Microbiome-pathogen interactions drive epidemiological dynamics of antibiotic resistance: A modeling study applied to nosocomial pathogen control

David RM Smith[1,2,3]*, Laura Temime[3,4†], Lulla Opatowski[1,2†]

[1]Institut Pasteur, Epidemiology and Modelling of Antibiotic Evasion (EMAE), Paris, France; [2]Université Paris-Saclay, UVSQ, Inserm, CESP, Anti-infective evasion and pharmacoepidemiology team, Montigny-Le-Bretonneux, France; [3]Modélisation, épidémiologie et surveillance des risques sanitaires (MESuRS), Conservatoire national des arts et métiers, Paris, France; [4]PACRI unit, Institut Pasteur, Conservatoire national des arts et métiers, Paris, France

Abstract The human microbiome can protect against colonization with pathogenic antibiotic-resistant bacteria (ARB), but its impacts on the spread of antibiotic resistance are poorly understood. We propose a mathematical modeling framework for ARB epidemiology formalizing within-host ARB-microbiome competition, and impacts of antibiotic consumption on microbiome function. Applied to the healthcare setting, we demonstrate a trade-off whereby antibiotics simultaneously clear bacterial pathogens and increase host susceptibility to their colonization, and compare this framework with a traditional strain-based approach. At the population level, microbiome interactions drive ARB incidence, but not resistance rates, reflecting distinct epidemiological relevance of different forces of competition. Simulating a range of public health interventions (contact precautions, antibiotic stewardship, microbiome recovery therapy) and pathogens (*Clostridioides difficile*, methicillin-resistant *Staphylococcus aureus*, multidrug-resistant Enterobacteriaceae) highlights how species-specific within-host ecological interactions drive intervention efficacy. We find limited impact of contact precautions for Enterobacteriaceae prevention, and a promising role for microbiome-targeted interventions to limit ARB spread.

*For correspondence:
david.smith@pasteur.fr

†These authors contributed equally to this work

Introduction

Bacteria are fundamental drivers of human health and disease. On one hand, bacterial pathogens are leading causes of global infectious disease burden, with antibiotic-resistant and healthcare-associated infections posing significant risks to patient safety and public health (*Cassini et al., 2019*; *Cassini et al., 2016*; *Friedman et al., 2016*; *Naylor et al., 2018*). On the other, the bacterial microbiome – the trillions of individual bacteria that collectively inhabit the human body – provides support to development and homeostasis, facilitates core physiological processes like digestion, and protects against diseases ranging from colitis to cancer (*Bäckhed et al., 2005*; *Kamada et al., 2013b*; *Lynch and Pedersen, 2016*; *Round and Mazmanian, 2009*; *Roy and Trinchieri, 2017*). The microbiome can also protect against colonization with infectious bacterial pathogens, a phenomenon known as colonization resistance, limiting their capacities to establish colonies, grow, persist, and transmit (*Bäumler and Sperandio, 2016*; *Buffie and Pamer, 2013*). This is perhaps best exemplified by the canonical *Clostridioides difficile*: growth within the intestine is inhibited by secondary metabolites of commensal gut bacteria, protecting colonized hosts from disease and limiting propagation of the infectious spores that drive between-host transmission (*Kamada et al., 2013a*;

Pamer, 2016). The human microbiome is purported to play a defensive role against a range of bacterial pathogens, but the mechanistic nature and epidemiological consequences of within-host microbiome-pathogen interactions are poorly understood.

This relationship between microbiome ecology and bacterial epidemiology is important in the context of widespread antibiotic use and global dissemination of high-risk pathogenic antibiotic-resistant bacteria (ARB). When prescribed appropriately, antibiotics target particular bacterial pathogens, but co-colonizing microbiota are also exposed (*Tedijanto et al., 2018*). This can unintentionally destabilize healthy microbial communities, resulting in dysbiosis, a state of population dynamic disequilibrium (*Bhalodi et al., 2019*; *Coyte et al., 2015*; *Dethlefsen and Relman, 2011*). Microbiome dysbiosis is associated with reduced abundance and diversity of commensal bacteria, impaired host immune responses, and loss of colonization resistance, altogether increasing host susceptibility to ARB colonization (*Kim et al., 2017*; *Sorbara and Pamer, 2019*; *Zhang et al., 2015*). Antibiotic-induced dysbiosis may further result in elevated expression of antibiotic resistance genes, increased rates of horizontal transfer of such genes, and ecological release, whereby subdominant ARB are released from competition via clearance of drug-sensitive bacteria, growing out into dominant colonies (*Doan et al., 2019*; *Letten et al., 2021*; *Ruppé et al., 2019*; *Stecher et al., 2013*). These associations may be particularly relevant for healthcare settings, where antibiotic use is widespread, and where microbiome dysbiosis is increasingly recognized as a key driver of ARB colonization and infection (*Baggs et al., 2018*; *Prescott et al., 2015*; *Ravi et al., 2019*). From a clinical perspective, this motivates a need for public health interventions that minimize or reverse harm to patient microbiota, from antibiotic stewardship, to fecal microbiota transplantation, to microbiome protective therapies. (*de Gunzburg et al., 2018*; *Relman and Lipsitch, 2018*).

In the face of uncertainty, mathematical modeling is a useful tool to analyze epidemiological dynamics of antibiotic resistance and evaluate control measures (*Heesterbeek et al., 2015*; *Opatowski et al., 2011*). However, an incomplete understanding of key eco-evolutionary principles is highlighted as a limitation to using modeling to predict future trends and inform decision-making (*Birkegård et al., 2018*; *Knight et al., 2019*). Disruption of the host microbiome is a long-standing theory explaining how antibiotics select for the spread of resistance at both the individual and population levels (*Lipsitch and Samore, 2002*), but most epidemiological models consider just one species of bacteria at a time, under the traditional assumption that antibiotic selection for resistance results from intraspecific competition between co-circulating strains (*Blanquart, 2019*; *Ramsay et al., 2018*; *Spicknall et al., 2013*). This simple framework has been particularly useful for bacteria like *Streptococcus pneumoniae* and *Staphylococcus aureus*, in which different strains – sometimes conceptualized as drug-sensitive vs. drug-resistant, or community-associated vs. healthcare-associated – are believed to be in close ecological competition (*Blanquart, 2019*; *Domenech de Cellès et al., 2011*; *Kardaś-Słoma et al., 2011*; *Pressley et al., 2010*; *van Kleef et al., 2013*).

Accounting for other forms of complexity in epidemiological models – from treatment intensity, to age-assortative contact behavior, to hospital referral networks, to animal-human interactions, to genetic linkage between resistance and non-resistance genes – has helped to unravel the many, disparate forces that contribute to drive the spread of resistance (*Blanquart et al., 2018*; *Cobey et al., 2017*; *Colijn and Cohen, 2015*; *Donker et al., 2017*; *Lehtinen et al., 2017*; *van Bunnik and Woolhouse, 2017*). Nevertheless, within-host bacterial competition remains a key mechanism of selection for antibiotic resistance dissemination, and an active area of research at the forefront of resistance modeling (*Lipsitch and Samore, 2002*; *Mulberry et al., 2020*; *Spicknall et al., 2013*). For instance, the 'mixed-carriage' model by Davies et al. demonstrates how intraspecific competition results in negative frequency-dependent selection for either of two competing strains, and provides a satisfying mechanistic explanation for widespread strain coexistence at the population level (*Davies et al., 2019*). However, contemporary work has stopped short of evaluating consequences of between-species competition on resistance epidemiology. Yet for many ARB, including emerging high-priority multidrug-resistant bacteria like extended-spectrum beta-lactamase (ESBL) producing Enterobacteriaceae, interactions with the host microbiome may be important mediators of nosocomial colonization dynamics (*Kim et al., 2017*; *Lerminiaux and Cameron, 2019*; *Pilmis et al., 2020*).

Here, we use mathematical modeling to evaluate how microbiome ecology and antibiotic consumption combine to drive the spread and control of antibiotic-resistant bacteria in the healthcare setting. This is presented in two parts. First, we propose a modeling framework for ARB colonization

dynamics, accounting for different within-host ecological interactions – including intraspecific pathogen strain competition, interspecific microbiome-pathogen competition, and horizontal gene transfer (HGT) – in the context of antibiotic treatment. Synthesizing these into a final model, we show how different combinations of ecological interactions drive antibiotic selection for the spread of resistance, with heterogeneous impacts on classic epidemiological indicators. Second, using parameter estimates from the literature, we apply this framework to simulate the nosocomial epidemiology of four high-risk ARB: *C. difficile*, methicillin-resistant *S. aureus* (MRSA), ESBL-producing *Escherichia coli* (ESBL-EC) and carbapenemase-producing *Klebsiella pneumoniae* (CP-KP). Expert elicitation interviews were conducted to characterize the clinical relevance of microbiome dysbiosis for each species, and to qualify and quantify interaction coefficients with uncertainty. By simulating a range of different public health interventions, we demonstrate the theoretical importance of microbiome-pathogen interactions as mediators of ARB epidemiology, and determining factors in the control of resistance dissemination.

Model and results

Part 1: A modeling framework for antibiotic resistance epidemiology in healthcare settings

We propose a series of five models describing colonization dynamics of an antibiotic-resistant bacterial *pathogen*, denoted P^R, among hospital inpatients in an acute care setting. Each model accounts for different within-host ecological interactions between P^R and other bacteria. Models are described using systems of ordinary differential equations (ODEs), and are evaluated deterministically using numerical integration. Across models, three primary epidemiological outcomes are calculated at steady-state equilibrium: P^R prevalence (the proportion of patients colonized), P^R incidence (the daily rate of colonization acquisition within the hospital), and the pathogen resistance rate (the proportion of patients colonized with the focal antibiotic-resistant strain P^R relative to a competing drug-sensitive strain P^S). We also derive and evaluate the basic reproduction number R_0 for P^R, an indicator of pathogen epidemicity representing the average number of patients expected to acquire a novel pathogen from an initial index patient. See Materials and methods for technical details, and the supplementary appendix for the complete modeling framework and assumptions (Appendix *Equation A1*).

A simple transmission model for bacterial colonization

We start with a Susceptible-Colonized transmission model (*Figure 1A*) representing a population of N hospital patients as either susceptible to colonization (S) or colonized (C^R) by P^R, the focal strain or species:

$$\frac{dS}{dt} = N \times (1-f) \times \mu - S \times (\lambda_R + \alpha_R + \mu) + C^R \times (\gamma_R + \sigma_R)$$
$$\frac{dC^R}{dt} = N \times f \times \mu + S \times (\lambda_R + \alpha_R) - C^R \times (\gamma_R + \sigma_R + \mu)$$

(1)

This model is adapted from classic colonization models of antibiotic-resistant bacteria (*Austin et al., 1997*), includes no ecological interactions with non-focal bacteria, and reflects a suite of common assumptions relevant to the healthcare setting, including: (i) a symmetric rate of patient admission and discharge μ, holding N constant; (ii) a proportion of patients colonized upon admission *f*, reflecting pathogen prevalence in the community; (iii) a dynamic rate of colonization acquisition $\lambda_R = \beta \times C^R/N$, for host-to-host transmission; (iv) a static rate of acquisition α_R, for endogenous routes of acquisition; (v) a rate of natural clearance γ_R; and (vi) a rate of effective antibiotic treatment σ_R. Note that all state variables are functions of time *t*, though this is omitted from ODEs for brevity.

Efficacy of antibiotic treatment is assumed to depend both on the distribution of antibiotics consumed in the hospital and on the intrinsic antibiotic resistance profile of P^R. We express this as

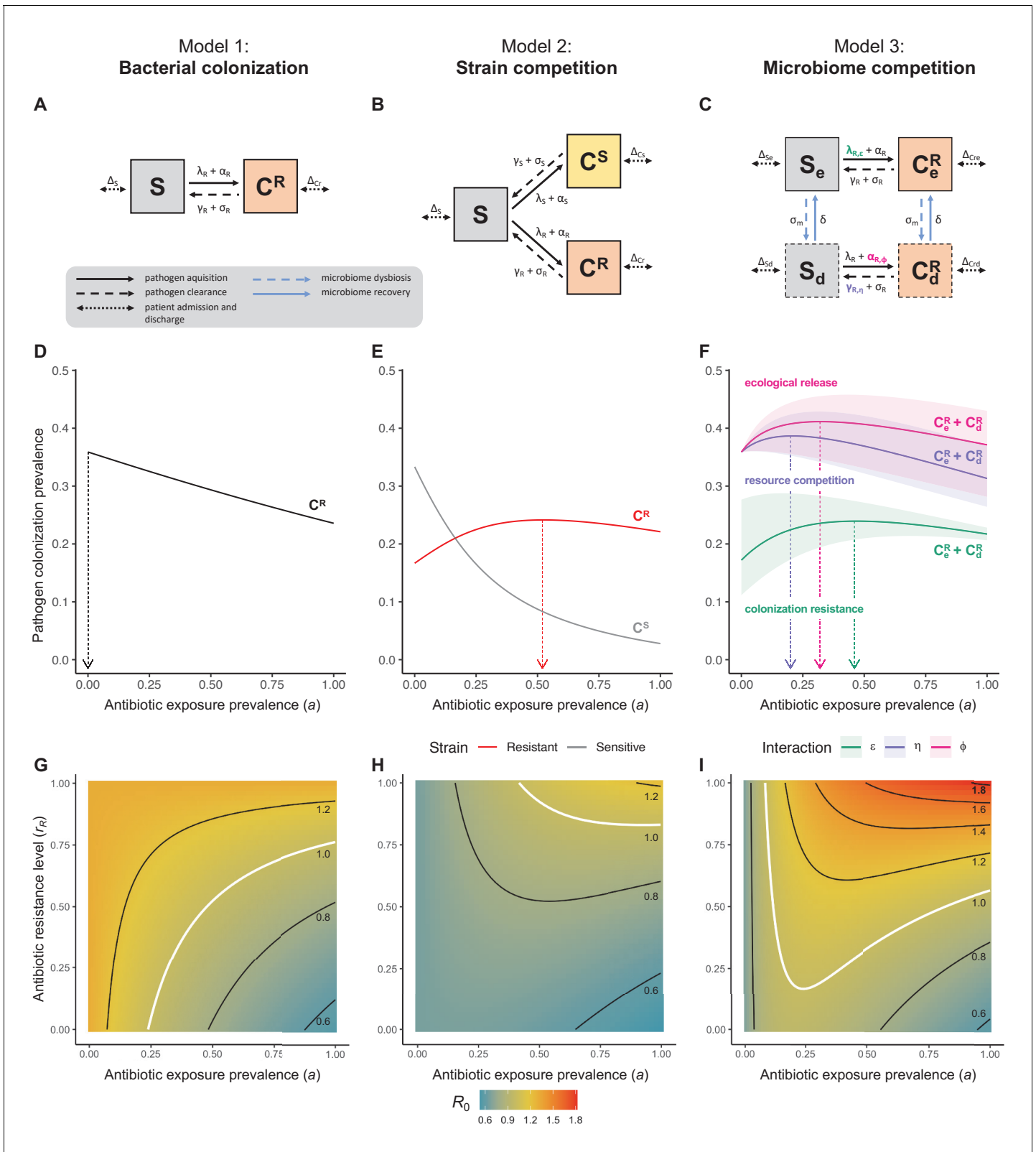$$\sigma_R = a \times (1 - r_R) \times \theta_C$$

(2)

Figure 1. Comparison of models describing bacterial colonization dynamics in healthcare settings: in contrast to predictions from a model with no ecological competition (A, D, G), models including strain competition (B, E, H) or microbiome competition (C, F, I) can explain how antibiotics select for the epidemiological spread of antibiotic-resistant bacteria. For all models, ODEs are integrated numerically using the same parameter values representing a generic nosocomial pathogen P^R (see **Appendix 1—table 1**). (A,B,C) Compartmental model diagrams representing corresponding ODE

Figure 1 continued on next page

Figure 1 continued

systems from the main text (A: *Equation 1*; B: *Equation 3*; C: *Equation 4*). (D,E,F) Pathogen colonization prevalence as a function of antibiotic exposure prevalence (a), assuming partial antibiotic resistance (r_R = 0.8). For (E) P^S and P^R circulate simultaneously, assuming strain-specific differences in antibiotic resistance (r_S = 0, r_R = 0.8), natural clearance (γ_S = 0.03 day^{-1}, γ_R = 0.06 day^{-1}) and transmission ($\lambda_S = \beta \times C^S/N$, $\lambda_R = \beta \times C^R/N$). For (F), epidemiological dynamics are evaluated independently for each interaction and superimposed (ε = colonization resistance; η = resource competition; ϕ = ecological release); shaded intervals represent outcomes across the range of values considered for each interaction (see *Figure 2*); and antibiotics are assumed to induce dysbiosis after 1 day (θ_m = 1 day^{-1}), from which microbiome stability recovers after 7 days (δ = 1/7 day^{-1}). Dashed vertical arrows denote the levels of antibiotic use that maximize P^R prevalence (the sum of colonized compartments C^R). (G,H,I) Numerical evaluation of the basic reproduction number (R_0) of P^R as a function of a and r_R. White contour lines indicate R_0 = 1, above which a single colonized patient admitted to a naïve hospital population is expected to trigger an outbreak. For I, all three microbiome-pathogen interactions are applied simultaneously using baseline values (ε = 0.5; η = 0.5; ϕ = 5).

where a is the hospital population's antibiotic exposure prevalence (the proportion of patients exposed to antibiotics at any t), θ_C is the antibiotic-induced clearance rate (the rate at which effective antibiotics clear pathogen colonization), and r_R is the antibiotic resistance level (the proportion of antibiotics that are ineffective against P^R). Modeling the latter as a continuous proportion reflects that bacteria are not necessarily fully drug-sensitive (r_R = 0) nor -resistant (r_R = 1), but can range in their sensitivity to different antibiotics ($0 \leq r_R \leq 1$). The resistance level r_R is thus a model input interpreted as an overall measure of the pathogen's innate degree of resistance to the particular antibiotics to which it is exposed.

Following models build upon these assumptions, representing the same pathogen P^R, but altering its ecological interactions with other bacteria from one model to the next. Models were evaluated over the same generic parameter space, to isolate impacts of model structure on epidemiological outcomes in the context of antibiotic use (see parameters in *Appendix 1—table 1*).

Antibiotic selection for resistance: the role of strain competition

Antibiotic consumption selects for the epidemiological spread of antibiotic-resistant bacteria (*Chatterjee et al., 2018*). To explain this mechanistically, a classic modeling assumption is that selection results from intraspecific competition between two or more drug-sensitive strains P^S and drug-resistant strains P^R (*Spicknall et al., 2013*). The reasoning goes: strains of the same species occupy the same ecological niche, so colonization with one strain inhibits colonization with another. In turn, antibiotics that preferentially clear P^S render the within-host niche available to potential colonization with co-circulating P^R, indirectly favouring P^R spread through the host population. A simple two-strain 'exclusive colonization' model (*Figure 1B*) can be written as:

$$\frac{dS}{dt} = -S \times (\lambda_S + \lambda_R + \alpha_S + \alpha_R) + C^S \times (\gamma_S + \sigma_S) + C^R \times (\gamma_R + \sigma_R) + \Delta_S$$

$$\frac{dC^S}{dt} = S \times (\lambda_S + \alpha_S) - C^S \times (\gamma_S + \sigma_S) + \Delta_{C^S} \quad (3)$$

$$\frac{dC^R}{dt} = S \times (\lambda_R + \alpha_R) - C^R \times (\gamma_R + \sigma_R) + \Delta_{C^R}$$

where patients can be colonized (C^S, C^R) by either strain (P^S, P^R). Subscripts S and R denote strain-specific rates, accounting for ecological differences between strains (e.g. antibiotic resistance levels, fitness costs of resistance; see Appendix *Equations 3–7*). Strains are labeled as sensitive or resistant, but here this is interpreted as relative ($r_S < r_R$). For simplicity, patient demography (admission and discharge) is given as Δ_j for each compartment j.

Unlike the single-strain Susceptible-Colonized model (*Figure 1D and G*), the strain competition model can explain how antibiotic consumption selects for the spread of resistance (*Figures 1E,H*). When P^R is resistant to all antibiotics (r_R = 1), its prevalence increases monotonically with increasing antibiotic exposure (*Appendix 1—figure 1*). When resistance is partial – when P^R is still cleared by antibiotics, but at a lower rate than P^S ($r_S < r_R < 1$) – selection for resistance can peak at intermediate antibiotic exposure, owing to a trade-off in how antibiotics both clear and facilitate P^R. As such, R_0 for P^R tends to increase with antibiotic use when P^R is highly resistant to antibiotics (high r_R), but decrease when still largely sensitive (low r_R).
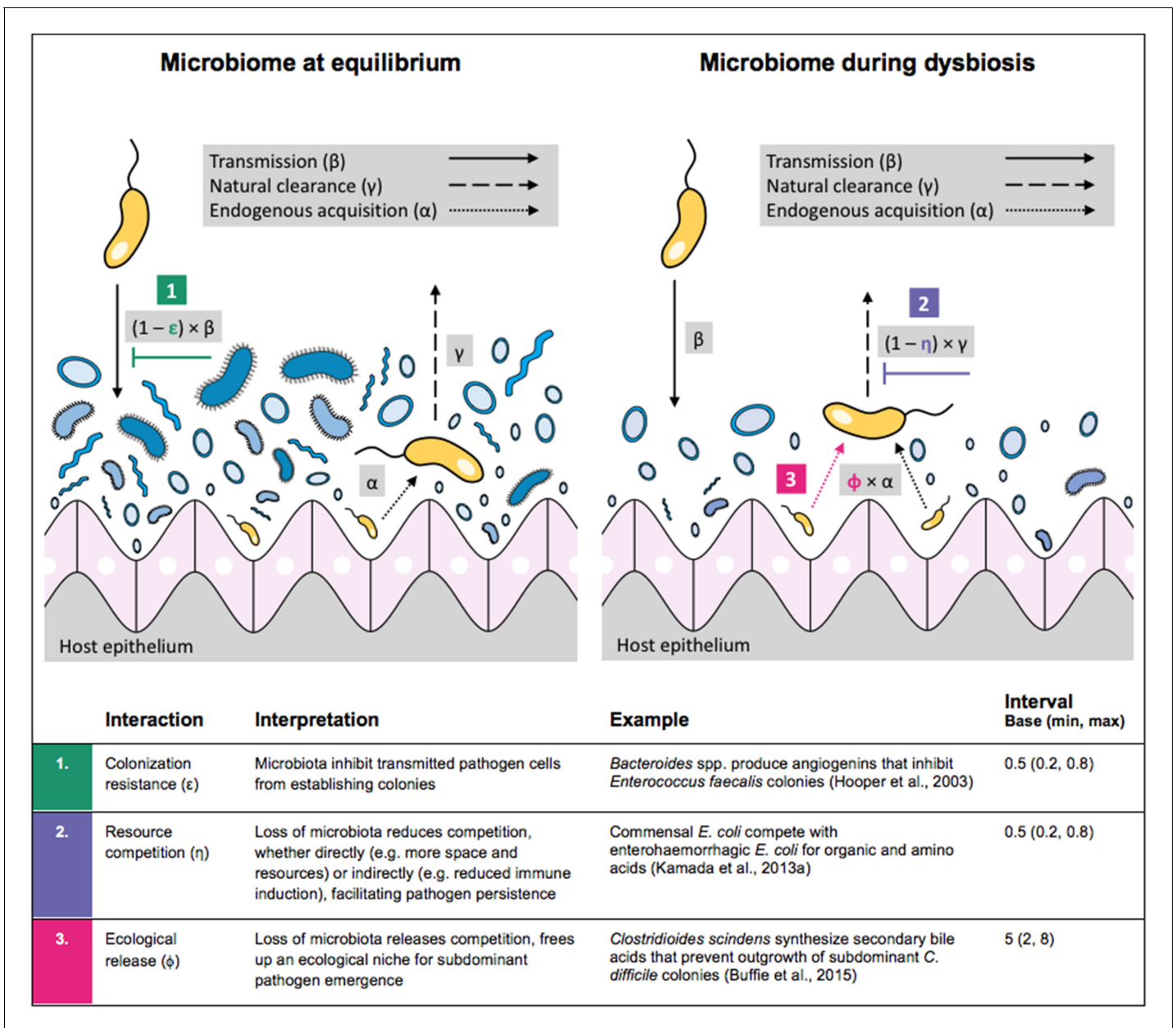
Figure 2. Illustration of within-host ecological interactions between the host microbiome (blue) and a transmissible bacterial pathogen P^R (yellow), and their impact on P^R's vital epidemiological parameters β (transmission rate), γ (clearance rate) and α (endogenous acquisition rate). To illustrate the latter: sub-dominant, non-transmissible P^R colonies inhibited by microbiota are represented by small cartoon pathogens, which can grow into dominant, transmissible colonies (large cartoon pathogens) via endogenous acquisition. Microbiome-pathogen interactions are assumed to differ between hosts with a stable microbiome at population dynamic equilibrium (left) and hosts experiencing antibiotic-induced microbiome dysbiosis (right). Interaction coefficients can be interpreted as terms explaining variation in host susceptibility to pathogen colonization, as depending on their recent history of antibiotic exposure. For interaction coefficient parameter values, broad intervals are assumed for the baseline analysis.

Most contemporary antibiotic resistance models are variants of this typology (*Blanquart, 2019*; *Spicknall et al., 2013*), but intraspecific strain competition is not the only mechanism by which antibiotic consumption can drive ARB spread (*Lipsitch and Samore, 2002*), and may have limited relevance for certain species, settings, timescales and epidemiological indicators.

Antibiotic selection for resistance: the role of microbiome competition

Antibiotic-induced microbiome dysbiosis is an alternative mechanism by which antibiotics may select for the spread of resistance. We propose a model in which (i) bacterial pathogens and commensal microbiota compete ecologically within the host, and (ii) antibiotic-induced dysbiosis disrupts these interactions, predisposing hosts to pathogen colonization. We consider three competitive within-host microbiome-pathogen interactions and conceptualize how they affect pathogen epidemiology (*Figure 2*; *Buffie et al., 2015*; *Hooper et al., 2003*; *Kamada et al., 2013a*). First, a stable microbiome can act as a barrier preventing introduced pathogens from establishing colonies. We modeled this *colonization resistance* (ε) as a reduced rate of pathogen transmission (β) to hosts with stable microbiota, $\beta_\varepsilon = (1 - \varepsilon) \times \beta$. Second, co-colonizing bacteria can compete for space, nutrients and other limited resources within the host. In this case, antibiotics that reduce the density of potential competitors may favour pathogen persistence. We modeled this *resource competition* (η) as a reduced rate of pathogen clearance (γ) among hosts undergoing dysbiosis, $\gamma_\eta = (1 - \eta) \times \gamma$. Lastly, microbiome dysbiosis can favor the emergence or outgrowth of subdominant pathogen colonies, and this *ecological release* (ϕ) was modeled as an increased rate of endogenous pathogen acquisition (α) upon dysbiosis, $\alpha_\phi = \phi \times \alpha$.

We integrate the microbiome, these three interactions, and antibiotic-induced microbiome dysbiosis into *Equation 1*. The resulting 'microbiome competition model' (*Figure 1C*) is given by

$$
\begin{aligned}
\frac{dS_e}{dt} &= -S_e \times \left(\lambda_{R,\varepsilon} + \alpha_R + \sigma_m\right) + S_d \times \delta + C_e^R \times \left(\gamma_R + \sigma_R\right) + \Delta_{S_e} \\
\frac{dS_d}{dt} &= S_e \times \sigma_m - S_d \times \left(\lambda_R + \alpha_{R,\phi} + \delta\right) + C_d^R \times \left(\gamma_{R,\eta} + \sigma_R\right) + \Delta_{S_d} \\
\frac{dC_e^R}{dt} &= S_e \times \left(\lambda_{R,\varepsilon} + \alpha_R\right) - C_e^R \times \left(\gamma_R + \sigma_m + \sigma_R\right) + C_d^R \times \delta + \Delta_{C_e^R} \\
\frac{dC_d^R}{dt} &= S_d \times \left(\lambda_R + \alpha_{R,\phi}\right) + C_e^R \times \sigma_m - C_d^R \times \left(\gamma_{R,\eta} + \delta + \sigma_R\right) + \Delta_{C_d^R}
\end{aligned}
\tag{4}
$$

describing colonization (C^R) with a single pathogen strain (P^R) across two host types: patients with a microbiome at dynamic equilibrium (subscript e) and those undergoing dysbiosis (subscript d). Antibiotics induce dysbiosis at a rate σ_m given by

$$
\sigma_m = \mathrm{a} \times \theta_m
\tag{5}
$$

such that microbiome dysbiosis depends on both antibiotic exposure prevalence (a) and the rate at which antibiotic exposure causes dysbiosis (θ_m). Accordingly, the same level of antibiotic exposure (a) can have asymmetric effects on microbiome stability (via θ_m) and P^R colonization (via $(1 - r_R) \times \theta_c$, as in *Equation 2*). Dysbiosis can result in long-term changes to microbiome composition, but ecological function and population dynamic stability tend to recover in the days or weeks following antibiotic therapy (*Lozupone et al., 2012*), represented here by microbiome recovery rate δ.

Included microbiome-pathogen interactions predict in different ways how antibiotic consumption selects for the epidemiological spread of antibiotic-resistant bacterial pathogens (*Figure 1F*). Like strain competition, microbiome competition underlies a trade-off in antibiotic selection: P^R prevalence and R_0 increase monotonically with antibiotic exposure when P^R is completely antibiotic-resistant ($r_R = 1$) (*Appendix 1—figure 1*), but can peak at intermediate antibiotic exposure when resistance is partial ($0 < r_R < 1$) because antibiotics simultaneously clear pathogen colonization and induce greater host susceptibility through dysbiosis (*Figure 1I*). This trade-off is more pronounced when multiple interactions are combined: when microbiota simultaneously limit multiple colonization processes (transmission, emergence, persistence), patients with stable microbiota are more protected from P^R colonization, but antibiotic use is predicted to have greater epidemiological costs, selecting more strongly for P^R spread (*Appendix 1—figure 2*).

Antibiotic selection for resistance: combining strain and microbiome competition

Strain competition and microbiome competition are not mutually exclusive: when combined in a two-strain 'microbiome-strain competition' model, different strains of the same pathogen species compete for hosts whose microbiota and history of antibiotic consumption influence susceptibility to

colonization. We assume that microbiome-pathogen interactions are species- and not strain-specific, that is that ε, η and ϕ apply equally to P^S and P^R. This is given by:

$$\frac{dS_e}{dt} = -S_e \times \left(\lambda_{S,\varepsilon} + \lambda_{R,\varepsilon} + \alpha_S + \alpha_R + \sigma_m\right) + S_d \times \delta + C_e^S \times \left(\gamma_S + \sigma_S\right) + C_e^R \times \left(\gamma_R + \sigma_R\right) + \Delta_{S_e}$$

$$\frac{dS_d}{dt} = -S_d \times \left(\lambda_S + \lambda_R + \alpha_{S,\phi} + \alpha_{R,\phi} + \delta\right) + S_e \times \sigma_m + C_d^S \times \left(\gamma_{S,\eta} + \sigma_S\right) + C_d^R \times \left(\gamma_{R,\eta} + \sigma_R\right) + \Delta_{S_d}$$

$$\frac{dC_e^S}{dt} = S_e \times \left(\lambda_{S,\varepsilon} + \alpha_S\right) + C_d^S \times \delta - C_e^S \times \left(\gamma_S + \sigma_S + \sigma_m\right) + \Delta_{C_e^S}$$

$$\frac{dC_d^S}{dt} = S_d \times \left(\lambda_S + \alpha_{S,\phi}\right) + C_e^S \times \sigma_m - C_d^S \times \left(\delta + \gamma_{S,\eta} + \sigma_S\right) + \Delta_{C_d^S}$$

$$\frac{dC_e^R}{dt} = S_e \times \left(\lambda_{R,\varepsilon} + \alpha_R\right) + C_d^R \times \delta - C_e^R \times \left(\gamma_R + \sigma_R + \sigma_m\right) + \Delta_{C_e^R}$$

$$\frac{dC_d^R}{dt} = S_d \times \left(\lambda_R + \alpha_{R,\phi}\right) + C_e^R \times \sigma_m - C_d^R \times \left(\delta + \gamma_{R,\eta} + \sigma_R\right) + \Delta_{C_d^R}$$

(6)

Introducing a drug-sensitive strain P^S to the microbiome model dampens R_0 of the focal strain P^R, because fewer patients are susceptible to colonization when the competing strain co-circulates in the population (*Appendix 1—figure 3*). However, antibiotic use makes way for P^R not only through preferential clearance of P^S, but remaining P^R also benefit from increased host susceptibility to colonization when antibiotics cause dysbiosis. Accordingly, antibiotics that both disrupt host microbiota and clear drug-sensitive pathogen strains tend to select more strongly for the spread of resistant strains than antibiotics that only target one or the other (*Figure 3*). Overall, antibiotics with stronger impacts on pathogen clearance (higher θ_C) lead to increased resistance rates, while consequences for P^R colonization prevalence are modest and depend on potential interactions with the microbiome. Conversely, antibiotics with stronger impacts on microbiome stability (higher θ_m) lead to higher prevalence, with only modest effects on resistance rates. Further, impacts of antibiotic treatment on resistance rates are greater when P^R resists a greater share of antibiotics (higher r_R), while impacts on prevalence are greater when microbiome-pathogen interactions are stronger (higher ε, η, ϕ) (*Appendix 1—figure 4*). Different microbiome-pathogen interactions also underlie distinct dynamic responses to theoretical public health interventions. For the same generic pathogen P^R, antibiotic stewardship interventions generally, but do not always prevent colonization, with predictions depending on the ecological interactions in effect (e.g. strain competition, microbiome competition), the impact of the intervention (e.g. reduced microbiome disruption, reduced overall prescribing), and the epidemiological outcome considered (e.g. colonization prevalence, resistance rate) (*Appendix 1—figure 5*).

Antibiotic selection for resistance: introducing interspecific horizontal gene transfer

Horizontal transfer of resistance-encoding genes may also contribute to hospital resistance dynamics (*Evans et al., 2020*; *Lerminiaux and Cameron, 2019*). We extend our model to include interspecific HGT, conceptualized as two-way within-host transfer of a focal resistance gene, either from a resistant pathogen strain P^R to co-colonizing microbiota, or from resistance-bearing microbiota to a co-colonizing drug-sensitive pathogen strain P^S. (See final model and assumptions, Appendix *Equations A1–A11*). Overall, an increasing rate of within-host HGT (χ) is found to drive increasing P^R prevalence (C^R), regardless of other microbiome-pathogen interactions (*Figure 4*). Under our modeling assumptions, HGT-driven gains in C^R result from symmetric declines in C^S, such that HGT's potential impact depends on the presence of both sufficient resistance donors and sufficient recipients. This results in non-linear feedbacks between HGT and other processes that drive strain prevalence (*Appendix 1—figure 7*). For instance, impacts of HGT on C^R are greatest at intermediate antibiotic exposure (a). This is linked to another antibiotic selection trade-off: higher a affords a selective advantage to P^R relative to P^S, increasing the potential impact of HGT on C^R; but higher a also reduces the pool of recipient C^S, ultimately limiting HGT's ability to drive C^R.

Part 2: Model application to high-risk nosocomial pathogens

We applied this modeling framework to simulate colonization dynamics of four nosocomial pathogens in the hospital setting: *C. difficile*, methicillin-resistant *S. aureus* (MRSA), extended-spectrum
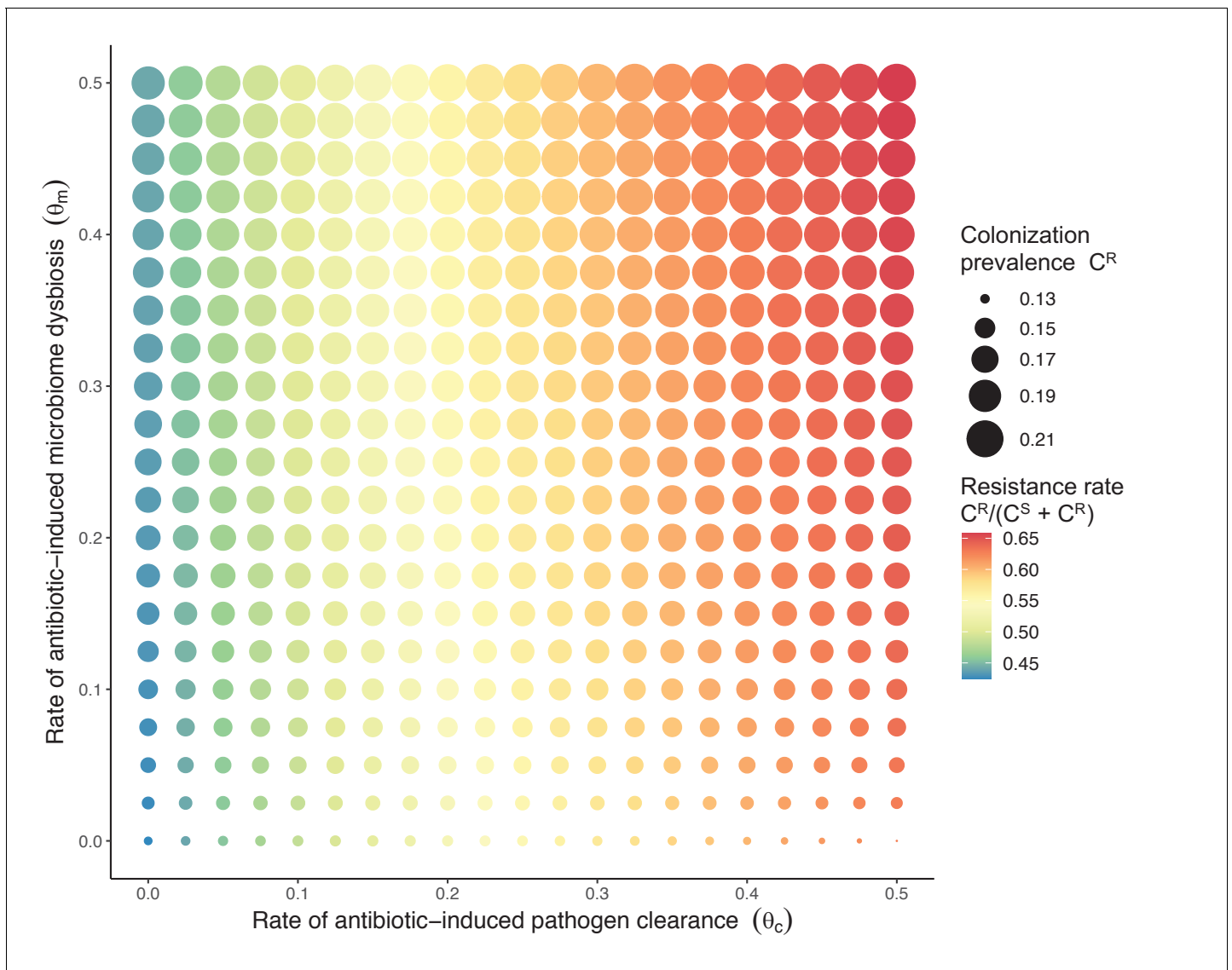
Figure 3. Strain competition and microbiome competition as simultaneous forces of antibiotic selection, with asymmetric impacts on epidemiological indicators. In a mixed microbiome-strain competition model (*Equation 6*), colonization prevalence of P^R (C^R; circle size) and the pathogen's resistance rate ($C^R/(C^S + C^R)$; color) depend on the relative rates at which antibiotics disrupt microbiota (θ_m) and clear pathogen colonization (θ_c). Antibiotics with a stronger effect on pathogen clearance (higher θ_c) increase the resistance rate, while antibiotics with a stronger effect on microbiota (higher θ_m) increase prevalence.

beta-lactamase-producing *E. coli* (ESBL-EC), and carbapenemase-producing *K. pneumoniae* (CP-KP). Data from the literature were used to parameterize the model to each pathogen (*Appendix 1—figure 5*, *Appendix 1—table 2–6*). Literature estimates for microbiome-pathogen interaction coefficients are scarce, and the species-specific relevance of different within-host interactions (intraspecific strain competition, microbiome competition, HGT) in the hospital environment are not well-defined. To characterize ecological interactions for each species and inform model structure, we conducted interviews with a panel of subject-matter experts in medical microbiology and antibiotic resistance epidemiology (details in Materials and methods). Based on their beliefs, all pathogens were assumed to compete with microbiota; MRSA, ESBL-EC and CP-KP were further assumed to compete intra-specifically with non-focal strains, for simplicity characterized as methicillin-sensitive *S. aureus* (MSSA), *E. coli* (EC), and *K. pneumoniae* (KP); and both ESBL resistance and carbapenem resistance were assumed to be borne by plasmids capable of horizontal transfer between patient microbiota and, respectively, EC and KP (*Figure 5A*). To quantify species-specific strengths of microbiome-
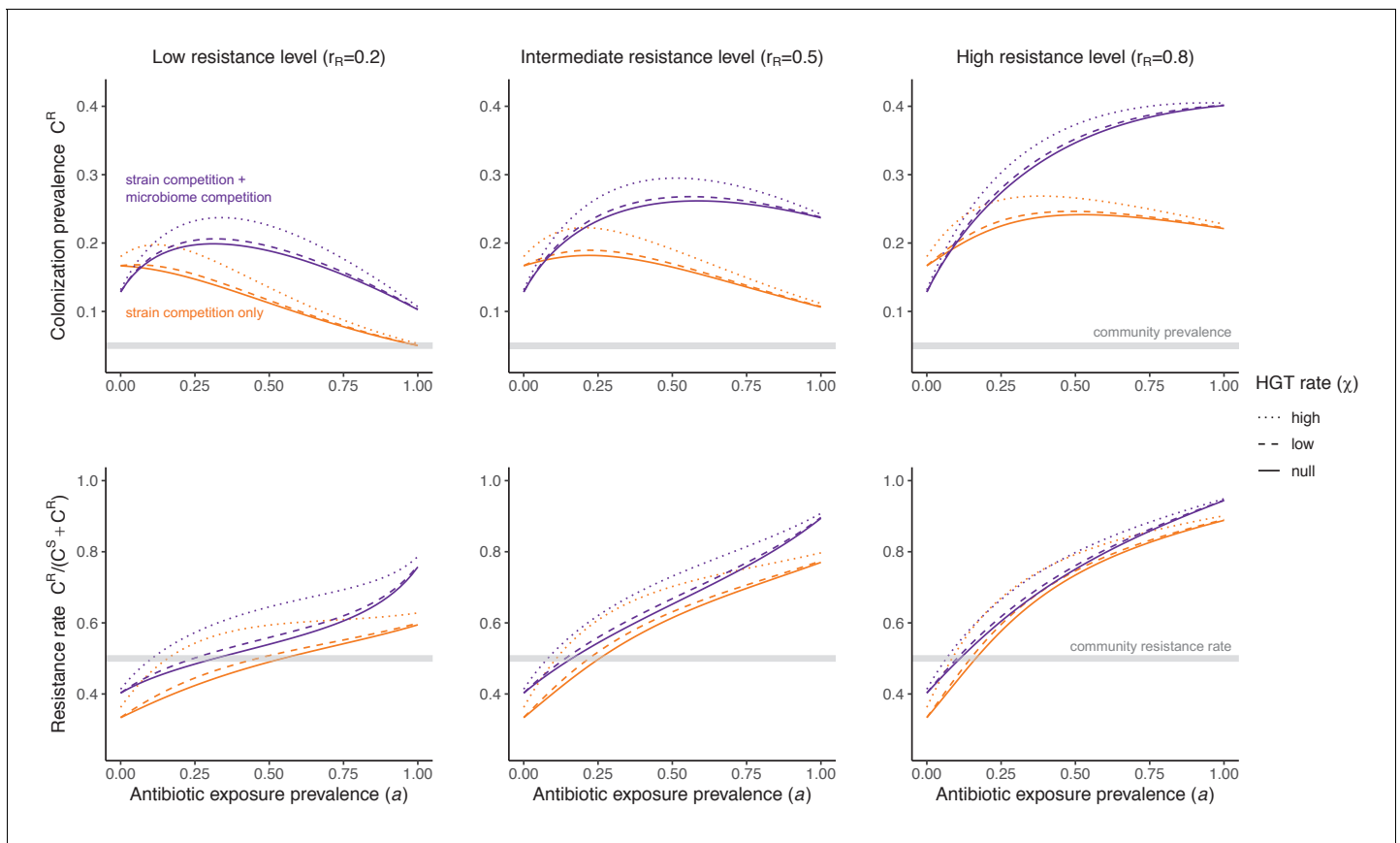
Figure 4. Impacts of horizontal gene transfer (HGT) on antibiotic selection for resistance. Allowing a resistance gene to transfer horizontally increases prevalence (top row) of the strain P^R that bears the gene, as well as its resistance rate (bottom row). The relative impact of HGT depends on the gene's rate of transfer (χ, line type), antibiotic exposure prevalence (a, x-axis), competitive interactions between pathogen strains and host microbiota (colors), the level of resistance conferred by the gene (r_R, columns), and any other parameters that drive the dynamics of donor and recipient strains. We assume that $\chi_d/\chi_e = 10$, such that the low HGT rate corresponds to $\{\chi_e=0.01\ \text{day}^{-1}, \chi_d=0.1\ \text{day}^{-1}\}$ and the high rate to $\{\chi_e=0.1\ \text{day}^{-1}, \chi_d=1\ \text{day}^{-1}\}$. Impacts of HGT on colonization incidence are shown in *Appendix 1—figure 6*. Alternative HGT assumptions are explored in *Appendix 1—figure 7A*.

pathogen interactions, within-host ecological parameters were translated into clinical parameters (*Appendix 1—table 7*), and experts were asked to quantify these using standardized expert elicitation methodology (*Figure 5B*, *Appendix 1—figures 8–10*).

Colonization dynamics for each ARB were modeled against a common backdrop of antibiotic consumption. This was parameterized at the level of antibiotic class, using national data from French hospitals in 2016 (*Appendix 1—table 8*; *Agence nationale de sécurité du médicament et des produits de santé, 2017*). Using data from the literature, antibiotic classes were assumed to vary in their impact on microbiome dysbiosis (very low, low, medium, or high rate of inducing dysbiosis) and on each pathogen strain (classified as sensitive, intermediate, or resistant) (*Figure 5C and D*; *Baggs et al., 2018*; *Brown et al., 2013*; *McCormack and Lalji, 2015*). For each of 10,000 Monte Carlo simulations, in which parameter values were sampled randomly from their respective probability distributions, epidemiological outcomes were evaluated at population dynamic equilibrium. For all outcomes, we compare results from simulations that include microbiome-pathogen interactions and dysbiosis ('microbiome simulations') and those that exclude them ('single-species simulations'). Multivariate sensitivity analyses were also conducted, using partial rank correlation coefficients (PRCCs) to evaluate impacts of parameter uncertainty on model outcomes (details in Methods).

Species-specific hospital colonization dynamics

Across simulations, *C. difficile* was the most prevalent pathogen (*Figure 6A*), MRSA had the highest resistance rate (*Figure 6B*), and ESBL-EC had the highest rate of incidence within the hospital
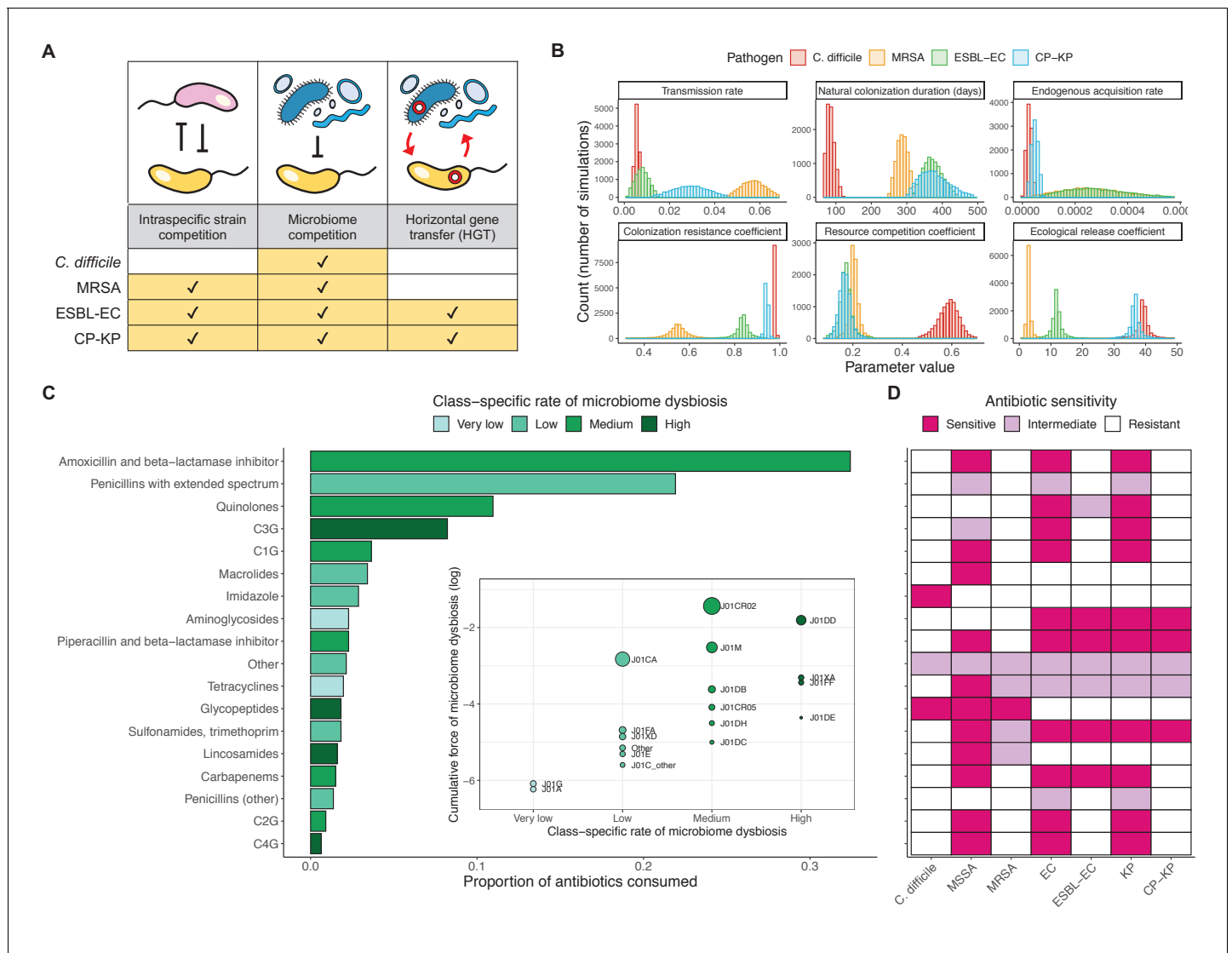
Figure 5. Characterizing the species-specific ecology of four selected antibiotic-resistant bacterial pathogens in the hospital setting. (**A**) Model structure: the within-host ecological interactions assumed for each pathogen, based on expert elicitation. (**B**) Simulation inputs: 95% distributions for selected model parameters drawn stochastically over 10,000 runs (all parameter distributions in *Appendix 1—table 2–6*). (**C**) The distribution of antibiotic classes consumed in French hospitals in 2016 (*Agence nationale de sécurité du médicament et des produits de santé, 2017*), shaded by their assumed impact on intestinal microbiome dysbiosis. Inset: the cumulative impact of each antibiotic class (given as ATC codes, see *Appendix 1— table 8* for corresponding names) on dysbiosis ($a_j \times e^{-k}$, see *Equation 7*); circle size represents each class's contribution to exposure prevalence (a_j). (**D**) Antibiograms for each pathogen strain and antibiotic class, adapted from the Therapeutics Education Collaboration (*McCormack and Lalji, 2015*).

(*Figure 6C*). CP-KP had the lowest prevalence, resistance rate and incidence, but was the pathogen most favoured by the hospital environment, its prevalence increasing by approximately 5.4-fold (95% uncertainty interval: 2.1–10.9) among hospital patients relative to baseline prevalence in the community (*Appendix 1—figure 12A*). For pathogens subject to intraspecific strain competition, resistance rates in the hospital also tended to exceed rates in the community (*Appendix 1—figure 12B*). Patient-to-patient transmission was the primary route of MRSA acquisition, while endogenous acquisition was the primary route for the enteric pathogens *C. difficile*, ESBL-EC and CP-KP (*Appendix 1—figure 13*). HGT played a potentially important but highly uncertain role for ESBL-EC and CP-KP, accounting for 8.7% (<0.01–49.7%) and 2.1% (<0.01–22.8%) of acquisition events, respectively. In multivariate sensitivity analysis, community prevalence (f_C for *C. difficile*, f_R for others) and rates of endogenous acquisition (α_R) had overall the strongest positive impacts (highest PRCCs) on hospital colonization prevalence across ARB, while rates of hospital admission/discharge (μ) and microbiome
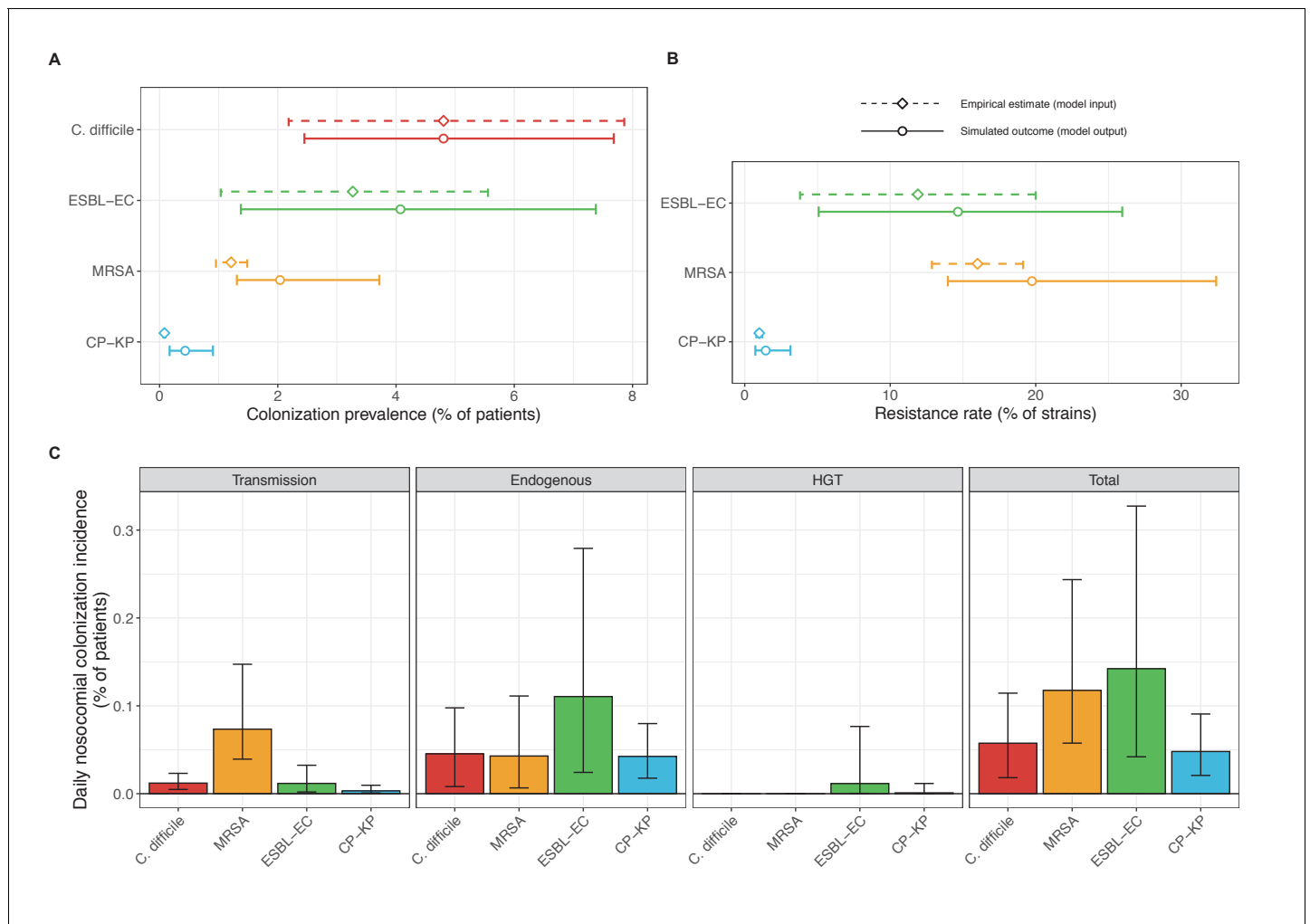
Figure 6. Baseline steady-state pathogen colonization outcomes. **(A)** Colonization prevalence, the percentage of patients colonized with the focal strain. Dashed lines (model inputs) represent assumed community prevalence, that is the proportion of patients already colonized upon hospital admission (see *Appendix 1—table 3–6*). Solid lines represent simulated prevalence within the hospital, as resulting from both importation from the community and within-hospital epidemiology. **(B)** Resistance rates, the proportion of *S. aureus* carriers bearing methicillin-resistant strains, *E. coli* carriers bearing ESBL-producing strains, and *K. pneumoniae* carriers bearing carbapenemase-producing strains. As in panel A, dashed lines (model inputs) represent assumed community resistance rates, and solid lines represent simulated resistance rates within the hospital. **(C)** Pathogen incidence (daily rate of within-hospital colonization acquisition), stratified by route of acquisition. Points (in panels A and B) and bar height (panel C) represent medians, and error bars represent 95% uncertainty intervals across 10,000 Monte Carlo simulations. For comparison, the same information for single-species simulations excluding the microbiome is presented in *Appendix 1—figure 11*.

recovery (δ) had the strongest negative impacts (lowest PRCCs; *Appendix 1—figure 14A*). For resistance rates, parameters with the strongest positive impacts (highest PRCCs) were community prevalence (f_R), the rate of endogenous acquisition (α_R) and the rate of antibiotic-induced pathogen clearance (θ_C). Parameters with the strongest negative impacts (lowest PRCCs) were rates of hospital admission/discharge (μ) and endogenous acquisition of competing drug-sensitive strains (α_S) (*Appendix 1—figure 14B*). Across ARB, prevalence estimates, but not resistance rates, were generally sensitive to microbiome parameters.

Microbiome ecology underlies epidemiological responses to public health interventions

We simulated three types of public health intervention, each across three levels of intervention compliance: (i) contact precautions, which reduced transmission rates of all strains by 20%, 35%, or 50%; (ii) antibiotic stewardship interventions, which reduced or modified hospital antibiotic consumption
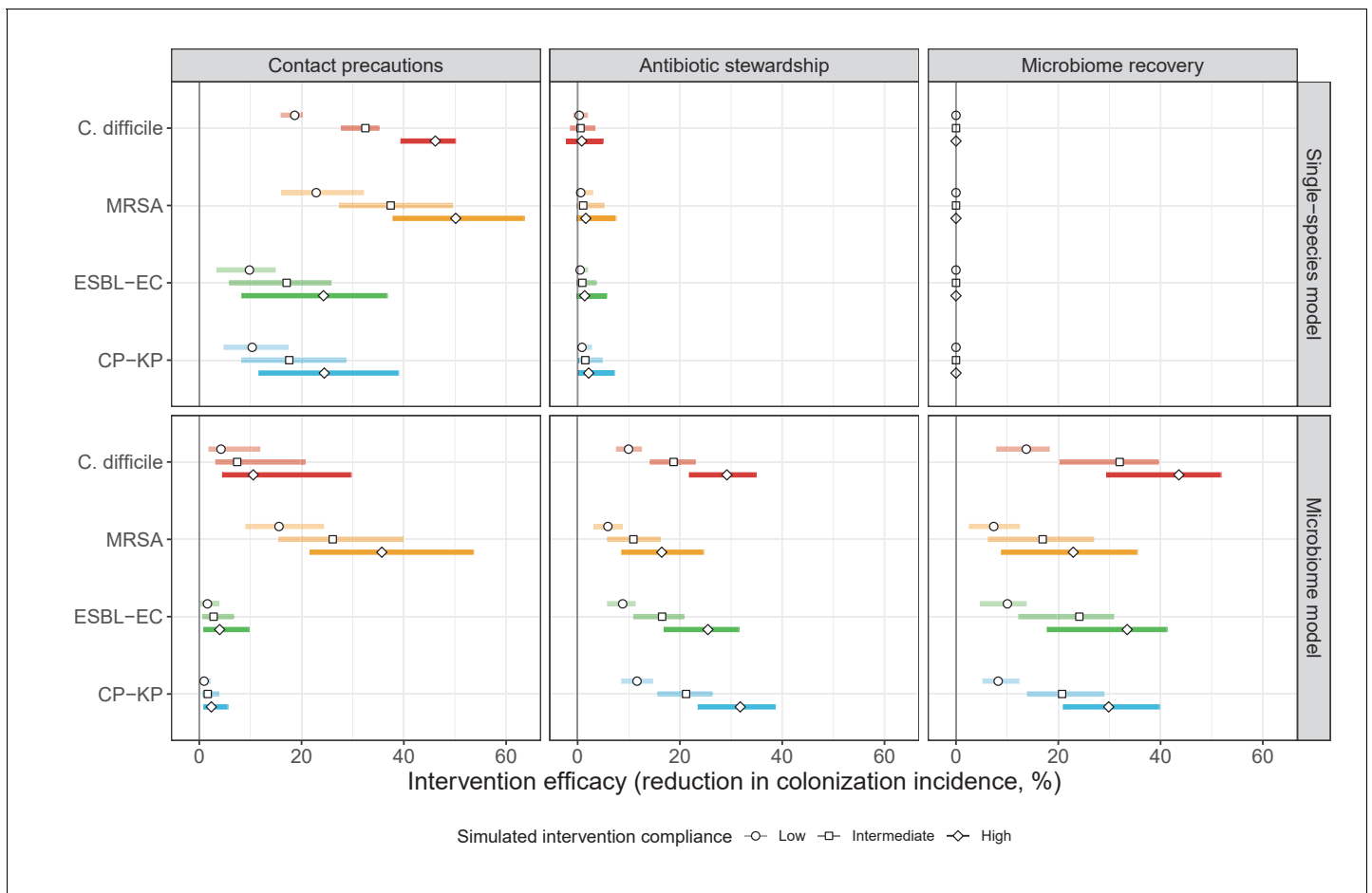
Figure 7. The microbiome drives pathogen-specific responses to simulated public health interventions (left panels, contact precautions; middle, antibiotic stewardship; right, microbiome recovery therapy). Top panels show results from simulations using classical 'single-species models' that only account for the focal pathogen species (including intraspecific strain competition for MRSA, ESBL-EC and CP-KP); bottom panels show simulation results when models also include microbiome-pathogen interactions and antibiotic-induced microbiome dysbiosis. For each intervention, three levels of intervention compliance (shading) are simulated. For antibiotic stewardship, simulation results are pooled across three different types of stewardship (see *Appendix 1—figure 17*). Points correspond to medians, and bars to 95% uncertainty intervals across 10,000 Monte Carlo simulations.

patterns by 20%, 35%, or 50%; and (iii) a theoretical 'microbiome recovery therapy' intervention that facilitates recovery from dysbiosis. We assumed a mean 2 day delay to microbiome recovery, and compliance levels corresponding to use among 10%, 30%, or 50% of antibiotic-exposed patients (see Materials and methods). Intervention efficacy was evaluated using: reduction in colonization incidence, 1 – IRR (where IRR is the incidence rate ratio of post-intervention to pre-intervention incidence); and reduction in the resistance rate, 1 – RRR (where RRR is the resistance rate ratio, the ratio of the post-intervention to pre-intervention resistance rate).

Efficacies of simulated interventions varied considerably by pathogen and type of intervention (*Figure 7*). Contact precautions were highly effective for reducing MRSA incidence, of intermediate efficacy for *C. difficile*, and minimally effective for ESBL-EC and CP-KP. Contact precautions had comparatively little impact on resistance rates, with a median 2–4% reduction across simulations and compliance levels for MRSA, 0–2% for CP-KP and negligible impact for ESBL-EC (*Appendix 1—figure 15*). These interventions were overall less effective in microbiome simulations, which tended to limit the role of between-host transmission (via colonization resistance) and favor the role of endogenous acquisition (via ecological release) in the hospital environment when compared to single-species simulations (*Appendix 1—figure 13*).

Antibiotic stewardship interventions led to substantial reductions in nosocomial incidence for all pathogens, but only when the microbiome was taken into account (*Figure 7*). Unlike contact

precautions, which only reduced incidence via transmission, stewardship reduced incidence through all acquisition routes, including HGT (*Appendix 1—figure 16*). Overall efficacy estimates and species-specific responses were similar across three types of stewardship considered (*Appendix 1—figure 17*). Pooling these together under intermediate compliance, colonization incidence was reduced by a median 20% for CP-KP, 18% for C. difficile, 15% for ESBL-EC, and 10% for MRSA. Single-species simulations excluding microbiome competition predicted negligible efficacy of all stewardship interventions for reducing incidence, and non-efficacy for *C. difficile*. Stewardship interventions also had a substantial impact on resistance rates, with overall greater reductions for CP-KP than MRSA and ESBL-EC, and similar outcomes across microbiome and single-species simulations (*Appendix 1—figure 15*).

Lastly, microbiome recovery therapy was potentially highly effective for limiting pathogen incidence, but efficacy varied greatly across different levels of intervention compliance (*Figure 7*). This intervention was most effective against *C. difficile*, of similar efficacy against ESBL-EC and CP-KP, and comparatively least effective against MRSA. Across pathogens, microbiome recovery therapy reduced incidence through all acquisition routes,(*Appendix 1—figure 16*) but had no clear impact on resistance rates (*Appendix 1—figure 15*).

Discussion

Antibiotics are essential medicines for the treatment and prevention of bacterial infections, but their use selects for the spread of pathogenic antibiotic-resistant bacteria (ARB), and can inadvertently disrupt the host microbiome and its associated immune function (*Buffie and Pamer, 2013*; *Chatterjee et al., 2018*; *Kim et al., 2017*). Within-host ecological interactions between co-colonizing bacteria can have important consequences for their colonization dynamics, which likely extend to influence the epidemiology of human pathogens in clinical settings. Yet microbiome ecology remains largely absent from the epidemiological modeling of antibiotic resistance (*Assab et al., 2017*; *Birkegård et al., 2018*; *Blanquart, 2019*; *Niewiadomska et al., 2019*), suggesting a need to better understand within-host competition between ARB and the host microbiome, its potential epidemiological consequences, and more broadly how antibiotics exert selection pressure on resistant bacteria (*Knight et al., 2019*). We present a modeling framework that includes within-host ecological costs of antibiotic use in the form of microbiome dysbiosis, incorporating a leading hypothesis for antibiotic selection into classical models of resistance epidemiology (*Austin et al., 1997*; *Lipsitch and Samore, 2002*). We formalize three examples of microbiome-pathogen competition potentially affected by dysbiosis, and show how they, either separately or in combination with other forces of selection, help explain how antibiotic use drives the spread of ARB in healthcare settings. We use probabilistic simulations to apply this framework across a panel of characteristic nosocomial pathogens and compare results to a traditional strain-based framework, demonstrating utility of a microbiome-oriented approach for modeling antibiotic resistance epidemiology and associated interventions.

MRSA, *C. difficile* and ESBL-producing Enterobacteriaceae are leading causes of antibiotic-resistant and healthcare-associated infection, while carbapenemase-producing Enterobacteriaceae represent emerging threats of particular concern due to limited therapeutic options for effective treatment of invasive infection (*Cassini et al., 2019*; *Jernigan et al., 2020*; *Miller et al., 2011*; *Rodríguez-Baño et al., 2018*). Antibiotic stewardship is a core component of public health efforts to limit the emergence and spread of these ARB in clinical settings (*Baur et al., 2017*), and an important focus of antibiotic resistance modeling (*Niewiadomska et al., 2019*). Different antibiotics vary in which organisms they intrinsically target, as well as pharmacodynamic factors like route of administration (e.g. oral vs. systemic), clearance mechanism (e.g. biliary vs. renal excretion) and site of absorption (e.g. small vs. large intestine). These differences affect the degree to which bacteria in different host niches are exposed to and cleared by different antibiotics, and are increasingly well described (*Bhalodi et al., 2019*; *Kim et al., 2017*; *Zhang et al., 2015*). Our findings suggest that asymmetric impacts of different antibiotics on competing commensal and pathogenic bacteria can drive antibiotic-driven selection for these high-risk ARB, with important consequences for resistance dynamics and stewardship efficacy.

Findings also suggest promise for interventions that effectively restore microbiome stability and associated colonization resistance as a means to control ARB spread. Fecal microbiota

transplantation is already used to treat recurrent *C. difficile* infection, and is under investigation for multidrug-resistant Enterobacteriaceae decolonization (*Davido et al., 2019a*; *Kassam et al., 2013*; *Saha et al., 2019*). However, its appropriateness for dysbiosis recovery in the absence of other clinical indications is unclear. Transplantation requires rigorous donor screening and close longitudinal follow-up, and cases of donor stool contaminated with toxicogenic and multidrug-resistant bacteria highlight non-negligible risks (*Gupta et al., 2021*; *Zellmer et al., 2021*). Alternative microbiome protective therapies now exist, like DAV132, a novel activated-charcoal product currently undergoing clinical trials. When co-administered with antibiotics by the oral route, DAV132 has been shown to absorb antibiotic residues in the colon and preserve the richness and composition of intestinal microbiota, while maintaining systemic antibiotic exposure (*de Gunzburg et al., 2018*; *de Gunzburg et al., 2015*; *Pinquier et al., 2021*). Modeling has been used previously to evaluate impacts of such microbiome-oriented interventions at the within-host level (*Guittar et al., 2021*; *Guk et al., 2021*), but knock-on impacts on ARB transmission dynamics and epidemiological burden are unknown. Our simulations were limited to a select few ARB, but our framework and findings likely have relevance for other bacteria known to interact with the microbiome, including vancomycin-resistant Enterococci and other multidrug-resistant Enterobacteriaceae (*Davido et al., 2019b*; *Stecher et al., 2013*). and could be further extended to explore impacts of the microbiome on resistance dynamics and intervention efficacy beyond healthcare settings.

Our simulations predicted colonization dynamics broadly consistent with previous findings from the literature. Input from the community was the main driver of hospital prevalence, and both prevalence and resistance rates tended to increase in the hospital relative to the community, as estimated in previous modeling studies (*Knight et al., 2018*; *MacFadden et al., 2019*). Findings reflected an important role for between-host nosocomial transmission for MRSA, as observed clinically (*Khader et al., 2019*; *Nadimpalli et al., 2020*), and a comparatively important role for endogenous acquisition for enteric ARB, as estimated elsewhere (*Bootsma et al., 2007*; *Gurieva et al., 2018*). Our estimates of intervention efficacy were more consistent with previous findings from the literature when microbiome interactions were taken into account. Contact precautions were effective for reducing incidence of MRSA and to a lesser extent *C. difficile*, but had limited impact against Enterobacteriaceae, consistent with clinical trials and modeling estimates. (*Khader et al., 2021*; *Luangasanatip et al., 2015*; *Maechler et al., 2020*). By contrast, simulated antibiotic stewardship interventions were broadly effective for reducing incidence across all included ARB. This is consistent with findings from a meta-analysis of clinical trials evaluating the efficacy of hospital antibiotic stewardship interventions for reducing incidence of ARB colonization and infection (*Baur et al., 2017*), which we updated to exclude studies co-implementing stewardship with alternative interventions (*Appendix 1—figure 18*). In comparison to our findings, estimates from the meta-analysis were associated with greater uncertainty across more heterogeneous interventions, but predicted the same rank order of efficacy across included ARB, and similar mean efficacy for *C. difficile* (19% from n=seven studies, vs. 18% under intermediate compliance in our simulations), ESBL-EC (18% from n=four studies, vs. 15%) and MRSA (12% from n=10 studies, vs. 10%), but higher efficacy for CP-KP (54% from n=one study, vs. 20%).

When excluding microbiome interactions, simulations predicted negligible efficacy of antibiotic stewardship interventions for controlling ARB incidence. Previous models have predicted efficacy using predominantly strain-based approaches, but often focus on resistance rates as the primary outcome, and in many cases assume that patient-to-patient transmission is the only route of colonization acquisition (*Niewiadomska et al., 2019*). Here, microbiome competition was found to have a large impact on incidence but comparatively little impact on resistance rates – both for the theoretical pathogen evaluated in Part 1 (*Figures 3* and *4*) and for the four ARB simulated in Part 2 (*Appendix 1—figures 12* and *14*) – underlying why stewardship interventions were of similar efficacy for reducing resistance rates across single-species and microbiome simulations (*Appendix 1—figure 15*). This reflects the importance of different forces of antibiotic selection for different epidemiological outcomes: while strain-based competition explains relative ecological dynamics of co-circulating strains, microbiome interactions may be better suited to explain how increasing antibiotic use favours ARB incidence, and how antibiotic stewardship and microbiome recovery interventions can help prevent colonization acquisition.

Under strain competition, pathogen colonization is limited by closely related strains sharing an ecological niche, with the same approximate epidemiological profile and transmission

characteristics. Competition against ARB is assumed to depend on the epidemic spread of competing strains, and removal of drug-sensitive strains releases antibiotic selection for resistance. By contrast, microbiome population structure is inherently stable, depending less on the epidemiological transmission of particular taxa, and more on host factors like diet, maternal inheritance, genetics, and antibiotic exposure (*Brito and Alm, 2016*). Despite great inter-individual diversity in microbiome composition, there is functional redundancy from one host to the next, such that colonization resistance and other forms of microbiome competition are shared across healthy hosts colonized with different taxa (*Bashan et al., 2016*; *Kim et al., 2017*). For these reasons, microbiome stability is modeled as a host trait reflecting the functional ecology of the microbiome in different population dynamic states, as opposed to a more traditional bacterial colonization process governed by rates of acquisition and clearance. This is clearly an oversimplification of real microbiome dynamics and complexity (*Hooks and O'Malley, 2017*), but is a useful approximation for the needs of epidemiological modeling, particularly in the absence of data, and reflects the universality of both human microbiome function and of the ecological impacts that antibiotics have on microbiome stability (*Bashan et al., 2016*).

Previous studies have modeled antibiotic exposure as a risk factor for ARB colonization, which can be interpreted as indirectly accounting for microbiome dysbiosis. In transmission models of *C. difficile*, ESBL-EC and *Pseudomonas aeruginosa*, among others, patients undergoing antibiotic therapy are assumed to be at greater risk of colonization and/or infection (*Gingras et al., 2016*; *Hurford et al., 2012*; *MacFadden et al., 2019*). An alternative approach has been to use antibiotic exposure as a coefficient on epidemiological parameters (e.g. transmission, endogenous acquisition), allowing ARB colonization rates to scale with antibiotic use (*Knight et al., 2018*). These strategies reflect widespread recognition that antibiotic use favours ARB acquisition, through erosion of colonization resistance or other supposed mechanisms, and independent of potential competition with other strains. The present work formalizes examples of the microbiome-pathogen interactions that underlie these assumptions, demonstrating their relevance to various epidemiological outcomes, distinguishing them from strain-based selection, and providing a framework for their application.

This study has a number of limitations. First, hospitals and healthcare settings are heterogeneous environments with non-random contact patterns and relatively small population sizes. Stochastic, individual-based models accounting for these factors reproduce more realistic nosocomial transmission dynamics than deterministic ODE simulations, allowing for local extinction events, super-spreaders, and other inherently random epidemiological phenomena. Nonetheless, our goal was to study how ecological mechanisms impact average epidemiological outcomes in the context of different model assumptions and parameter uncertainty, and in this context, ODE modeling was the more appropriate tool, particularly for widely endemic ARB like *C. difficile*, MRSA and ESBL-EC. Still, further insights could certainly be gained by accounting for additional complexity and stochastic heterogeneity in future work, from within-host spatial organization (*Estrela et al., 2015*), to patient and staff contact behavior (*Duval et al., 2019*), to inter-institutional or inter-ward meta-population dynamics (*Shapiro et al., 2020*). These distinctions may be particularly important for rare or non-endemic ARB (e.g. CP-KP in some regions). Second, our evaluation of strain competition was limited to exclusive colonization, a widely used approach (an estimated 12% of published strain competition models allow co-colonization or -infection) (*Niewiadomska et al., 2019*). Yet alternative models predict unique impacts on resistance dynamics (*Spicknall et al., 2013*), and explicit consideration of higher resolution within-host population dynamics has been shown to better reproduce empirical findings in previous work (*Davies et al., 2019*). Further, our exclusive colonization approach precluded assessment of intraspecific HGT, which may have different impacts on resistance dynamics than interspecific HGT.

Third, Monte Carlo simulations were limited by the availability of species-specific model parameters from the literature, in some instances necessitating use of previous modeling results, approximations, or estimates from small studies in specific locations, making the generalizability of results unclear. For instance, Khader et al. estimated a four-fold difference in MRSA transmission rates between hospitals and nursing homes (*Khader et al., 2019*). Such differences could have a substantial impact on dynamics and estimated intervention efficacy, with higher transmission rates favouring use of contact precautions, and higher rates of endogenous acquisition favouring antibiotic stewardship (in the context of a high ecological release coefficient). Uncertainty in endogenous acquisition rates may be particularly important: in multivariate sensitivity analyses, this parameter emerged as a

key driver of both colonization prevalence and resistance rates across ARB (*Appendix 1—figure 14*). Further, data used to estimate class-specific rates of microbiome dysbiosis are specific to the gut; class-specific data for dysbiosis of the skin, the preferred niche of *S. aureus*, were not available. This may over-estimate impacts of dysbiosis on MRSA colonization dynamics.

Finally, the nature of microbiome-pathogen interactions and their epidemiological consequences remain poorly understood and largely unquantified. We show in theory why these interactions matter at the population level, but empirical data were unavailable to inform their parameterization. Instead, we translated microbiome-pathogen competition coefficients into clinical parameters, designed a structured expert elicitation protocol, and conducted interviews allowing subject-matter experts to quantify their beliefs. Although these estimates are subject to substantial bias and uncertainty, they facilitated species-specific characterization of the epidemiological impact of microbiome dysbiosis, and represent useful proxy measures in the absence of clinical data. More broadly, our characterizations of microbiome-pathogen interactions are conceptual, and were mapped mechanistically to particular colonization processes (transmission, clearance, endogenous acquisition), but we note that in other contexts terms like *colonization resistance, resource competition* and *ecological release* may map to specific biochemical processes that could affect epidemiological parameters in different ways.

Despite data limitations, epidemiological conclusions from Monte Carlo simulations were largely consistent with empirical findings (discussed above), suggesting that final parameter distributions were reasonable approximations. Uncertainty in parameter inputs translated to uncertainty in model outputs, reflecting the knowledge gaps underlying our simulations (*Appendix 1—figure 14*). This is exemplified by HGT and its highly uncertain role in driving colonization incidence; to date, HGT modeling has largely been limited to within-host dynamics, and impacts on epidemiological dynamics are only just beginning to come to light (*Evans et al., 2020*; *Leclerc et al., 2019*; *Lerminiaux and Cameron, 2019*). Increasing availability and synthesis of high-quality within-host microbiological data will help to further characterize epidemiological impacts of microbiome-pathogen interactions. Studies are needed that describe ecological impacts of antibiotic exposure on microbiome population structure across control and treatment groups, with longitudinal follow-up evaluating subsequent nosocomial ARB colonization risk. In the absence of clinical data, insights from experiments and within-host models nonetheless suggest that antibiotic disruption of microbiome-pathogen competition is a key driver of selection for resistance (*Baumgartner et al., 2020*; *Estrela and Brown, 2018*; *O'Brien et al., 2021*; *Shaw et al., 2019*; *Stein et al., 2013*; *Tepekule et al., 2019*). The present work highlights the importance of extending these within-host concepts to the population level. Links between within- and between-host dynamics have been widely studied in various contexts, including the theory underlying the evolution of parasite life history and antimicrobial resistance (*Day et al., 2011*; *Greischar et al., 2019*; *zur Wiesch et al., 2011*), but remain largely absent from clinical models of antibiotic resistance (*Blanquart, 2019*). A clear extension of the present work is to explicitly account for simultaneous within- and between-host processes using nested models (*Birkegård et al., 2018*; *Niewiadomska et al., 2019*). However, such models do not necessarily provide more epidemiological clarity, especially when data are lacking and simple heuristic parameters can capture epidemiological consequences of within-host processes (*Gog et al., 2015*; *Mideo et al., 2008*).

In conclusion, we have proposed a mathematical modeling framework for the epidemiology of antibiotic-resistant bacteria that accounts for their potential interactions with the host microbiome. This model simplifies into accessible epidemiological parameters what are in reality highly complex ecological systems, comprising a staggering diversity of microbes and interactions among them. We demonstrate that accounting for at least some of this ecological complexity may help to explain how antibiotics select for the epidemiological spread of resistance, how antibiotic stewardship works to reduce pathogen colonization incidence, and how interventions favouring healthy microbiome function may help to mitigate the epidemiological burden of antibiotic resistance.

Materials and methods

Mathematical models of bacterial colonization

We evaluated ODE systems describing colonization dynamics of bacterial pathogens in the healthcare setting. The final model, comprising pathogen colonization (*Equation 1*), intraspecific strain competition (*Equation 3*), microbiome-pathogen competition (*Equation 4*), and horizontal gene transfer (HGT), is given alongside all assumptions in the supplementary appendix (Appendix *Equation A1*). ODEs were integrated numerically to calculate steady-state epidemiological outcomes for nosocomial P^R colonization: colonization prevalence (the sum of all compartments C^R), colonization incidence (the daily rate of C^R acquisition), and the resistance rate ($C^R/(C^S + C^R)$). (See Appendix 1 for technical details, and R and Mathematica files available online at https://github.com/drmsmith/microbiomeR [*Smith, 2021*; copy archived at swh:1:rev:a3682a24970d79e4-f748952ecc49fcdb16adf48f].) For each model, outcomes were evaluated over the same parameter space representing a generic pathogen P^R (parameters in *Appendix 1—table 1*), while varying specific parameters through univariate and bivariate analysis to assess their impacts on dynamic equilibria in the context of different modeling assumptions. We focused on impacts of the patient population's antibiotic exposure prevalence (a), rates of antibiotic-induced pathogen clearance (θ_c) and microbiome dysbiosis (θ_m), the focal pathogen's intrinsic antibiotic resistance level (r_R), and mediating impacts of microbiome-pathogen competition (ε, η, ϕ) and horizontal gene transfer (χ_e, χ_d).

Monte Carlo simulations over parameter distributions

We applied the final model to simulate epidemiological dynamics of four high-risk nosocomial pathogens, varying the within-host ecological interactions in effect for each (*Figure 5A*). For MRSA, ESBL-EC and CP-KP, the focal pathogen was taken as the 'drug-resistant' strain P^R, while the 'drug-sensitive' strain P^S was taken to represent all other co-circulating strains of the same species. We simulated colonization dynamics using these model characterizations and accounted for parameter uncertainty using Monte Carlo methods. Specifically, 10,000 unique parameter vectors Ω were created by drawing random values for each parameter from its respective probability distribution (parameters in *Appendix 1—table 2–6*). For each Ω, epidemiological outcomes (prevalence, incidence, resistance rate) were calculated as above. Final outcome distributions were reported as the median and 95% uncertainty interval, that is the 50th (2.5th–97.5th) percentiles across all simulations.

Parameterizing models for application to specific nosocomial pathogens

Models were parameterized using estimates from the literature, prioritizing clinical studies from the French hospital setting where available. We used expert elicitation to inform model structure and quantify parameter values for microbiome-pathogen interactions. This involved development of a protocol and questionnaire (provided separately), designed using established expert elicitation methodologies for quantitative estimation of unknown parameter values (*Johnson et al., 2010*). To facilitate more reliable parameter interpretation, microbiome-pathogen coefficients were translated into clinical parameters, for example relative risks of pathogen colonization among hospital patients undergoing dysbiosis relative to those with stable microbiota (*Appendix 1—table 7*). Expert estimates were quantified with uncertainty using the MATCH Uncertainty Elicitation Tool (*Morris et al., 2014*), and final parameter distributions were generated by pooling their individual distributions while maintaining estimated species rank order (*Appendix 1—figure 8–10*).

Characterizing ecological impacts of antibiotic consumption

Antibiotic exposure prevalence was quantified at the level of antibiotic class using nationally representative antibiotic consumption data from French hospitals in 2016 (*Agence nationale de sécurité du médicament et des produits de santé, 2017*). A study from American hospitals in 2006–2012 was used to further stratify antibiotics with ATC code J01F into J01FA and J01FF, J01X into J01XA and J01XD, and J01DD+DE into J01DD and J01DE (*Baggs et al., 2016*). Final antibiotic consumption data are presented in *Appendix 1—table 8*. To simulate class-specific rates of microbiome

dysbiosis, we used a four-point log-linear scale of intestinal microbiome disruption from *Brown et al., 2013*. For interpretation, we present classes as inducing dysbiosis at a high, medium, low, or very low rate. This scale was supplemented with data for additional antibiotic classes from *Baggs et al., 2018*. Applied to our model, the rate that antibiotic treatment induces dysbiosis (σ_m) is given by

$$\sigma_m = a \times \theta_m \times \sum_{k=0}^{3} \left(a_k \times e^{-k} \right) \tag{7}$$

where a_k is the proportion of antibiotics consumed of each group k, and where the most ecologically disruptive group (k=0) causes dysbiosis a mean 12 hr after antibiotic exposure (θ_m = 2 day^{-1}), with classes in less disruptive groups (k=1,2,3) causing dysbiosis at successively slower rates (*Figure 5C*).

To characterize class-specific effects on pathogen clearance, characteristic antibiograms for all strains were adapted from an online compendium from the Therapeutics Education Collaboration (*Figure 5D*; *McCormack and Lalji, 2015*). Each strain i was classified as sensitive ($r_{i,j} = 0$), of intermediate sensitivity ($0 < r_{i,j} < 1$), or resistant ($r_{i,j} = 1$) to each antibiotic class j. Overall, the rate that antibiotic treatment clears each strain is given by:

$$\sigma_i = a \times \theta_C \times \sum_{j=1}^{18} \left(a_j \times r_{i,j} \right) \tag{8}$$

across the included classes. Under these assumptions, MRSA was resistant to the greatest proportion of antibiotics consumed in hospital (median r_R = 94.5%), followed by *C. difficile* (94.3%), CP-KP (91.7%) and ESBL-EC (84.8%); competing 'drug-sensitive' strains bore considerably less resistance median r_S = 33.0% for MSSA and 23.0% for both *E. coli* and *K. pneumoniae*.

Sensitivity analyses

Two distinct sensitivity analyses were conducted. First, to evaluate the impact of microbiome competition on model outcomes, a second lot of 'single-species simulations' was run after removing microbiome-pathogen interactions from all Ω ($\varepsilon = 0$, $\eta = 0$, $\phi = 1$, $\chi = 0$). Second, the impact of parameter uncertainty on model outcomes was evaluated. For each pathogen, model parameter values were re-sampled from their distributions (*Appendix 1—table 2–6*) using Latin Hypercube Sampling over 10,000 iterations, epidemiological outcomes were re-calculated at population dynamic equilibrium, and partial rank correlation coefficients were calculated between each parameter and the pathogen's (i) colonization prevalence and (ii) resistance rate (using the R package *pse*) (*Chalom and Prado, 2013*; *Marino et al., 2008*).

Public health interventions

Three public health interventions were incorporated into the final model (see Appendix *Equations A12–A15*). First, contact precautions were assumed to represent physical or behavioral barriers that block opportunities for transmission, reducing transmission rates by the same fraction τ_{ipc} across all pathogens relative to baseline. Second, antibiotic stewardship programmes were assumed to alter antibiotic consumption patterns in the hospital. Two main types were considered: antibiotic reduction, which limits overall antibiotic prescribing by a fraction τ_{asp}, and antibiotic restriction, which adjusts the distribution of antibiotic classes consumed in the hospital by the same fraction. We considered two types of restriction, the first favouring classically narrow-spectrum antibiotics (e.g. macrolides) over broad-spectrum (e.g. quinolones), and the second favouring antibiotics that cause dysbiosis at very low or low rates (k={3,2}) over those causing dysbiosis at medium or high rates (k={1,0}) (see *Appendix 1—table 8* for antibiotic classification). Third, microbiome recovery therapy was assumed to trigger recovery at rate 0.5 day^{-1} and was apportioned to the fraction τ_{pbt} of patients. Overall, different values assumed for intervention parameters (τ_{ipc}, τ_{asp}, τ_{pbt}) are interpreted as different levels of compliance to the respective interventions. Intervention efficacy was evaluated using the IRR and RRR (defined in Model and Results). Outcomes were matched across Monte Carlo simulations, such that IRRs and RRRs were calculated for each intervention and compliance level for each Ω. The distribution of outcomes is expressed as the median and 95% uncertainty interval.

Acknowledgements

Additional information

Funding

Author contributions

David RM Smith, Conceptualization, Data curation, Formal analysis, Investigation, Visualization, Methodology, Writing - original draft, Writing - review and editing; Laura Temime, Lulla Opatowski, Conceptualization, Supervision, Funding acquisition, Writing - review and editing

Author ORCIDs

David RM Smith https://orcid.org/0000-0002-7330-4262
Laura Temime https://orcid.org/0000-0002-8850-5403

Decision letter and Author response

Decision letter https://doi.org/10.7554/eLife.68764.sa1
Author response https://doi.org/10.7554/eLife.68764.sa2

Additional files

Supplementary files

- Supplementary file 1. Expert elicitation protocol.
- Transparent reporting form

Data availability

Model equations and parameter values are provided in the manuscript, as well as in supporting R files and a Mathematica notebook available online at https://github.com/drmsmith/microbiomeR (copy archived at https://archive.softwareheritage.org/swh:1:rev:a3682a24970d79e4f748952ecc49fcdb16adf48f).

References

Abbara S, Cazanave C, Dubée V, D'humières C, Jauréguiberry S, Kernéis S, Lefort A, Lepeule R, Pilmis B, Nguyen LL. 2020. Classement pragmatique des antibiotiques en fonction de leur spectre et de leur impact écologique à des fins éducatives : résultats d'une enquête Delphi pour le jeu éducatif « Dawaa ». *Médecine Et Maladies Infectieuses* **50**:S60. DOI: https://doi.org/10.1016/j.medmal.2020.06.115

Agence nationale de sécurité du médicament et des produits de santé. 2017. *La Consommation D'antibiotiques en France en 2016 – Rapport De l'ANSM.* http://www.ordre.pharmacien.fr/Communications/Les-actualites/La-consommation-d-antibiotiques-en-France-en-2016-rapport-de-l-ANSM

Alfandari S, Robert J, Péan Y, Rabaud C, Bedos JP, Varon E, Lepape A, Bru JP, Gauzit R. 2015. Antibiotic use and good practice in 314 french hospitals: the 2010 SPA2 prevalence study. *Médecine Et Maladies Infectieuses* **45**:475–480. DOI: https://doi.org/10.1016/j.medmal.2015.10.001

Archambaud C, Derré-Bobillot A, Lapaque N, Rigottier-Gois L, Serror P. 2019. Intestinal translocation of enterococci requires a threshold level of enterococcal overgrowth in the lumen. *Scientific Reports* **9**:8926. DOI: https://doi.org/10.1038/s41598-019-45441-3, PMID: 31222056

Arda B, Sipahi OR, Yamazhan T, Tasbakan M, Pullukcu H, Tunger A, Buke C, Ulusoy S. 2007. Short-term effect of antibiotic control policy on the usage patterns and cost of antimicrobials, mortality, nosocomial infection rates and antibacterial resistance. *Journal of Infection* **55**:41–48. DOI: https://doi.org/10.1016/j.jinf.2007.02.014, PMID: 17512598

Assab R, Nekkab N, Crépey P, Astagneau P, Guillemot D, Opatowski L, Temime L. 2017. Mathematical models of infection transmission in healthcare settings: recent advances from the use of network structured data. *Current Opinion in Infectious Diseases* **30**:410–418. DOI: https://doi.org/10.1097/QCO.0000000000000390, PMID: 28570284

Austin DJ, Kakehashi M, Anderson RM. 1997. The transmission dynamics of antibiotic-resistant Bacteria: the relationship between resistance in commensal organisms and antibiotic consumption. *Proceedings of the Royal Society of London. Series B: Biological Sciences* **264**:1629–1638. DOI: https://doi.org/10.1098/rspb.1997.0227, PMID: 9404026

Bäckhed F, Ley RE, Sonnenburg JL, Peterson DA, Gordon JI. 2005. Host-bacterial mutualism in the human intestine. *Science* **307**:1915–1920. DOI: https://doi.org/10.1126/science.1104816, PMID: 15790844

Baggs J, Fridkin SK, Pollack LA, Srinivasan A, Jernigan JA. 2016. Estimating national trends in inpatient antibiotic use among US hospitals from 2006 to 2012. *JAMA Internal Medicine* **176**:1639–1648. DOI: https://doi.org/10.1001/jamainternmed.2016.5651, PMID: 27653796

Baggs J, Jernigan JA, Halpin AL, Epstein L, Hatfield KM, McDonald LC. 2018. Risk of subsequent Sepsis within 90 days after a hospital stay by type of antibiotic exposure. *Clinical Infectious Diseases* **66**:1004–1012. DOI: https://doi.org/10.1093/cid/cix947, PMID: 29136126

Bar-Yoseph H, Hussein K, Braun E, Paul M. 2016. Natural history and decolonization strategies for ESBL/carbapenem-resistant Enterobacteriaceae carriage: systematic review and meta-analysis. *Journal of Antimicrobial Chemotherapy* **71**:2729–2739. DOI: https://doi.org/10.1093/jac/dkw221, PMID: 27317444

Barbut F. 1996. Prevalence and pathogenicity of Clostridium difficile in hospitalized patients. *Archives of Internal Medicine* **156**:1449. DOI: https://doi.org/10.1001/archinte.1996.00440120107012

Bashan A, Gibson TE, Friedman J, Carey VJ, Weiss ST, Hohmann EL, Liu YY. 2016. Universality of human microbial dynamics. *Nature* **534**:259–262. DOI: https://doi.org/10.1038/nature18301, PMID: 27279224

Baumgartner M, Bayer F, Pfrunder-Cardozo KR, Buckling A, Hall AR. 2020. Resident microbial communities inhibit growth and antibiotic-resistance evolution of *Escherichia coli* in human gut microbiome samples. *PLOS Biology* **18**:e3000465. DOI: https://doi.org/10.1371/journal.pbio.3000465, PMID: 32310938

Bäumler AJ, Sperandio V. 2016. Interactions between the Microbiota and pathogenic Bacteria in the gut. *Nature* **535**:85–93. DOI: https://doi.org/10.1038/nature18849, PMID: 27383983

Baur D, Gladstone BP, Burkert F, Carrara E, Foschi F, Döbele S, Tacconelli E. 2017. Effect of antibiotic stewardship on the incidence of infection and colonisation with antibiotic-resistant Bacteria and Clostridium difficile infection: a systematic review and meta-analysis. *The Lancet Infectious Diseases* **17**:990–1001. DOI: https://doi.org/10.1016/S1473-3099(17)30325-0, PMID: 28629876

Bernier A, Delarocque-Astagneau E, Ligier C, Vibet M-A, Guillemot D, Watier L. 2014. Outpatient antibiotic use in France between 2000 and 2010: after the nationwide campaign, it is time to focus on the elderly. *Antimicrobial Agents and Chemotherapy* **58**:71–77. DOI: https://doi.org/10.1128/AAC.01813-13

Bhalodi AA, van Engelen TSR, Virk HS, Wiersinga WJ. 2019. Impact of antimicrobial therapy on the gut microbiome. *Journal of Antimicrobial Chemotherapy* **74**:i6–i15. DOI: https://doi.org/10.1093/jac/dky530, PMID: 30690540

Birkegård AC, Halasa T, Toft N, Folkesson A, Græsbøll K. 2018. Send more data: a systematic review of mathematical models of antimicrobial resistance. *Antimicrobial Resistance & Infection Control* **7**:117. DOI: https://doi.org/10.1186/s13756-018-0406-1, PMID: 30288257

Blanquart F, Lehtinen S, Lipsitch M, Fraser C. 2018. The evolution of antibiotic resistance in a structured host population. *Journal of the Royal Society Interface* **15**:20180040. DOI: https://doi.org/10.1098/rsif.2018.0040, PMID: 29925579

Blanquart F. 2019. Evolutionary epidemiology models to predict the dynamics of antibiotic resistance. *Evolutionary Applications* **12**:365–383. DOI: https://doi.org/10.1111/eva.12753, PMID: 30828361

Bootsma MC, Bonten MJ, Nijssen S, Fluit AC, Diekmann O. 2007. An algorithm to estimate the importance of bacterial acquisition routes in hospital settings. *American Journal of Epidemiology* **166**:841–851. DOI: https://doi.org/10.1093/aje/kwm149, PMID: 17644823

Borde JP, Litterst S, Ruhnke M, Feik R, Hübner J, deWith K, Kaier K, Kern WV. 2015. Implementing an intensified antibiotic stewardship programme targeting cephalosporin and fluoroquinolone use in a 200-bed community hospital in Germany. *Infection* **43**:45–50. DOI: https://doi.org/10.1007/s15010-014-0693-2, PMID: 25344419

Brito IL, Alm EJ. 2016. Tracking strains in the microbiome: insights from metagenomics and models. *Frontiers in Microbiology* **7**:712. DOI: https://doi.org/10.3389/fmicb.2016.00712, PMID: 27242733

Brown KA, Khanafer N, Daneman N, Fisman DN. 2013. Meta-Analysis of antibiotics and the risk of Community-Associated Clostridium difficile infection. *Antimicrobial Agents and Chemotherapy* **57**:2326–2332. DOI: https://doi.org/10.1128/AAC.02176-12

Buffie CG, Bucci V, Stein RR, McKenney PT, Ling L, Gobourne A, No D, Liu H, Kinnebrew M, Viale A, Littmann E, van den Brink MR, Jenq RR, Taur Y, Sander C, Cross JR, Toussaint NC, Xavier JB, Pamer EG. 2015. Precision microbiome reconstitution restores bile acid mediated resistance to Clostridium difficile. *Nature* **517**:205–208. DOI: https://doi.org/10.1038/nature13828, PMID: 25337874

Buffie CG, Pamer EG. 2013. Microbiota-mediated colonization resistance against intestinal pathogens. *Nature Reviews Immunology* **13**:790–801. DOI: https://doi.org/10.1038/nri3535, PMID: 24096337

Burdet C, Nguyen TT, Duval X, Ferreira S, Andremont A, Guedj J, Mentré F, the DAV132-CL-1002 Study Group. 2019. Impact of antibiotic gut exposure on the temporal changes in microbiome diversity. *Antimicrobial Agents and Chemotherapy* **63**:19. DOI: https://doi.org/10.1128/AAC.00820-19

Cassini A, Plachouras D, Eckmanns T, Abu Sin M, Blank HP, Ducomble T, Haller S, Harder T, Klingeberg A, Sixtensson M, Velasco E, Weiß B, Kramarz P, Monnet DL, Kretzschmar ME, Suetens C. 2016. Burden of six Healthcare-Associated infections on european population health: estimating Incidence-Based Disability-Adjusted life years through a population Prevalence-Based modelling study. *PLOS Medicine* **13**:e1002150. DOI: https://doi.org/10.1371/journal.pmed.1002150, PMID: 27755545

Cassini A, Högberg LD, Plachouras D, Quattrocchi A, Hoxha A, Simonsen GS, Colomb-Cotinat M, Kretzschmar ME, Devleesschauwer B, Cecchini M, Ouakrim DA, Oliveira TC, Struelens MJ, Suetens C, Monnet DL, Burden of AMR Collaborative Group. 2019. Attributable deaths and disability-adjusted life-years caused by infections with antibiotic-resistant Bacteria in the EU and the european economic area in 2015: a population-level modelling analysis. *The Lancet Infectious Diseases* **19**:56–66. DOI: https://doi.org/10.1016/S1473-3099(18)30605-4, PMID: 30409683

Chalom A, Prado P. 2013. *Pse: Parameter Space Exploration with Latin Hypercubes*. https://cran.r-project.org/web/packages/pse/pse.pdf

Chatterjee A, Modarai M, Naylor NR, Boyd SE, Atun R, Barlow J, Holmes AH, Johnson A, Robotham JV. 2018. Quantifying drivers of antibiotic resistance in humans: a systematic review. *The Lancet Infectious Diseases* **18**:e368–e378. DOI: https://doi.org/10.1016/S1473-3099(18)30296-2, PMID: 30172580

Chong Y, Shimoda S, Yakushiji H, Ito Y, Miyamoto T, Kamimura T, Shimono N, Akashi K. 2013. Antibiotic rotation for febrile neutropenic patients with hematological malignancies: clinical significance of antibiotic heterogeneity. *PLOS ONE* **8**:e54190. DOI: https://doi.org/10.1371/journal.pone.0054190, PMID: 23372683

Cobey S, Baskerville EB, Colijn C, Hanage W, Fraser C, Lipsitch M. 2017. Host population structure and treatment frequency maintain balancing selection on drug resistance. *Journal of the Royal Society Interface* **14**:20170295. DOI: https://doi.org/10.1098/rsif.2017.0295, PMID: 28835542

Coello R, Glynn JR, Gaspar C, Picazo JJ, Fereres J. 1997. Risk factors for developing clinical infection with methicillin-resistant *Staphylococcus aureus* (MRSA) amongst hospital patients initially only colonized with MRSA. *Journal of Hospital Infection* **37**:39–46. DOI: https://doi.org/10.1016/S0195-6701(97)90071-2, PMID: 9321727

Colijn C, Cohen T. 2015. How competition governs whether moderate or aggressive treatment minimizes antibiotic resistance. *eLife* **4**:e10559. DOI: https://doi.org/10.7554/eLife.10559, PMID: 26393685

Coyte KZ, Schluter J, Foster KR. 2015. The ecology of the microbiome: networks, competition, and stability. *Science* **350**:663–666. DOI: https://doi.org/10.1126/science.aad2602, PMID: 26542567

Cravo Oliveira Hashiguchi T, Ait Ouakrim D, Padget M, Cassini A, Cecchini M. 2019. Resistance proportions for eight priority antibiotic-bacterium combinations in OECD, EU/EEA and G20 countries 2000 to 2030: a modelling study. *Eurosurveillance* **24**:1800445. DOI: https://doi.org/10.2807/1560-7917.ES.2019.24.20.1800445

Davido B, Batista R, Dinh A, de Truchis P, Terveer EM, Roberts B, Kuijper EJ, Caballero S. 2019a. Fifty shades of graft: how to improve the efficacy of faecal Microbiota transplantation for decolonization of antibiotic-resistant Bacteria. *International Journal of Antimicrobial Agents* **53**:553–556. DOI: https://doi.org/10.1016/j.ijantimicag.2019.03.008, PMID: 30880228

Davido B, Batista R, Fessi H, Michelon H, Escaut L, Lawrence C, Denis M, Perronne C, Salomon J, Dinh A. 2019b. Fecal Microbiota transplantation to eradicate vancomycin-resistant enterococci colonization in case of an outbreak. *Médecine Et Maladies Infectieuses* **49**:214–218. DOI: https://doi.org/10.1016/j.medmal.2018.11.002

Davies NG, Flasche S, Jit M, Atkins KE. 2019. Within-host dynamics shape antibiotic resistance in commensal Bacteria. *Nature Ecology & Evolution* **3**:440–449. DOI: https://doi.org/10.1038/s41559-018-0786-x

Day T, Alizon S, Mideo N. 2011. Bridging scales in the evolution of infectious disease life histories: theory. *Evolution* **65**:3448–3461. DOI: https://doi.org/10.1111/j.1558-5646.2011.01394.x

de Gunzburg J, Ducher A, Modess C, Wegner D, Oswald S, Dressman J, Augustin V, Feger C, Andremont A, Weitschies W, Siegmund W. 2015. Targeted adsorption of molecules in the Colon with the novel adsorbent-

based medicinal product, DAV132: a proof of concept study in healthy subjects. *The Journal of Clinical Pharmacology* **55**:10–16. DOI: https://doi.org/10.1002/jcph.359, PMID: 25042595

de Gunzburg J, Ghozlane A, Ducher A, Le Chatelier E, Duval X, Ruppé E, Armand-Lefevre L, Sablier-Gallis F, Burdet C, Alavoine L, Chachaty E, Augustin V, Varastet M, Levenez F, Kennedy S, Pons N, Mentré F, Andremont A. 2018. Protection of the human gut microbiome from antibiotics. *The Journal of Infectious Diseases* **217**:628–636. DOI: https://doi.org/10.1093/infdis/jix604, PMID: 29186529

de Wit R, Bouvier T. 2006. 'Everything is everywhere, but, the environment selects'; what did Baas Becking and Beijerinck really say? *Environmental Microbiology* **8**:755–758. DOI: https://doi.org/10.1111/j.1462-2920.2006.01017.x, PMID: 16584487

Dethlefsen L, Relman DA. 2011. Incomplete recovery and individualized responses of the human distal gut Microbiota to repeated antibiotic perturbation. *PNAS* **108**:4554–4561. DOI: https://doi.org/10.1073/pnas.1000087107, PMID: 20847294

Di Ruscio F, Guzzetta G, Bjørnholt JV, Leegaard TM, Moen AEF, Merler S, Freiesleben de Blasio B. 2019. Quantifying the transmission dynamics of MRSA in the community and healthcare settings in a low-prevalence country. *PNAS* **116**:14599–14605. DOI: https://doi.org/10.1073/pnas.1900959116, PMID: 31262808

Doan T, Hinterwirth A, Worden L, Arzika AM, Maliki R, Abdou A, Kane S, Zhong L, Cummings SL, Sakar S, Chen C, Cook C, Lebas E, Chow ED, Nachamkin I, Porco TC, Keenan JD, Lietman TM. 2019. Gut microbiome alteration in MORDOR I: a community-randomized trial of mass azithromycin distribution. *Nature Medicine* **25**:1370–1376. DOI: https://doi.org/10.1038/s41591-019-0533-0, PMID: 31406349

Domenech de Cellès M, Opatowski L, Salomon J, Varon E, Carbon C, Boëlle P-Y, Guillemot D. 2011. Intrinsic epidemicity of Streptococcus pneumoniae depends on strain serotype and antibiotic susceptibility pattern. *Antimicrobial Agents and Chemotherapy* **55**:5255–5261. DOI: https://doi.org/10.1128/AAC.00249-11

Donker T, Henderson KL, Hopkins KL, Dodgson AR, Thomas S, Crook DW, Peto TEA, Johnson AP, Woodford N, Walker AS, Robotham JV. 2017. The relative importance of large problems far away versus small problems closer to home: insights into limiting the spread of antimicrobial resistance in England. *BMC Medicine* **15**:86. DOI: https://doi.org/10.1186/s12916-017-0844-2, PMID: 28446169

Dubrovskaya Y, Papadopoulos J, Scipione MR, Altshuler J, Phillips M, Mehta SA. 2012. Antibiotic stewardship for intra-abdominal infections: early impact on antimicrobial use and patient outcomes. *Infection Control & Hospital Epidemiology* **33**:427–429. DOI: https://doi.org/10.1086/664765, PMID: 22418644

Durham DP, Olsen MA, Dubberke ER, Galvani AP, Townsend JP. 2016. Quantifying Transmission of *Clostridium difficile* within and outside Healthcare Settings . *Emerging Infectious Diseases* **22**:608–616. DOI: https://doi.org/10.3201/eid2204.150455

Duval A, Obadia T, Boëlle PY, Fleury E, Herrmann JL, Guillemot D, Temime L, Opatowski L, i-Bird Study group. 2019. Close proximity interactions support transmission of ESBL-K. pneumoniae but not ESBL-*E. coli* in healthcare settings. *PLOS Computational Biology* **15**:e1006496. DOI: https://doi.org/10.1371/journal.pcbi.1006496, PMID: 31145725

Ebrahimi F, Mózes J, Monostori J, Górácz O, Fésűs A, Majoros L, Szarka K, Kardos G. 2016. Comparison of rates of fecal colonization with extended-spectrum beta-lactamase-producing enterobacteria among patients in different wards, outpatients and medical students. *Microbiology and Immunology* **60**:285–294. DOI: https://doi.org/10.1111/1348-0421.12373, PMID: 26959958

Estrela S, Whiteley M, Brown SP. 2015. The demographic determinants of human microbiome health. *Trends in Microbiology* **23**:134–141. DOI: https://doi.org/10.1016/j.tim.2014.11.005, PMID: 25500524

Estrela S, Brown SP. 2018. Community interactions and spatial structure shape selection on antibiotic resistant lineages. *PLOS Computational Biology* **14**:e1006179. DOI: https://doi.org/10.1371/journal.pcbi.1006179, PMID: 29927925

Evans DR, Griffith MP, Sundermann AJ, Shutt KA, Saul MI, Mustapha MM, Marsh JW, Cooper VS, Harrison LH, Van Tyne D. 2020. Systematic detection of horizontal gene transfer across genera among multidrug-resistant Bacteria in a single hospital. *eLife* **9**:e53886. DOI: https://doi.org/10.7554/eLife.53886, PMID: 32285801

Frank MO, Batteiger BE, Sorensen SJ, Hartstein AI, Carr JA, McComb JS, Clark CD, Abel SR, Mikuta JM, Jones RB. 1997. Decrease in expenditures and selected nosocomial infections following implementation of an antimicrobial-prescribing improvement program. *Clinical Performance and Quality Health Care* **5**:180–188. PMID: 10176026

Friedman ND, Temkin E, Carmeli Y. 2016. The negative impact of antibiotic resistance. *Clinical Microbiology and Infection* **22**:416–422. DOI: https://doi.org/10.1016/j.cmi.2015.12.002, PMID: 26706614

Gingras G, Guertin MH, Laprise JF, Drolet M, Brisson M. 2016. Mathematical modeling of the transmission dynamics of Clostridium difficile infection and colonization in healthcare settings: a systematic review. *PLOS ONE* **11**:e0163880. DOI: https://doi.org/10.1371/journal.pone.0163880, PMID: 27690247

Gog JR, Pellis L, Wood JL, McLean AR, Arinaminpathy N, Lloyd-Smith JO. 2015. Seven challenges in modeling pathogen dynamics within-host and across scales. *Epidemics* **10**:45–48. DOI: https://doi.org/10.1016/j.epidem.2014.09.009, PMID: 25843382

Greischar MA, Beck-Johnson LM, Mideo N. 2019. Partitioning the influence of ecology across scales on parasite evolution. *Evolution* **73**:2175–2188. DOI: https://doi.org/10.1111/evo.13840

Grohs P, Kernéis S, Sabatier B, Lavollay M, Carbonnelle E, Rostane H, Souty C, Meyer G, Gutmann L, Mainardi JL. 2014. Fighting the spread of AmpC-hyperproducing Enterobacteriaceae: beneficial effect of replacing ceftriaxone with cefotaxime. *Journal of Antimicrobial Chemotherapy* **69**:786–789. DOI: https://doi.org/10.1093/jac/dkt403, PMID: 24159154

Guittar J, Koffel T, Shade A, Klausmeier CA, Litchman E. 2021. Resource competition and host feedbacks underlie regime shifts in gut Microbiota. *The American Naturalist* **198**:1–12. DOI: https://doi.org/10.1086/714527, PMID: 34143726

Guk J, Guedj J, Burdet C, Andremont A, de Gunzburg J, Ducher A, Mentré F. 2021. Modeling the effect of DAV132, a novel Colon-Targeted adsorbent, on fecal concentrations of moxifloxacin and gut Microbiota diversity in healthy volunteers. *Clinical Pharmacology & Therapeutics* **109**:1045–1054. DOI: https://doi.org/10.1002/cpt.1977, PMID: 32617960

Gupta S, Mullish BH, Allegretti JR. 2021. Fecal Microbiota transplantation: the evolving risk landscape. *American Journal of Gastroenterology* **116**:647–656. DOI: https://doi.org/10.14309/ajg.0000000000001075, PMID: 33982930

Gurieva T, Dautzenberg MJD, Gniadkowski M, Derde LPG, Bonten MJM, Bootsma MCJ. 2018. The transmissibility of Antibiotic-Resistant Enterobacteriaceae in intensive care units. *Clinical Infectious Diseases* **66**:489–493. DOI: https://doi.org/10.1093/cid/cix825, PMID: 29020273

Heesterbeek H, Anderson RM, Andreasen V, Bansal S, De Angelis D, Dye C, Eames KT, Edmunds WJ, Frost SD, Funk S, Hollingsworth TD, House T, Isham V, Klepac P, Lessler J, Lloyd-Smith JO, Metcalf CJ, Mollison D, Pellis L, Pulliam JR, et al. 2015. Modeling infectious disease dynamics in the complex landscape of global health. *Science* **347**:aaa4339. DOI: https://doi.org/10.1126/science.aaa4339, PMID: 25766240

Hooks KB, O'Malley MA. 2017. Dysbiosis and its discontents. *mBio* **8**:17. DOI: https://doi.org/10.1128/mBio.01492-17

Hooper LV, Stappenbeck TS, Hong CV, Gordon JI. 2003. Angiogenins: a new class of microbicidal proteins involved in innate immunity. *Nature Immunology* **4**:269–273. DOI: https://doi.org/10.1038/ni888, PMID: 12548285

Hurford A, Morris AM, Fisman DN, Wu J. 2012. Linking antimicrobial prescribing to antimicrobial resistance in the ICU: before and after an antimicrobial stewardship program. *Epidemics* **4**:203–210. DOI: https://doi.org/10.1016/j.epidem.2012.12.001, PMID: 23351372

Jernigan JA, Hatfield KM, Wolford H, Nelson RE, Olubajo B, Reddy SC, McCarthy N, Paul P, McDonald LC, Kallen A, Fiore A, Craig M, Baggs J. 2020. Multidrug-Resistant bacterial infections in U.S. hospitalized patients, 2012-2017. *New England Journal of Medicine* **382**:1309–1319. DOI: https://doi.org/10.1056/NEJMoa1914433, PMID: 32242356

Johnson SR, Tomlinson GA, Hawker GA, Granton JT, Grosbein HA, Feldman BM. 2010. A valid and reliable belief elicitation method for bayesian priors. *Journal of Clinical Epidemiology* **63**:370–383. DOI: https://doi.org/10.1016/j.jclinepi.2009.08.005, PMID: 19926253

Kamada N, Chen GY, Inohara N, Núñez G. 2013a. Control of pathogens and pathobionts by the gut Microbiota. *Nature Immunology* **14**:685–690. DOI: https://doi.org/10.1038/ni.2608, PMID: 23778796

Kamada N, Seo SU, Chen GY, Núñez G. 2013b. Role of the gut Microbiota in immunity and inflammatory disease. *Nature Reviews Immunology* **13**:321–335. DOI: https://doi.org/10.1038/nri3430, PMID: 23618829

Kardaś-Słoma L, Boëlle PY, Opatowski L, Brun-Buisson C, Guillemot D, Temime L. 2011. Impact of antibiotic exposure patterns on selection of Community-Associated Methicillin-Resistant *Staphylococcus aureus* in hospital settings. *Antimicrobial Agents and Chemotherapy* **55**:4888–4895. DOI: https://doi.org/10.1128/AAC.01626-10

Kassam Z, Lee CH, Yuan Y, Hunt RH. 2013. Fecal Microbiota transplantation for Clostridium difficile infection: systematic review and meta-analysis. *American Journal of Gastroenterology* **108**:500–508. DOI: https://doi.org/10.1038/ajg.2013.59, PMID: 23511459

Khader K, Thomas A, Jones M, Toth D, Stevens V, Samore MH, CDC Modeling Infectious Diseases in Healthcare Program (MInD-Healthcare). 2019. Variation and trends in transmission dynamics of Methicillin-resistant *Staphylococcus aureus* in veterans affairs hospitals and nursing homes. *Epidemics* **28**:100347. DOI: https://doi.org/10.1016/j.epidem.2019.100347, PMID: 31171468

Khader K, Thomas A, Stevens V, Visnovsky L, Nevers M, Toth D, Keegan LT, Jones M, Rubin M, Samore MH. 2021. Association between contact precautions and transmission of Methicillin-Resistant *Staphylococcus aureus* in veterans affairs hospitals. *JAMA Network Open* **4**:e210971. DOI: https://doi.org/10.1001/jamanetworkopen.2021.0971, PMID: 33720369

Kim S, Covington A, Pamer EG. 2017. The intestinal Microbiota: antibiotics, colonization resistance, and enteric pathogens. *Immunological Reviews* **279**:90–105. DOI: https://doi.org/10.1111/imr.12563, PMID: 28856737

Knight GM, Costelloe C, Deeny SR, Moore LSP, Hopkins S, Johnson AP, Robotham JV, Holmes AH. 2018. Quantifying where human acquisition of antibiotic resistance occurs: a mathematical modelling study. *BMC Medicine* **16**:137. DOI: https://doi.org/10.1186/s12916-018-1121-8, PMID: 30134939

Knight GM, Davies NG, Colijn C, Coll F, Donker T, Gifford DR, Glover RE, Jit M, Klemm E, Lehtinen S, Lindsay JA, Lipsitch M, Llewelyn MJ, Mateus ALP, Robotham JV, Sharland M, Stekel D, Yakob L, Atkins KE. 2019. Mathematical modelling for antibiotic resistance control policy: do we know enough? *BMC Infectious Diseases* **19**:1011. DOI: https://doi.org/10.1186/s12879-019-4630-y, PMID: 31783803

Kouyos R, Klein E, Grenfell B. 2013. Hospital-community interactions foster coexistence between methicillin-resistant strains of *Staphylococcus aureus*. *PLOS Pathogens* **9**:e1003134. DOI: https://doi.org/10.1371/journal.ppat.1003134, PMID: 23468619

Laurent F, Lelièvre H, Cornu M, Vandenesch F, Carret G, Etienne J, Flandrois JP. 2001. Fitness and competitive growth advantage of new gentamicin-susceptible MRSA clones spreading in french hospitals. *Journal of Antimicrobial Chemotherapy* **47**:277–283. DOI: https://doi.org/10.1093/jac/47.3.277, PMID: 11222560

Leclerc QJ, Lindsay JA, Knight GM. 2019. Mathematical modelling to study the horizontal transfer of antimicrobial resistance genes in Bacteria: current state of the field and recommendations. *Journal of the Royal Society Interface* **16**:20190260. DOI: https://doi.org/10.1098/rsif.2019.0260, PMID: 31409239

Lehtinen S, Blanquart F, Croucher NJ, Turner P, Lipsitch M, Fraser C. 2017. Evolution of antibiotic resistance is linked to any genetic mechanism affecting bacterial duration of carriage. *PNAS* **114**:1075–1080. DOI: https://doi.org/10.1073/pnas.1617849114, PMID: 28096340

Lerminiaux NA, Cameron ADS. 2019. Horizontal transfer of antibiotic resistance genes in clinical environments. *Canadian Journal of Microbiology* **65**:34–44. DOI: https://doi.org/10.1139/cjm-2018-0275, PMID: 30248271

Letten AD, Baumgartner M, Pfrunder-Cardozo KR, Levine JM, Hall AR. 2021. Human-associated Microbiota suppress invading Bacteria even under disruption by antibiotics. *The ISME Journal* **15**:2809–2812. DOI: https://doi.org/10.1038/s41396-021-00929-7, PMID: 33712700

Leung V, Gill S, Sauve J, Walker K, Stumpo C, Powis J. 2011. Growing a "positive culture" of antimicrobial stewardship in a community hospital. *The Canadian Journal of Hospital Pharmacy* **64**:314–320. DOI: https://doi.org/10.4212/cjhp.v64i5.1065, PMID: 22479082

Lipsitch M, Samore MH. 2002. Antimicrobial use and antimicrobial resistance: a population perspective. *Emerging Infectious Diseases* **8**:347–354. DOI: https://doi.org/10.3201/eid0804.010312

Lozupone CA, Stombaugh JI, Gordon JI, Jansson JK, Knight R. 2012. Diversity, stability and resilience of the human gut Microbiota. *Nature* **489**:220–230. DOI: https://doi.org/10.1038/nature11550, PMID: 22972295

Luangasanatip N, Hongsuwan M, Limmathurotsakul D, Lubell Y, Lee AS, Harbarth S, Day NP, Graves N, Cooper BS. 2015. Comparative efficacy of interventions to promote hand hygiene in hospital: systematic review and network meta-analysis. *BMJ* **351**:h3728. DOI: https://doi.org/10.1136/bmj.h3728, PMID: 26220070

Lübbert C, Schumacher U, Stareprawo S, Claus J, Heeß-Erler G, Fiebig C, de With K, Wilhelms D, Kekulé AS, Klöss T, Moritz S, University Hospital Halle (Saale). 2014. Can the antibiotic prescription practice in a hospital be influenced by in-house guidelines? an interventional study at the university hospital halle Germany. *Deutsche Medizinische Wochenschrift* **139**:2578–2584. DOI: https://doi.org/10.1055/s-0034-1387220, PMID: 25271804

Lynch SV, Pedersen O. 2016. The human intestinal microbiome in health and disease. *New England Journal of Medicine* **375**:2369–2379. DOI: https://doi.org/10.1056/NEJMra1600266, PMID: 27974040

MacFadden DR, Fisman DN, Hanage WP, Lipsitch M. 2019. The relative impact of community and hospital antibiotic use on the selection of Extended-spectrum Beta-lactamase-producing *Escherichia coli*. *Clinical Infectious Diseases* **69**:182–188. DOI: https://doi.org/10.1093/cid/ciy978, PMID: 30462185

Mach R, Vlcek J, Prusova M, Batka P, Rysavy V, Kubena A. 2007. Impact of a multidisciplinary approach on antibiotic consumption, cost and microbial resistance in a czech hospital. *Pharmacy World & Science* **29**:565–572. DOI: https://doi.org/10.1007/s11096-006-9059-x, PMID: 17610145

Maechler F, Schwab F, Hansen S, Fankhauser C, Harbarth S, Huttner BD, Diaz-Agero C, Lopez N, Canton R, Ruiz-Garbajosa P, Blok H, Bonten MJ, Kloosterman F, Schotsman J, Cooper BS, Behnke M, Golembus J, Kola A, Gastmeier P, R-GNOSIS WP5 study group. 2020. Contact isolation versus standard precautions to decrease acquisition of extended-spectrum β-lactamase-producing enterobacterales in non-critical care wards: a cluster-randomised crossover trial. *The Lancet Infectious Diseases* **20**:575–584. DOI: https://doi.org/10.1016/S1473-3099(19)30626-7, PMID: 32087113

Malani AN, Richards PG, Kapila S, Otto MH, Czerwinski J, Singal B. 2013. Clinical and economic outcomes from a community hospital's antimicrobial stewardship program. *American Journal of Infection Control* **41**:145–148. DOI: https://doi.org/10.1016/j.ajic.2012.02.021, PMID: 22579261

Marino S, Hogue IB, Ray CJ, Kirschner DE. 2008. A methodology for performing global uncertainty and sensitivity analysis in systems biology. *Journal of Theoretical Biology* **254**:178–196. DOI: https://doi.org/10.1016/j.jtbi.2008.04.011, PMID: 18572196

Marra AR, de Almeida SM, Correa L, Silva M, Martino MD, Silva CV, Cal RG, Edmond MB, dos Santos OF. 2009. The effect of limiting antimicrobial therapy duration on antimicrobial resistance in the critical care setting. *American Journal of Infection Control* **37**:204–209. DOI: https://doi.org/10.1016/j.ajic.2008.06.008, PMID: 18986735

McCormack J, Lalji F. 2015. *Antibiotic Sensitivity Chart*. http://therapeuticseducation.org/sites/therapeuticseducation.org/files/Antibiotic_Sensitivity_December_2015.pdf

Melnyk AH, Wong A, Kassen R. 2015. The fitness costs of antibiotic resistance mutations. *Evolutionary Applications* **8**:273–283. DOI: https://doi.org/10.1111/eva.12196, PMID: 25861385

Meyer E, Schwab F, Pollitt A, Bettolo W, Schroeren-Boersch B, Trautmann M. 2010. Impact of a change in antibiotic prophylaxis on total antibiotic use in a surgical intensive care unit. *Infection* **38**:19–24. DOI: https://doi.org/10.1007/s15010-009-9115-2, PMID: 19904488

Mideo N, Alizon S, Day T. 2008. Linking within- and between-host dynamics in the evolutionary epidemiology of infectious diseases. *Trends in Ecology & Evolution* **23**:511–517. DOI: https://doi.org/10.1016/j.tree.2008.05.009

Miller BA, Chen LF, Sexton DJ, Anderson DJ. 2011. Comparison of the Burdens of Hospital-Onset, Healthcare Facility-Associated *Clostridium difficile* Infection and of Healthcare-Associated Infection due to Methicillin-Resistant *Staphylococcus aureus* in Community Hospitals. *Infection Control & Hospital Epidemiology* **32**:387–390. DOI: https://doi.org/10.1086/659156

Miyawaki K, Miwa Y, Tomono K, Kurokawa N. 2010. Impact of antimicrobial stewardship by infection control team in a japanese teaching hospital. *Yakugaku Zasshi* **130**:1105–1111. DOI: https://doi.org/10.1248/yakushi.130.1105, PMID: 20686215

Morris DE, Oakley JE, Crowe JA. 2014. A web-based tool for eliciting probability distributions from experts. *Environmental Modelling & Software* **52**:1–4. DOI: https://doi.org/10.1016/j.envsoft.2013.10.010

Mulberry N, Rutherford A, Colijn C. 2020. Systematic comparison of coexistence in models of drug-sensitive and drug-resistant pathogen strains. *Theoretical Population Biology* **133**:150–158. DOI: https://doi.org/10.1016/j.tpb.2019.12.001, PMID: 31887315

Nadimpalli G, O'Hara LM, Pineles L, Lebherz K, Johnson JK, Calfee DP, Miller LG, Morgan DJ, Harris AD. 2020. Patient to healthcare personnel transmission of MRSA in the non-intensive care unit setting. *Infection Control & Hospital Epidemiology* **41**:601–603. DOI: https://doi.org/10.1017/ice.2020.10, PMID: 32036800

Naylor NR, Atun R, Zhu N, Kulasabanathan K, Silva S, Chatterjee A, Knight GM, Robotham JV. 2018. Estimating the burden of antimicrobial resistance: a systematic literature review. *Antimicrobial Resistance & Infection Control* **7**:58. DOI: https://doi.org/10.1186/s13756-018-0336-y, PMID: 29713465

Niewiadomska AM, Jayabalasingham B, Seidman JC, Willem L, Grenfell B, Spiro D, Viboud C. 2019. Population-level mathematical modeling of antimicrobial resistance: a systematic review. *BMC Medicine* **17**:81. DOI: https://doi.org/10.1186/s12916-019-1314-9, PMID: 31014341

Opatowski L, Guillemot D, Boëlle PY, Temime L. 2011. Contribution of mathematical modeling to the fight against bacterial antibiotic resistance. *Current Opinion in Infectious Diseases* **24**:279–287. DOI: https://doi.org/10.1097/QCO.0b013e3283462362, PMID: 21467930

O'Brien S, Baumgartner M, Hall AR. 2021. Species interactions drive the spread of ampicillin resistance in human-associated gut Microbiota. *Evolution, Medicine, and Public Health* **9**:256–266. DOI: https://doi.org/10.1093/emph/eoab020

Pamer EG. 2016. Resurrecting the intestinal Microbiota to combat antibiotic-resistant pathogens. *Science* **352**:535–538. DOI: https://doi.org/10.1126/science.aad9382, PMID: 27126035

Pantel A, Marchandin H, Prère MF, Boutet-Dubois A, Brieu-Roche N, Gaschet A, Davin-Regli A, Sotto A, Lavigne JP. 2015. Faecal carriage of carbapenemase-producing Gram-negative bacilli in hospital settings in southern france. *European Journal of Clinical Microbiology & Infectious Diseases* **34**:899–904. DOI: https://doi.org/10.1007/s10096-014-2298-1, PMID: 25532506

Peto Z, Benko R, Matuz M, Csullog E, Molnar A, Hajdu E. 2008. Results of a local antibiotic management program on antibiotic use in a tertiary intensive care unit in Hungary. *Infection* **36**:560–564. DOI: https://doi.org/10.1007/s15010-008-7377-8, PMID: 19011742

Pilmis B, Cattoir V, Lecointe D, Limelette A, Grall I, Mizrahi A, Marcade G, Poilane I, Guillard T, Bourgeois Nicolaos N, Zahar JR, Le Monnier A. 2018. Carriage of ESBL-producing Enterobacteriaceae in French hospitals: the PORTABLSE study. *Journal of Hospital Infection* **98**:247–252. DOI: https://doi.org/10.1016/j.jhin.2017.11.022, PMID: 29222035

Pilmis B, Le Monnier A, Zahar JR. 2020. Gut Microbiota, antibiotic therapy and antimicrobial resistance: a narrative review. *Microorganisms* **8**:269. DOI: https://doi.org/10.3390/microorganisms8020269, PMID: 32079318

Pinquier JL, Varastet M, Meyers D, Sayah-Jeanne S, Féger C, Gaumétou O, Corbel T, de Gunzburg J, Mentré F, Ducher A. 2021. A Colon-Targeted adsorbent (DAV132) does not affect the pharmacokinetics of warfarin or clonazepam in healthy subjects. *Clinical Pharmacology in Drug Development* **10**:908–917. DOI: https://doi.org/10.1002/cpdd.901, PMID: 33434399

Prescott HC, Dickson RP, Rogers MA, Langa KM, Iwashyna TJ. 2015. Hospitalization type and subsequent severe sepsis. *American Journal of Respiratory and Critical Care Medicine* **192**:581–588. DOI: https://doi.org/10.1164/rccm.201503-0483OC, PMID: 26016947

Pressley J, D'Agata EM, Webb GF. 2010. The effect of co-colonization with community-acquired and hospital-acquired methicillin-resistant *Staphylococcus aureus* strains on competitive exclusion. *Journal of Theoretical Biology* **264**:645–656. DOI: https://doi.org/10.1016/j.jtbi.2010.03.036, PMID: 20347850

Rafii F, Sutherland JB, Cerniglia CE. 2008. Effects of treatment with antimicrobial agents on the human colonic microflora. *Therapeutics and Clinical Risk Management* **4**:1343–1358. DOI: https://doi.org/10.2147/tcrm.s4328, PMID: 19337440

Ramsay DE, Invik J, Checkley SL, Gow SP, Osgood ND, Waldner CL. 2018. Application of dynamic modelling techniques to the problem of antibacterial use and resistance: a scoping review. *Epidemiology and Infection* **146**:2014–2027. DOI: https://doi.org/10.1017/S0950268818002091, PMID: 30062979

Ravi A, Halstead FD, Bamford A, Casey A, Thomson NM, van Schaik W, Snelson C, Goulden R, Foster-Nyarko E, Savva GM, Whitehouse T, Pallen MJ, Oppenheim BA. 2019. Loss of microbial diversity and pathogen domination of the gut Microbiota in critically ill patients. *Microbial Genomics* **5**:000293. DOI: https://doi.org/10.1099/mgen.0.000293

Relman DA, Lipsitch M. 2018. Microbiome as a tool and a target in the effort to address antimicrobial resistance. *PNAS* **115**:12902–12910. DOI: https://doi.org/10.1073/pnas.1717163115, PMID: 30559176

Rodríguez-Baño J, Gutiérrez-Gutiérrez B, Machuca I, Pascual A. 2018. Treatment of infections caused by Extended-Spectrum-Beta-Lactamase-, AmpC-, and Carbapenemase-Producing Enterobacteriaceae. *Clinical Microbiology Reviews* **31**:17. DOI: https://doi.org/10.1128/CMR.00079-17

Round JL, Mazmanian SK. 2009. The gut Microbiota shapes intestinal immune responses during health and disease. *Nature Reviews Immunology* **9**:313–323. DOI: https://doi.org/10.1038/nri2515, PMID: 19343057

Roy S, Trinchieri G. 2017. Microbiota: a key orchestrator of Cancer therapy. *Nature Reviews Cancer* **17**:271–285. DOI: https://doi.org/10.1038/nrc.2017.13, PMID: 28303904

Ruppé E, Ghozlane A, Tap J, Pons N, Alvarez AS, Maziers N, Cuesta T, Hernando-Amado S, Clares I, Martínez JL, Coque TM, Baquero F, Lanza VF, Máiz L, Goulenok T, de Lastours V, Amor N, Fantin B, Wieder I,

Andremont A, et al. 2019. Prediction of the intestinal resistome by a three-dimensional structure-based method. *Nature Microbiology* **4**:112–123. DOI: https://doi.org/10.1038/s41564-018-0292-6, PMID: 30478291

Saha S, Tariq R, Tosh PK, Pardi DS, Khanna S. 2019. Faecal Microbiota transplantation for eradicating carriage of multidrug-resistant organisms: a systematic review. *Clinical Microbiology and Infection* **25**:958–963. DOI: https://doi.org/10.1016/j.cmi.2019.04.006, PMID: 30986562

Scanvic A, Denic L, Gaillon S, Giry P, Andremont A, Lucet JC. 2001. Duration of colonization by methicillin-resistant *Staphylococcus aureus* after hospital discharge and risk factors for prolonged carriage. *Clinical Infectious Diseases* **32**:1393–1398. DOI: https://doi.org/10.1086/320151, PMID: 11317238

Schön T, Sandelin LL, Bonnedahl J, Hedebäck F, Wistedt A, Brudin L, Jarnheimer PÅ. 2011. A comparative study of three methods to evaluate an intervention to improve empirical antibiotic therapy for acute bacterial infections in hospitalized patients. *Scandinavian Journal of Infectious Diseases* **43**:251–257. DOI: https://doi.org/10.3109/00365548.2010.544326, PMID: 21171827

Shapiro JT, Leboucher G, Myard-Dury AF, Girardo P, Luzzati A, Mary M, Sauzon JF, Lafay B, Dauwalder O, Laurent F, Lina G, Chidiac C, Couray-Targe S, Vandenesch F, Flandrois JP, Rasigade JP. 2020. Metapopulation ecology links antibiotic resistance, consumption, and patient transfers in a network of hospital wards. *eLife* **9**: e54795. DOI: https://doi.org/10.7554/eLife.54795, PMID: 33106223

Shaw LP, Bassam H, Barnes CP, Walker AS, Klein N, Balloux F. 2019. Modelling microbiome recovery after antibiotics using a stability landscape framework. *The ISME Journal* **13**:1845–1856. DOI: https://doi.org/10.1038/s41396-019-0392-1, PMID: 30877283

Shenoy ES, Paras ML, Noubary F, Walensky RP, Hooper DC. 2014. Natural history of colonization with methicillin-resistant *Staphylococcus aureus* (MRSA) and vancomycin-resistant Enterococcus (VRE): a systematic review. *BMC Infectious Diseases* **14**:177. DOI: https://doi.org/10.1186/1471-2334-14-177, PMID: 24678646

Simor AE, Yake SL, Tsimidis K. 1993. Infection due to Clostridium difficile among elderly residents of a long-term-care facility. *Clinical Infectious Diseases* **17**:672–678. DOI: https://doi.org/10.1093/clinids/17.4.672, PMID: 7903557

Smith RL, Evans HL, Chong TW, McElearney ST, Hedrick TL, Swenson BR, Scheld WM, Pruett TL, Sawyer RG. 2008. Reduction in rates of methicillin-resistant *Staphylococcus aureus* infection after introduction of quarterly linezolid-vancomycin cycling in a surgical intensive care unit. *Surgical Infections* **9**:423–431. DOI: https://doi.org/10.1089/sur.2007.024, PMID: 18759679

Smith DRM. 2021. microbiomeR. *Software Heritage*. swh:1:rev:a3682a24970d79e4f748952ecc49fcdb16adf48f. https://archive.softwareheritage.org/swh:1:dir:b9466325c11d19e7bc3962c2c4b913dd88d701b8;origin=https://github.com/drmsmith/microbiomeR;visit=swh:1:snp:111f1edd0d2dbcdc7509e028d86125d72f7d7650;anchor=swh:1:rev:a3682a24970d79e4f748952ecc49fcdb16adf48f

Sorbara MT, Pamer EG. 2019. Interbacterial mechanisms of colonization resistance and the strategies pathogens use to overcome them. *Mucosal Immunology* **12**:1–9. DOI: https://doi.org/10.1038/s41385-018-0053-0, PMID: 29988120

Spicknall IH, Foxman B, Marrs CF, Eisenberg JN. 2013. A modeling framework for the evolution and spread of antibiotic resistance: literature review and model categorization. *American Journal of Epidemiology* **178**:508–520. DOI: https://doi.org/10.1093/aje/kwt017, PMID: 23660797

Stecher B, Maier L, Hardt WD. 2013. 'Blooming' in the gut: how dysbiosis might contribute to pathogen evolution. *Nature Reviews Microbiology* **11**:277–284. DOI: https://doi.org/10.1038/nrmicro2989, PMID: 23474681

Stein RR, Bucci V, Toussaint NC, Buffie CG, Rätsch G, Pamer EG, Sander C, Xavier JB. 2013. Ecological modeling from time-series inference: insight into dynamics and stability of intestinal Microbiota. *PLOS Computational Biology* **9**:e1003388. DOI: https://doi.org/10.1371/journal.pcbi.1003388, PMID: 24348232

Takesue Y, Nakajima K, Ichiki K, Ishihara M, Wada Y, Takahashi Y, Tsuchida T, Ikeuchi H. 2010. Impact of a hospital-wide programme of heterogeneous antibiotic use on the development of antibiotic-resistant Gram-negative Bacteria. *Journal of Hospital Infection* **75**:28–32. DOI: https://doi.org/10.1016/j.jhin.2009.11.022, PMID: 20346536

Tan C, Vermeulen M, Wang X, Zvonar R, Garber G, Daneman N. 2017. Variability in antibiotic use across Ontario acute care hospitals. *Journal of Antimicrobial Chemotherapy* **72**:554–563. DOI: https://doi.org/10.1093/jac/dkw454, PMID: 27856724

Tedijanto C, Olesen SW, Grad YH, Lipsitch M. 2018. Estimating the proportion of bystander selection for antibiotic resistance among potentially pathogenic bacterial flora. *PNAS* **115**:E11988–E11995. DOI: https://doi.org/10.1073/pnas.1810840115, PMID: 30559213

Tepekule B, Uecker H, Derungs I, Frenoy A, Bonhoeffer S. 2017. Modeling antibiotic treatment in hospitals: a systematic approach shows benefits of combination therapy over cycling, mixing, and mono-drug therapies. *PLOS Computational Biology* **13**:e1005745. DOI: https://doi.org/10.1371/journal.pcbi.1005745, PMID: 28915236

Tepekule B, Abel Zur Wiesch P, Kouyos RD, Bonhoeffer S. 2019. Quantifying the impact of treatment history on plasmid-mediated resistance evolution in human gut Microbiota. *PNAS* **116**:23106–23116. DOI: https://doi.org/10.1073/pnas.1912188116, PMID: 31666328

Touat M, Opatowski M, Brun-Buisson C, Cosker K, Guillemot D, Salomon J, Tuppin P, de Lagasnerie G, Watier L. 2019. A payer perspective of the hospital inpatient additional care costs of antimicrobial resistance in France: a matched Case-Control study. *Applied Health Economics and Health Policy* **17**:381–389. DOI: https://doi.org/10.1007/s40258-018-0451-1, PMID: 30506456

van Bunnik BAD, Woolhouse MEJ. 2017. Modelling the impact of curtailing antibiotic usage in food animals on antibiotic resistance in humans. *Royal Society Open Science* **4**:161067. DOI: https://doi.org/10.1098/rsos.161067, PMID: 28484624

van den Driessche P. 2017. Reproduction numbers of infectious disease models. *Infectious Disease Modelling* **2**: 288–303. DOI: https://doi.org/10.1016/j.idm.2017.06.002, PMID: 29928743

van Kleef E, Robotham JV, Jit M, Deeny SR, Edmunds WJ. 2013. Modelling the transmission of healthcare associated infections: a systematic review. *BMC Infectious Diseases* **13**:294. DOI: https://doi.org/10.1186/1471-2334-13-294, PMID: 23809195

van Kleef E, Deeny SR, Jit M, Cookson B, Goldenberg SD, Edmunds WJ, Robotham JV. 2016. The projected effectiveness of Clostridium difficile vaccination as part of an integrated infection control strategy. *Vaccine* **34**: 5562–5570. DOI: https://doi.org/10.1016/j.vaccine.2016.09.046, PMID: 27727031

Vidal-Navarro L, Pfeiffer C, Bouziges N, Sotto A, Lavigne JP. 2010. Faecal carriage of multidrug-resistant Gram-negative bacilli during a non-outbreak situation in a french university hospital. *Journal of Antimicrobial Chemotherapy* **65**:2455–2458. DOI: https://doi.org/10.1093/jac/dkq333, PMID: 20813808

Yeo CL, Chan DS, Earnest A, Wu TS, Yeoh SF, Lim R, Jureen R, Fisher D, Hsu LY. 2012. Prospective audit and feedback on antibiotic prescription in an adult hematology-oncology unit in Singapore. *European Journal of Clinical Microbiology & Infectious Diseases* **31**:583–590. DOI: https://doi.org/10.1007/s10096-011-1351-6, PMID: 21845470

Zellmer C, Sater MRA, Huntley MH, Osman M, Olesen SW, Ramakrishna B. 2021. Shiga Toxin-Producing *Escherichia coli* transmission via fecal Microbiota transplant. *Clinical Infectious Diseases : An Official Publication of the Infectious Diseases Society of America* **72**:e876–e880. DOI: https://doi.org/10.1093/cid/ciaa1486, PMID: 33159210

Zhang M, Jiang Z, Li D, Jiang D, Wu Y, Ren H, Peng H, Lai Y. 2015. Oral antibiotic treatment induces skin Microbiota dysbiosis and influences wound healing. *Microbial Ecology* **69**:415–421. DOI: https://doi.org/10.1007/s00248-014-0504-4, PMID: 25301498

Zou YM, Ma Y, Liu JH, Shi J, Fan T, Shan YY, Yao HP, Dong YL. 2015. Trends and correlation of antibacterial usage and bacterial resistance: time series analysis for antibacterial stewardship in a chinese teaching hospital (2009-2013). *European Journal of Clinical Microbiology & Infectious Diseases* **34**:795–803. DOI: https://doi.org/10.1007/s10096-014-2293-6, PMID: 25487131

zur Wiesch PA, Kouyos R, Engelstädter J, Regoes RR, Bonhoeffer S. 2011. Population biological principles of drug-resistance evolution in infectious diseases. *The Lancet Infectious Diseases* **11**:236–247. DOI: https://doi.org/10.1016/S1473-3099(10)70264-4, PMID: 21371657

Appendix 1

Model and assumptions
ODEs

The final ODE system, which incorporates horizontal gene transfer (HGT) of a transmissible resistance gene R into the mixed microbiome-strain competition model (*Equation 6* in the main text), is given by:

$$
\begin{aligned}
\frac{dS_{e,s}}{dt} &= -S_{e,s} \times \left(\lambda_{S,\varepsilon} + \lambda_{R,\varepsilon} + \alpha_S + \alpha_R + \sigma_m\right) + S_{d,s} \times \delta + C_{e,s}^S \times \left(\gamma_S + \sigma_S\right) \\
&\quad + C_{e,s}^R \times \left(\gamma_R + \sigma_R\right) + \Delta_{S_{e,s}} \\
\frac{dS_{e,r}}{dt} &= -S_{e,r} \times \left(\lambda_{S,\varepsilon} + \lambda_{R,\varepsilon} + \alpha_S + \alpha_R + \sigma_m\right) + S_{d,r} \times \delta + C_{e,r}^S \times \left(\gamma_S + \sigma_S\right) \\
&\quad + C_{e,r}^R \times \left(\gamma_R + \sigma_R\right) + \Delta_{S_{e,r}} \\
\frac{dS_{d,s}}{dt} &= S_{e,s} \times \left((1-\omega) \times \sigma_m\right) - S_{d,s} \times \left(\lambda_S + \lambda_R + \alpha_{S,\phi} + \alpha_{R,\phi} + \delta\right) + C_{d,s}^S \times \left(\gamma_{S,\eta} + \sigma_S\right) + \\
&\quad C_{d,s}^R \times \left(\gamma_{R,\eta} + \sigma_R\right) + \Delta_{S_{d,s}} \\
\frac{dS_{d,r}}{dt} &= S_{e,s} \times \left(\omega \times \sigma_m\right) + S_{e,r} \times \sigma_m - S_{d,r} \times \left(\lambda_S + \lambda_R + \alpha_{S,\phi} + \alpha_{R,\phi} + \delta\right) + C_{d,r}^S \times \left(\gamma_{S,\eta} + \sigma_S\right) \\
&\quad + C_{d,r}^R \times \left(\gamma_{R,\eta} + \sigma_R\right) + \Delta_{S_{d,r}} \\
\frac{dC_{e,s}^S}{dt} &= S_{e,s} \times \left(\lambda_{S,\varepsilon} + \alpha_S\right) - C_{e,s}^S \times \left(\gamma_S + \sigma_S + \sigma_m\right) + C_{d,s}^S \times \delta + \Delta_{C_{e,s}^S} \\
\frac{dC_{e,r}^S}{dt} &= S_{e,r} \times \left(\lambda_{S,\varepsilon} + \alpha_S\right) - C_{e,r}^S \times \left(\gamma_S + \sigma_S + \sigma_m + \chi_e\right) + C_{d,r}^S \times \delta + \Delta_{C_{e,r}^S} \\
\frac{dC_{d,s}^S}{dt} &= S_{d,s} \times \left(\lambda_S + \alpha_{S,\phi}\right) + C_{e,s}^S \times \left((1-\omega) \times \sigma_m\right) - C_{d,s}^S \times \left(\gamma_{S,\eta} + \sigma_S + \delta\right) + \Delta_{C_{d,s}^S} \\
\frac{dC_{d,r}^S}{dt} &= S_{d,r} \times \left(\lambda_S + \alpha_{S,\phi}\right) + C_{e,s}^S \times \left(\omega \times \sigma_m\right) + C_{e,r}^S \times \sigma_m - C_{d,r}^S \times \left(\gamma_{S,\eta} + \sigma_S + \delta + \chi_d\right) + \Delta_{C_{d,r}^S} \\
\frac{dC_{e,s}^R}{dt} &= S_{e,s} \times \left(\lambda_{R,\varepsilon} + \alpha_R\right) - C_{e,s}^R \times \left(\gamma_R + \sigma_R + \sigma_m + \chi_e\right) + C_{d,s}^R \times \delta + \Delta_{C_{e,s}^R} \\
\frac{dC_{e,r}^R}{dt} &= S_{e,r} \times \left(\lambda_{R,\varepsilon} + \alpha_R\right) + C_{e,r}^S \times \chi_e + C_{e,s}^R \times \chi_e - C_{e,r}^R \times \left(\gamma_R + \sigma_R + \sigma_m\right) + C_{d,r}^R \times \delta + \Delta_{C_{e,r}^R} \\
\frac{dC_{d,s}^R}{dt} &= S_{d,s} \times \left(\lambda_R + \alpha_{R,\phi}\right) + C_{e,s}^R \times \left((1-\omega) \times \sigma_m\right) - C_{d,s}^R \times \left(\gamma_{R,\eta} + \sigma_R + \delta + \chi_d\right) + \Delta_{C_{d,s}^R} \\
\frac{dC_{d,r}^R}{dt} &= S_{d,r} \times \left(\lambda_R + \alpha_{R,\phi}\right) + C_{d,r}^S \times \chi_d + C_{e,s}^R \times \left(\omega \times \sigma_m\right) + C_{e,r}^R \times \sigma_m + C_{d,s}^R \times \chi_d - \\
&\quad C_{d,r}^R \times \left(\gamma_{R,\eta} + \sigma_R + \delta\right) + \Delta_{C_{d,r}^R}
\end{aligned}
$$

(A1)

This system of equations describes epidemiological colonization dynamics of a bacterial pathogen among host classes $H_{j,k}$, corresponding to patients of pathogen colonization status H (S, C^S, C^R), microbiome status j (e, equilibrium; or d, dysbiosis) and microbiome resistance profile k (s, not bearing R; r, bearing R). Equations can be found in an R file and Mathematica notebook available online (https://github.com/drmsmith/microbiomeR), and modeling assumptions are listed below.

Patient demography

We assume constant population size (N=1), balanced by a daily rate of hospital admission and discharge μ. The number of patients in each compartment is expressed as proportions of the total population. The proportion of patients entering each compartment j is given by admission fractions f_j. These are interpreted as representing prevalence of different host types in the community, which are assumed to be stable over time and unaffected by hospital dynamics. For simplicity, demography is expressed as Δ_j for each class j, which expand to:

$$\Delta_{S_{e,s}} = \mu \times \left((1-f_C) \times (1-f_d) \times (1-f_\omega) - S_{e,s}\right)$$
$$\Delta_{S_{e,r}} = \mu \times \left((1-f_C) \times (1-f_d) \times f_\omega - S_{e,r}\right)$$
$$\Delta_{S_{d,s}} = \mu \times \left((1-f_C) \times f_d \times (1-f_\omega) - S_{d,s}\right)$$
$$\Delta_{S_{d,r}} = \mu \times \left((1-f_C) \times f_d \times f_\omega - S_{d,r}\right)$$
$$\Delta_{C_{e,s}^S} = \mu \times \left(f_C \times (1-f_R) \times (1-f_d) \times (1-f_\omega) - C_{e,s}^S\right)$$
$$\Delta_{C_{e,r}^S} = \mu \times \left(f_C \times (1-f_R) \times (1-f_d) \times f_\omega - C_{e,r}^S\right)$$
$$\Delta_{C_{d,s}^S} = \mu \times \left(f_C \times (1-f_R) \times f_d \times (1-f_\omega) - C_{d,s}^S\right) \quad \text{(A2)}$$
$$\Delta_{C_{d,r}^S} = \mu \times \left(f_C \times (1-f_R) \times f_d \times f_\omega - C_{d,r}^S\right)$$
$$\Delta_{C_{e,s}^R} = \mu \times \left(f_C \times f_R \times (1-f_d) \times (1-f_\omega) - C_{e,s}^R\right)$$
$$\Delta_{C_{e,r}^R} = \mu \times \left(f_C \times f_R \times (1-f_d) \times f_\omega - C_{e,r}^R\right)$$
$$\Delta_{C_{d,s}^R} = \mu \times \left(f_C \times f_R \times f_d \times (1-f_\omega) - C_{d,s}^R\right)$$
$$\Delta_{C_{d,r}^R} = \mu \times \left(f_C \times f_R \times f_d \times f_\omega - C_{e,s}^R\right)$$

where f_C is the proportion of patients colonized with the pathogen upon admission, f_R is the proportion of colonized patients bearing the focal resistant strain (i.e. the community resistance rate), f_d is the proportion of patients undergoing dysbiosis upon hospital admission, and f_ω is the proportion of admitted patients with microbiota bearing R.

Pathogen epidemiology

Pathogen colonization can be acquired through dynamic patient-to-patient *transmission* via the dynamic force of infection λ, which is defined as the product of the pathogen's intrinsic transmission rate (β) and the prevalence of patients colonized at a particular time *t*. For each strain P^j, with *j* in {S, R}, this is given by

$$\lambda_j = \frac{\beta \times \left(C_{e,s}^j + C_{e,r}^j + C_{d,s}^j + C_{d,r}^j\right)}{N} \quad \text{(A3)}$$

In hospital environments, pathogen colonization incidence also results from *endogenous acquisition* (α). This subsumes alternative routes of acquisition not resulting from direct patient-to-patient transmission, and can include processes like translocation and within-host outgrowth of a subdominant/non-detectable/non-transmissible colony (into a dominant/detectable/transmissible colony) (*Archambaud et al., 2019*; *Bootsma et al., 2007*; *Duval et al., 2019*; *Gurieva et al., 2018*). This reflects the tenet that 'everything is everywhere, but the environment selects' (*de Wit and Bouvier, 2006*). We assume that pathogen colonization is not acquired endogenously among patients undergoing antibiotic treatment capable of clearing that pathogen, such that for each strain P^j,

$$\alpha_j = \alpha' \times \left(1 - \mathrm{a} \times (1 - r_j)\right) \quad \text{(A4)}$$

where α′ is the baseline rate in untreated patients. For the hospital simulation study (below), available literature estimates for endogenous acquisition rates were not strain-specific. These were generated by scaling species-specific rates by the baseline prevalence of each strain in the community, or

$$\alpha_S = \alpha' \times \left(1 - \mathrm{a} \times (1 - r_S)\right) \times (1 - f_R)$$
$$\alpha_R = \alpha' \times \left(1 - \mathrm{a} \times (1 - r_R)\right) \times f_R \quad \text{(A5)}$$

Pathogen colonization is naturally cleared by the host at rate γ. To reflect potential metabolic costs associated with bearing antibiotic resistance genes (*Melnyk et al., 2015*), we assumed that C^R

(colonization with the resistant strain) is naturally cleared at a faster rate than C^S (colonization with the sensitive strain), such that $\gamma_S < \gamma_R$. This is given by

$$\gamma_R = \gamma_S \times (1 + c) \tag{A6}$$

where c is interpreted as the fitness cost of bearing R.

Antibiotic resistance

Pathogen colonization is cleared by antibiotics according to strain-specific rates of effective antibiotic treatment, given by

$$\begin{aligned} \sigma_S &= a \times (1 - r_S) \times \theta_C \\ \sigma_R &= a \times (1 - r_R) \times \theta_C \end{aligned} \tag{A7}$$

Antibiotic exposure prevalence a is applied independently of colonization status to reflect high estimated rates of bystander selection for ARB, which predominantly colonize patients asymptomatically, are rarely detected and only opportunistically cause disease (*Tedijanto et al., 2018*). Among patients exposed to effective antibiotic therapy, pathogen colonization is cleared at a constant rate θ_C. The proportion of antibiotics that are ineffective is given by the antibiotic resistance level r_j, which is a proportion reflecting the pathogen's innate resistance to the antibiotics to which it is exposed, ranging from complete antibiotic sensitivity ($r_j = 0$) to complete resistance ($r_j = 1$), For model application, effective antibiotic treatment is considered at the level of antibiotic class, with rates for each class varying across strains and species (see main text *Equation 8*).

Microbiome dynamics

Patient microbiota are considered in terms of their population dynamic stability, and are assumed either to be at stable equilibrium or undergoing temporary dysbiosis (population dynamic disequilibrium). Microbiome stability is disrupted via antibiotic treatment according to

$$\sigma_m = a \times \theta_m \tag{A8}$$

For model application, rates of antibiotic-induced microbiome dysbiosis are also considered at the level of antibiotic class (see main text *Equation 7*). Microbiome stability recovers at rate δ, but only among patients not actively undergoing antibiotic treatment, such that

$$\delta = \delta' \times (1 - a) \tag{A9}$$

where δ' is the baseline rate in untreated hosts. Further, during model application we assume that microbiota can still recover among patients exposed to aminoglycosides and tetracyclines, the antibiotic classes inducing microbiome dysbiosis at the lowest rate (k=3, see Materials and methods), such that

$$\delta = \delta' \times (1 - a \times (1 - a_{k=3})) \tag{A10}$$

Microbiome-pathogen competition

We assume that the host microbiome and the focal pathogen compete ecologically within the host, such that host microbiota limit pathogen transmission, persistence and endogenous acquisition. We propose three examples of microbiome-pathogen competition – colonization resistance (ε), resource competition (η), and ecological release (ϕ) – and conceptualize how they affect pathogen colonization processes, and by extension how microbiome dysbiosis predisposes patients to pathogen colonization (see *Figure 2* in the main text). Interactions are given by

$$\begin{aligned} \beta_\varepsilon &= (1 - \varepsilon) \times \beta \\ \gamma_\eta &= (1 - \eta) \times \gamma \\ \alpha_\phi &= \phi \times \alpha \end{aligned} \tag{1}$$

where, respectively, ε reduces the transmission rate to patients with stable microbiota, η reduces the clearance rate among patients undergoing dysbiosis, and ϕ favours endogenous acquisition among patients undergoing dysbiosis. We assume that microbiome-pathogen interactions are species- and not strain-specific, that is that ε, η and ϕ apply equally to P^S and P^R.

Horizontal gene transfer

HGT is conceptualized as two-way within-host transfer of the focal resistance gene R, either from an R-bearing pathogen strain P^R to co-colonizing microbiota, or from R-bearing microbiota to a co-colonizing drug-sensitive pathogen strain P^S. For simplicity, we assumed (i) a symmetric rate of HGT (χ) from each donor, (ii) no loss of resistance upon donation, (iii) no accumulation of resistance (e.g. plasmid copy number dependence), (iv) that all patients bear microbiota capable of receiving and transferring R, (v) that dysbiosis can accelerate the rate of transfer ($\chi_d \geq \chi_e$), (vi) no impact of R on rates of microbiome dysbiosis and recovery, (vii) that a proportion f_ω of patients are admitted to hospital with microbiota bearing R, and lastly (viii) that microbiota of a proportion ω of patients can spontaneously acquire R subsequent to dysbiosis. The latter assumption was made to reflect increased expression of antibiotic resistance genes among host microbiota following antibiotic therapy, and can be interpreted as a corollary to endogenous pathogen acquisition (*Ruppé et al., 2019*).

Public health interventions

Three public health interventions τ were incorporated into Appendix *Equation A1* for subsequent model application. First, contact precautions were assumed to represent physical or behavioral barriers that block opportunities for transmission, reducing transmission rates by the same fraction τ_{ipc} across all pathogens relative to baseline. This is given by

$$\beta_{ipc} = \left(1 - \tau_{ipc}\right) \times \beta \tag{A12}$$

Second, antibiotic stewardship programmes were assumed to alter antibiotic consumption patterns in the hospital. Two main types were considered: antibiotic reduction, which limits overall antibiotic prescribing by a fraction τ_{asp}, given by

$$a_{asp} = \left(1 - \tau_{asp}\right) \times a \tag{A13}$$

and antibiotic restriction, which adjusts the distribution of antibiotic classes consumed in the hospital. We considered two types of restriction, the first favouring classically narrow-spectrum antibiotics (e.g. macrolides) over broad-spectrum (e.g. quinolones), and the second favouring antibiotics that cause dysbiosis at very low or low rates (k={3,2}) over those causing dysbiosis at medium or high rates (k={1,0}). For both, the proportion of antibiotics in the restricted group ($p_{restrict}$) was reduced by the same fraction τ_{asp} without adjusting the distribution of antibiotics consumed within that group, given by

$$p_{restrict|asp} = p_{restrict} - \tau_{asp} \tag{A14}$$

and the proportion of non-restricted antibiotics was increased symmetrically. With this structure, τ_{asp} alters antibiotic consumption for the same proportion of hospital patients across all three stewardship interventions. In all simulations, $p_{restrict} > \tau_{asp}$.

Third, microbiome recovery therapy was assumed to trigger recovery at rate 0.5 day^{-1} and was apportioned to the fraction τ_{pbt} of patients, such that the overall rate of microbiome recovery when including these interventions (δ_{pbt}) is given by

$$\delta_{pbt} = \delta + 0.5 \times \tau_{pbt} \tag{A15}$$

For simplicity, different values assumed for intervention parameters (τ_{ipc}, τ_{asp}, τ_{pbt}) are interpreted as different levels of compliance to the respective interventions.

Part 1: Model evaluation and parameterization

R_0 expressions

R_0 was calculated for P^R across **Equations 1, 3, 4 and 6** from the main text (see Mathematica notebook), and was interpreted as the expected number of secondary patients colonized by an index patient in a fully susceptible (uncolonized) hospital population (i.e. at *disease-free equilibrium*, DFE, as indicated by the equilibrium symbol ˆ above state variables). To reflect this epidemiological context, we made two additional assumptions specifically for R_0 calculations: no C^R input from the community ($f_R=0$), and that the rate of endogenous acquisition α_R scales linearly with current colonization prevalence C^R. R_0 expressions were derived following **van den Driessche, 2017**.

For the susceptible-colonized model,

$$R_0 = \hat{S}\frac{\beta + \alpha_R}{\gamma_R + \sigma_R + \mu} \tag{A16}$$

where $\hat{S} = 1$, such that pathogens with higher rates of transmission (β) and endogenous acquisition (α_R) have higher R_0, while those with higher rates of natural clearance (γ_R) have lower R_0. Higher rates of effective antibiotic treatment (σ_R) and patient admission and discharge (μ) also reduce R_0.

For the strain competition model, we derive R_0 for P^R assuming that P^S is at endemic equilibrium with input from the community ($f_C > 0$, $f_R = 0$). In this context, the same R_0 expression was found as for the susceptible-colonized model (Appendix *Equation A16*), except R_0 is reduced because of a lower equilibrium prevalence of susceptible hosts when P^S is endemic ($\hat{S}<1$). DFE were not found analytically for models with strain competition and were solved numerically (details below).

For the microbiome model, R_0 was calculated using next-generation theory as the spectral radius of the next-generation matrix (NGM),

$$R_0 = \rho(\mathbf{NGM}) \tag{A17}$$

where NGM is the product of the transmission matrix **F** (describing the rates at which existing colonies cause colonization in new hosts) and the inverse transition matrix **V** (describing the rates at which colonized hosts shift between colonized classes or are removed). These are given by

$$\mathbf{F} = \begin{pmatrix} (\alpha_R + (1-\varepsilon) \times \beta) \times \hat{S}_e & (\alpha_R + (1-\varepsilon) \times \beta) \times \hat{S}_e \\ (\alpha_R \times \phi + \beta) \times \hat{S}_d & (\alpha_R \times \phi + \beta) \times \hat{S}_d \end{pmatrix} \tag{A18}$$

and

$$\mathbf{V} = \begin{pmatrix} \gamma_R + \sigma_R + \sigma_m + \mu & -\delta \\ -\sigma_m & \delta + (1-\eta) \times \gamma_R + \sigma_R + \mu \end{pmatrix} \tag{A19}$$

which give

$$R_0 = \frac{\hat{S}_e \times (\alpha_R + (1-\varepsilon) \times \beta)(\delta + (1-\eta) \times \gamma_R + \sigma_m + \sigma_R + \mu) + \hat{S}_d \times (\alpha_R \times \phi + \beta)(\delta + \gamma_R + \sigma_m + \sigma_R + \mu)}{(\sigma_R + \mu)(\delta + \sigma_m + \sigma_R + \mu) + (\delta + \sigma_R + \mu + (1-\eta) \times (\sigma_m + \sigma_R + \mu)) \times \gamma_R + (1-\eta) \times \gamma_R^2} \tag{A20}$$

where the two terms in the numerator correspond to pathogen acquisition, respectively, in hosts with a stable microbiome and in those undergoing dysbiosis. Antibiotic-induced dysbiosis (σ_m) and treatment (σ_R) are found in both numerator and denominator.

When assuming no microbiome-pathogen interactions ($\varepsilon = 0$, $\eta = 0$, $\phi = 1$), DFE is

$$\{\hat{S}_e, \hat{S}_d, \hat{C}_e, \hat{C}_d\} = \left\{ \frac{\mu \times (1-f_d) + \delta}{\sigma_m + \mu + \delta}, \frac{\mu \times f_d + \sigma_m}{\sigma_m + \mu + \delta}, 0, 0 \right\} \tag{A21}$$

and R_0 reduces to the same expression as given by the susceptible-colonized model

$$R_0 = \frac{\beta + \alpha_R}{\gamma_R + \sigma_R + \mu} \tag{A22}$$

With two strains, as in the microbiome-strain competition model, the same R_0 expression is found for P^R as the single-strain model, but when P^S is endemic,

$$\hat{S}_e + \hat{S}_d < 1 \tag{A23}$$

so strain competition dampens R_0 relative to the single-strain microbiome competition model. R_0 expressions are evaluated numerically in *Figure 1* and *Appendix 1—figure 2* and *3*.

Epidemiological outcomes
Colonization prevalence

Colonization prevalence was defined as the proportion of hospital patients colonized (C^R) by the focal drug-resistant strain (P^R) at endemic equilibrium:

$$C^R = \hat{C}_{e,s}^R + \hat{C}_{e,r}^R + \hat{C}_{d,s}^R + \hat{C}_{d,r}^R \tag{A24}$$

Colonization prevalence of the drug-sensitive strain P^S was also calculated:

$$C^S = \hat{C}_{e,s}^S + \hat{C}_{e,r}^S + \hat{C}_{d,s}^S + \hat{C}_{d,r}^S \tag{A25}$$

These were found by substituting a corresponding vector of numerical parameter values Ω and solving ODE systems through numerical integration. Solutions were found using the lsoda method of the function *ode* from the package *deSolve* in R (version 3.6.0). For evaluation of the theoretical pathogen (part 1), solutions were corroborated using the function NSolve in Mathematica.

Resistance rate

The resistance rate was defined as the proportion of patients colonized with the focal resistant strain P^R relative to the sensitive strain P^S, calculated using equilibrium prevalence values as $C^R/(C^S + C^R)$.

Colonization incidence

Nosocomial colonization incidence was defined as the daily rate of colonization acquisition within the hospital, calculated separately for each route of acquisition. For P^R, incidence rates corresponding to transmission (inc_β), endogenous acquisition (inc_α) and HGT (inc_χ) were calculated as

$$
\begin{aligned}
inc_\beta &= \int_t^{t+1} \lambda_{R,\varepsilon} \times (S_{e,s} + S_{e,r}) + \lambda_R \times (S_{d,s} + S_{d,r}) \, dt \\
inc_\alpha &= \int_t^{t+1} \alpha_R \times (S_{e,s} + S_{e,r}) + \alpha_{R,\phi} \times (S_{d,s} + S_{d,r}) \, dt \\
inc_\chi &= \int_t^{t+1} \chi_e \times C_{e,r}^S + \chi_d \times C_{d,r}^S \, dt
\end{aligned}
\tag{A26}
$$

We evaluated incidence at dynamic equilibrium by solving ODE systems numerically for each Ω, then using resulting equilibria as initial values for subsequent numerical integration to calculate incidence from time t to $t+1$.

Parameter space for P^R colonization

Appendix 1—table 1. Parameter values and ranges for the generic pathogen P^R evaluated over five different colonization models (*Figures 1*, *3* and *4*, and *Appendix 1—figures 1–7*).
For endogenous acquisition and microbiome recovery, rates presented are assumed rates in untreated hosts, represented by the' (prime) symbol. Model 1: susceptible-colonized model; Model 2: strain competition model; Model 3: microbiome competition model; Model 4: microbiome-strain competition model; Model 5: microbiome-strain competition model with HGT.

			Value	Model				
Symbol	Parameter	Unit	{Range}	1	2	3	4	5

Continued on next page

Appendix 1—table 1 continued

| Symbol	Parameter	Unit	Value {Range}	Model 1	2	3	4	5
Pathogen colonization								
β	Transmission rate	day^{-1}	0.2	X	X	X	X	X
α'	Endogenous acquisition rate	day^{-1}	0.01	X	X	X	X	X
γ	natural clearance rate	day^{-1}	0.03	X	X	X	X	X
c	Fitness cost of resistance	/	1	X	X	X	X	X
Patient demography								
μ	Admission / discharge rate	day^{-1}	0.1	X	X	X	X	X
f_C	Admission fraction (colonized)	/	0.1	X	X	X	X	X
f_R	Admission fraction (bearing resistant strain)	/	0.5	X	X	X	X	X
f_d	Admission fraction (dysbiosis)	/	0			X	X	X
f_ω	Admission fraction (microbiota bearing resistance gene)	/	0					X
Antibiotics								
a	Antibiotic exposure prevalence	/	0.2 {0–1}	X	X	X	X	X
r_R	Antibiotic resistance level (P^R)	/	0.8 {0–1}	X	X	X	X	X
r_S	Antibiotic resistance level (P^S)	/	0	X			X	X
θ_c	Antibiotic-induced pathogen clearance rate	day^{-1}	0.2	X	X	X	X	X
θ_m	Antibiotic-induced microbiome dysbiosis rate	day^{-1}	1			X	X	X
Microbiome ecology								
ϵ	Colonization resistance	/	0.5 {0.2–0.8}			X	X	X
η	Resource competition	/	0.5 {0.2–0.8}			X	X	X
ϕ	Ecological release	/	5 {2–8}			X	X	X
χ_e	HGT rate (equilibrium)	day^{-1}	{0, 0.01, 0.1}					X
χ_d	HGT rate (dysbiosis)	day^{-1}	$\chi_e \times 10$					X
δ'	Microbiome recovery rate	day^{-1}	0.143			X	X	X
ω	Proportion of patients acquiring the resistance gene among microbiota following antibiotic exposure	/	0.01					X

Part 1: Supplementary results

Here, we expand on results for Part one from the main text. For both strain competition and microbiome competition models, C^R increases monotonically with antibiotic use under the assumption of complete antibiotic resistance (r_R = 1) (*Appendix 1—figure 1*). In *Appendix 1—figure 2*, we evaluate R_0 in the context of each microbiome-pathogen interaction separately, and in concert, over a range of assumed values. This demonstrates how colonization resistance dampens pathogen R_0, while resource competition and ecological release augment it. Taken together, strong microbiome-pathogen interactions can protect patients from P^R colonization in some conditions (e.g. at low a and r_R), while predisposing them to P^R colonization in others (high a and r_R). In *Appendix 1—figure 3*, we demonstrate numerically that introducing a drug-sensitive strain P^S to the microbiome model reduces R_0 of P^R. In *Appendix 1—figure 4*, we again demonstrate how the strength of a pathogen's microbiome interactions (ϵ, η, ϕ) and the level of antibiotic resistance for P^R (r_R) drive epidemiological consequences of antibiotic use, here disentangling the role of antibiotic-induced pathogen clearance (θ_c) from antibiotic-induced microbiome dysbiosis (θ_m). In *Appendix 1—figure 5*, we simulate dynamic responses of P^R to public health interventions. First, dynamic equilibria were found, from which ODEs were integrated for an additional 365 days, evaluating C^R and the resistance rate over

time in the context of each microbiome-pathogen interaction (separately and in concert). We introduced theoretical interventions at days 90 (halving r_R from 0.8 to 0.4), 180 (halving θ_m from 1.0 to 0.5), and 270 (halving a from 0.2 to 0.1), demonstrating that an otherwise identical pathogen can experience diverse, and sometimes opposing responses to public health interventions in the context of different microbiome-pathogen interactions and epidemiological outcomes.

In *Appendix 1—figure 6*, we show how HGT impacts P^R colonization incidence, in contrast to prevalence and resistance rate as presented in *Figure 4* in the main text. In *Appendix 1—figure 7*, we demonstrate effects of HGT on pathogen colonization outcomes. First, we vary key epidemiological parameters over broad ranges to show how the absolute impact of HGT depends on how other parameters mediate colonization dynamics (*Appendix 1—figure 7A*). Second, we show how increasing the rate of HGT in hosts undergoing dysbiosis (χ_d), while holding the rate constant in hosts with stable microbiota (χ_e), augments HGT's impact but does not substantively shift the level of antibiotic exposure that maximizes C^R (*Appendix 1—figure 7B*). Third, we demonstrate how effects of HGT depend on characteristics of the resistance gene being transmitted (*Appendix 1—figure 7C*). For instance, a metabolically costly but highly drug-resistant gene R ($c = 2$, $r_R = 0.8$) is potentially disadvantageous for the pathogen species as a whole at low antibiotic use (reducing total pathogen prevalence) but advantageous at high antibiotic use (increasing total prevalence).
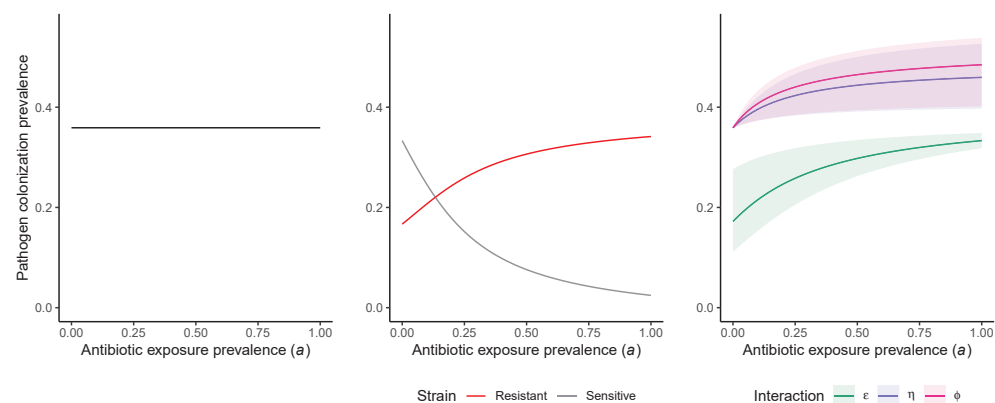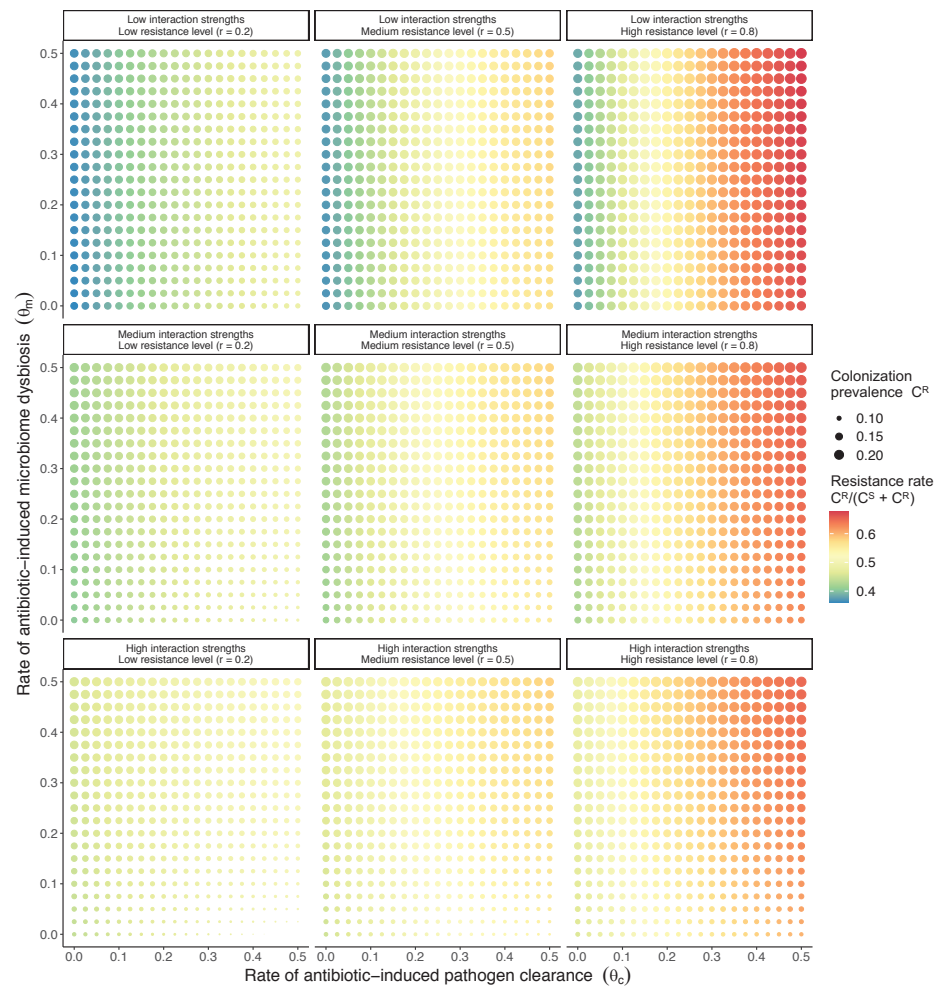

Appendix 1—figure 1. Antibiotic selection for the epidemiological spread of an antibiotic-resistant bacterial pathogen P^R with full resistance to all antibiotics ($r_R = 1$; for the middle panel, $r_S = 0$). As in *Figure 1* in the main text, we compare results from the susceptible-colonized model (left), strain competition model (middle) and microbiome competition model (right). There are no selection trade-offs here because antibiotics have no epidemiological 'benefit', i.e. no ability to clear P^R. See *Appendix 1—table 1* for parameter values.
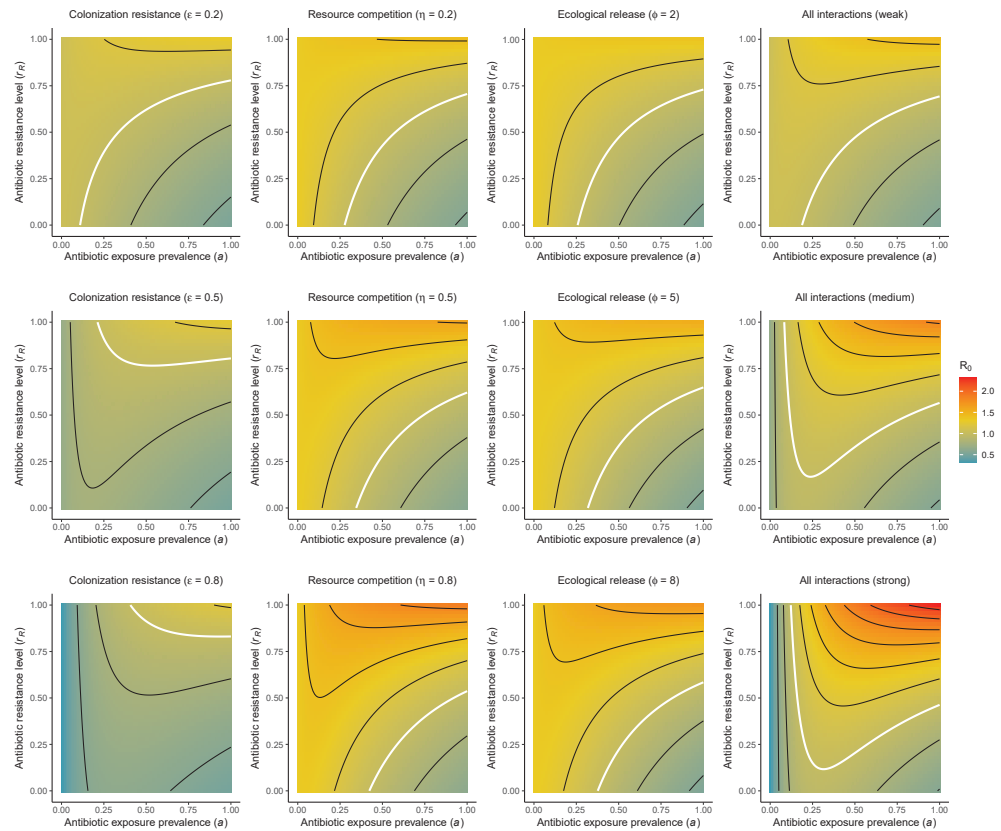
Appendix 1—figure 2. Different microbiome-pathogen interactions of different strengths (figure sub-titles) mediate how antibiotic use (a, x-axis) and resistance (r_R, y-axis) drive R_0 for P^R (z-axis, color). White contour lines indicate $R_0=1$, and each successive black contour line represents an incremental change of 0.2. Microbiome-pathogen interactions are included separately (columns 1, 2, 3) and together (column 4), and their strengths are varied from weak (top row) to medium (middle row) to strong (bottom row) using values from *Figure 2* in the main text. See *Appendix 1—table 1* for all parameter values.
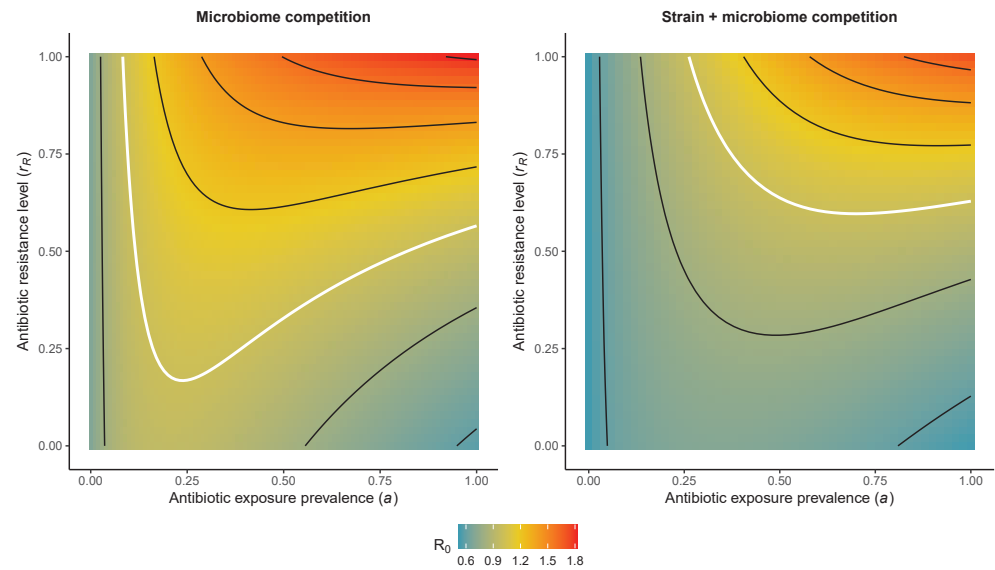
Appendix 1—figure 3. Introducing strain competition to the microbiome competition model reduces R_0 for P^R. Over the whole parameter space, the focal strain P^R of a two-strain microbiome competition model (right) has a lower R_0 than the same pathogen evaluated in the absence of strain competition (left). We assume the competing strain P^S is at endemic equilibrium and is completely sensitive to antibiotics ($r_S=0$). White contour lines indicate $R_0=1$, and each successive black contour line represents an incremental change of 0.2. See *Appendix 1—table 1* for all parameter values.

Appendix 1—figure 4. Antibiotic selection for the spread of an antibiotic-resistant pathogen strain P^R depends on the strength of its interactions with microbiota (rows) and its level of resistance to antibiotics r_R (columns). We assume complete antibiotic sensitivity for P^S ($r_S = 0$), and low, medium, and high interactions strengths correspond to values in *Figure 2* in the main text, and columns in *Appendix 1—figure 2* ({$\varepsilon = 0.2$, $\eta = 0.2$, $\phi = 2$}, {$\varepsilon = 0.5$, $\eta = 0.5$, $\phi = 5$} and {$\varepsilon = 0.8$, $\eta = 0.8$, $\phi = 8$}, respectively). See *Appendix 1—table 1* for all parameter values.
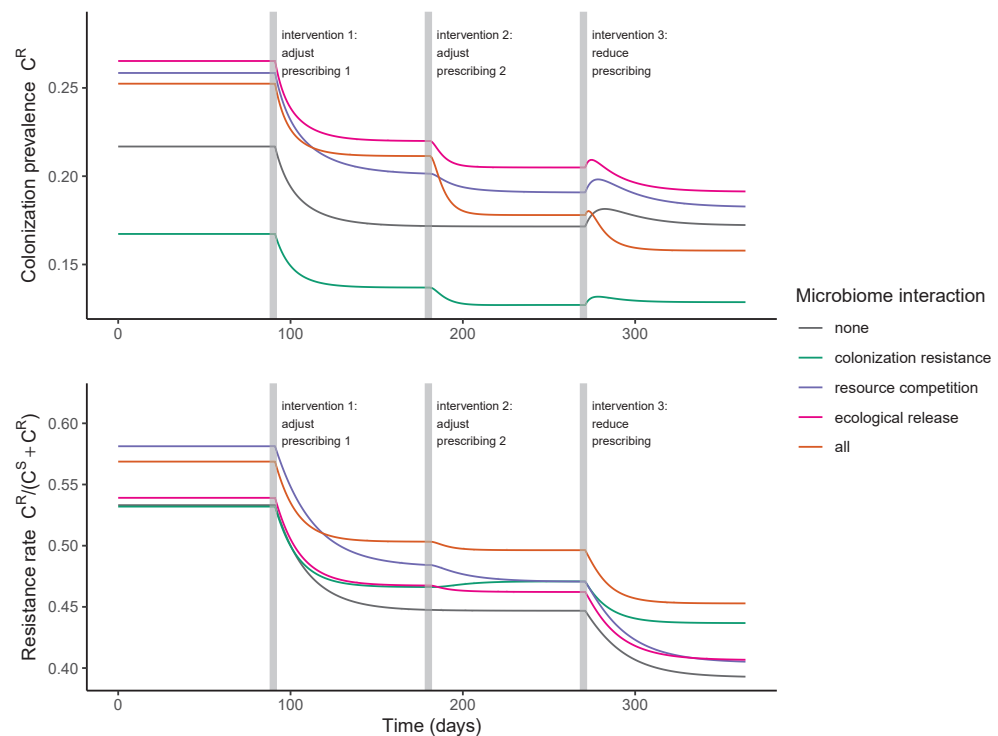
Appendix 1—figure 5. Antibiotic prescribing interventions have mixed impacts on P^R colonization dynamics, depending on the microbiome interactions in effect (colors) and the epidemiological outcomes measured (top: colonization prevalence; bottom: the resistance rate). ODEs were integrated numerically for the baseline pathogen P^R, introducing successive interventions at 3, 6, and 9 months. Interventions represent changes to parameter values corresponding to presumed changes in antibiotic consumption: for intervention 1, P^R's resistance level r_R was halved from 0.8 to 0.4; for intervention 2, the rate of antibiotic-induced microbiome dysbiosis θ_m was halved from 1 to 0.5; and for intervention 3, the baseline antibiotic exposure prevalence a was halved from 0.2 to 0.1. See *Appendix 1—table 1* for all parameter values.
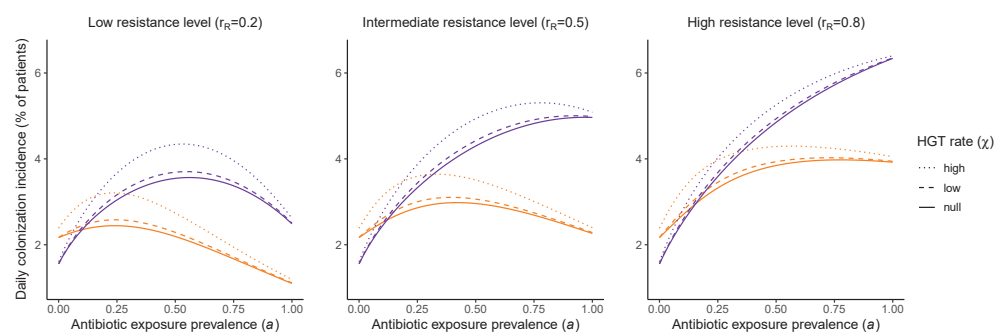
Appendix 1—figure 6. Impacts of horizontal gene transfer (HGT) on steady-state daily colonization incidence of P^R. The relative impact of HGT depends on the gene's rate of transfer (χ, line type), antibiotic exposure prevalence (a, x-axis), competitive interactions between pathogen strains and host microbiota (colors: purple=combined strain and microbiome competition; orange=strain competition only), and the level of resistance conferred by the gene (r_R, columns). Assumptions match those for *Figure 4* in the main text. See *Appendix 1—table 1* for all parameter values.
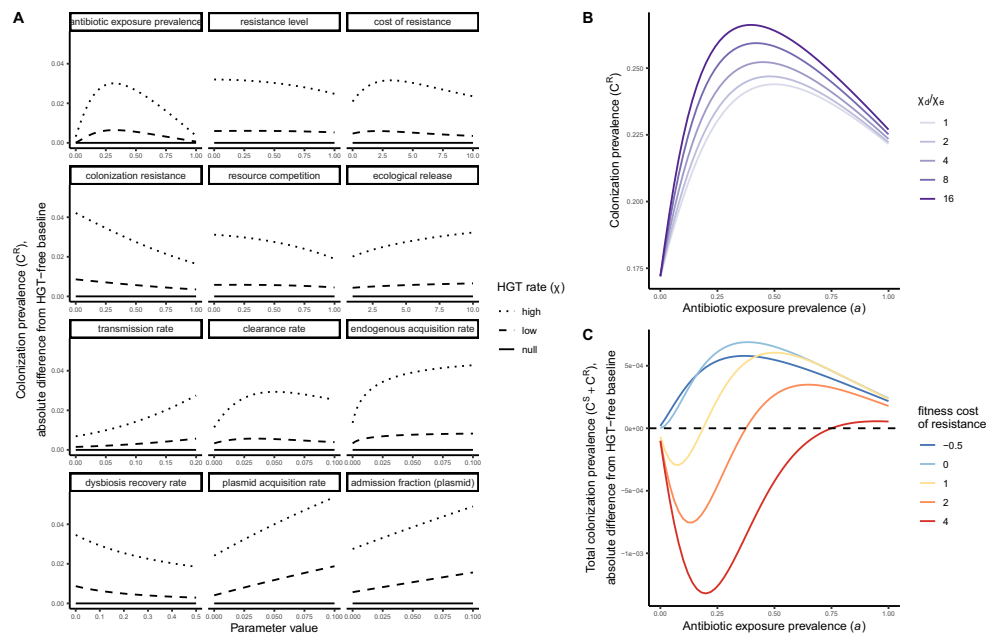
Appendix 1—figure 7. Impacts of HGT on pathogen colonization dynamics are tied to other parameters that mediate the prevalence of competing pathogen strains. (**A**) The absolute difference in P^R colonization prevalence when including HGT (dashed and dotted lines) compared to prevalence in the absence of HGT (solid horizontal line) depends on assumed values of other parameters (panels) that drive colonization dynamics. For brevity, ω is described as the plasmid acquisition rate, and f_ω as the plasmid admission fraction. (**B**) Assuming a higher rate of HGT in patients undergoing dysbiosis (χ_d) than in patients with stable microbiota (χ_e) has a modest impact on C^R. Here, χ_e is held constant at $\chi_e=0.05$, such that changes in the fraction χ_d/χ_e result from corresponding increases in χ_d. (**C**) Impacts of HGT on total pathogen prevalence ($C^S + C^R$) depend on how selectively (dis)advantageous the resistance gene R is for the pathogen bearing it. Here, we show total prevalence (both strains) as proportional to a model assuming the same parameter values but excluding HGT (dashed horizontal line). Colors represent different fitness costs of resistance c, demonstrating that HGT not only changes the relative frequency of competing strains, but can feed forward to alter total prevalence of all strains, tending to increase total prevalence when R has little metabolic cost (low c), but decrease prevalence when R is costly (high c). See *Appendix 1—table 1* for all parameter values.

Part 2: Model application, species characterization, and parameterization
Host and pathogen parameterization

Appendix 1—table 2. Parameters and probability distributions for baseline hospital and host parameters applied across all ARB.

Symbol	Parameter	Unit	Distribution	Reference	Reference setting	Notes
μ	Admission / discharge rate	day^{-1}	1 / Normal (8, 2.55)	*Touat et al., 2019*	French hospitals	/

Continued on next page

Appendix 1—table 2 continued

Symbol	Parameter	Unit	Distribution	Reference	Reference setting	Notes
f_d	Admission fraction (dysbiosis)	/	Normal (0.0756, 0.0190)	*Bernier et al., 2014*	French community	Taken as proportion of the French community exposed to antibiotics in previous 28 days, extrapolating weekly reimbursed antibiotic prescriptions/1000 inhabitants (18.9, 9.6–28.3) to 4 weeks and assuming independent prescriptions = 75.6 (38.4–113.2) prescriptions/1000 inhabitants
a	Antibiotic exposure prevalence	/	Normal (0.195, 0.0195)	*Alfandari et al., 2015*	314 French hospitals	/
$r_{i,j}$	Antibiotic resistance level	/	if sensitive, 0; if resistant, 1; if intermediate sensitivity, $r_{i,j} \sim$ Uniform (0,1)			For all strains *i*, the resistance level to each antibiotic class *j* depends on whether the strain is classified as sensitive, resistant, or of intermediate sensitivity in its assumed antibiogram
θ_c	Antibiotic-induced pathogen clearance rate	day^{-1}	1 / Uniform (1, 10)	*Tepekule et al., 2017*	Simulation study	/
θ_m	Antibiotic-induced microbiome dysbiosis rate	day^{-1}	1 / Normal (2, 0.4)	*Bhalodi et al., 2019*	Mixed	Circumstantial evidence of same-day microbiome disruption following antibiotic therapy; assumed an average minimum 12 hr to disruption
δ'	Microbiome recovery rate	day^{-1}	1 / Normal (28, 10.71)	*Burdet et al., 2019*; *Rafii et al., 2008*	Mixed; French hospital	Across studies in a review of antibiotic-induced microbiome disruption, intestinal microflora were observed to 'return to normal' 1–49 days after antibiotic cessation; in a French hospital, two measures of microbiome diversity were observed to 'return to normal' after 16–21 days.

Appendix 1—table 3. Parameters and probability distributions for *C. difficile*.

Symbol	Parameter	Unit	Distribution	Reference	Reference setting	Notes
β	Transmission rate	day^{-1}	Normal (0.00555, 0.000944)	*van Kleef et al., 2016*	English hospitals (modeling study)	Mean of point estimates of the daily probability of transmission from colonized patients (0.0037) and infected patients (0.0074)
α'	Endogenous acquisition rate	day^{-1}	Normal (0.0000253, 0.0000114)	*Durham et al., 2016*	USA hospitals (modeling study)	Proxy measure: the estimated daily rate of progression from colonization to infection in hospital patients, divided by the relative risk of progression in patients exposed to antibiotics
γ	Natural clearance rate	day^{-1}	Normal (0.0119, 0.00170)	*Simor et al., 1993*	Canadian care home	Fit longitudinal colonization data using exponential decay model

Continued on next page

Appendix 1—table 3 continued

Symbol	Parameter	Unit	Distribution	Reference	Reference setting	Notes
f_C	Admission fraction (colonized)	/	Binomial (229, 0.048) / 229	*Barbut, 1996*	11 French hospitals	Stool prevalence among asymptomatic patients
r	Antibiotic resistance level	/	median 94.3%, (range 93.3–95.4%)	estimated	/	Cumulative resistance level across simulated antibiotic consumption data and assumed antibiograms
ε	Colonization resistance	/	1–1 / Cauchy (52.85, 1.62)	estimated	/	From expert opinion
η	Resource competition	/	$(1/\gamma)/(1/\gamma +$ Cauchy (121.11, 4.85))	estimated	/	From expert opinion
ϕ	Ecological release	/	Cauchy (39.22 0.922)	estimated	/	From expert opinion

Appendix 1—table 4. Parameters and probability distributions for *S. aureus*.

Symbol	Parameter	Unit	Distribution	Reference	Reference setting	Notes
β	Transmission rate	day^{-1}	Normal (0.057, 0.0057)	*Di Ruscio et al., 2019*	Norwegian hospitals (modeling study)	/
α'	Endogenous acquisition rate	day^{-1}	Normal (0.0016, 0.0008)	*Coello et al., 1997*; *Di Ruscio et al., 2019*	Spanish hospital	Proxy measure: the estimated daily rate of progression from colonization to infection in hospital patients
γ	Natural clearance rate	day^{-1}	1 / Normal (287, 17.9)	*Shenoy et al., 2014*	Mixed	/
c	Fitness cost of resistance	/	Normal (0.2, 0.02)	*Kouyos et al., 2013*; *Laurent et al., 2001*	French hospitals	Growth cultures showed 20% fitness benefit to MSSA over MRSA strains
f_C	Admission fraction (colonized)	/	Normal (0.0757, 0.00364)	*Cravo Oliveira Hashiguchi et al., 2019*; *Scanvic et al., 2001*	French hospitals	Estimated as the proportion of patients arriving to a French hospital with MRSA colonization, divided by the estimated proportion of *S. aureus* strains that are methicillin-resistant in France
f_R	Admission fraction (bearing resistant strain)	/	Normal (0.16, 0.016)	*Cravo Oliveira Hashiguchi et al., 2019*	France	/
r_S	Antibiotic resistance level (MSSA)	/	median 33.1% (range 17.2–48.9%)	estimated	/	Cumulative resistance level across simulated antibiotic consumption data and assumed antibiograms
r_R	Antibiotic resistance level (MRSA)	/	median 94.5% (range 90.8–98.2%)	estimated	/	Cumulative resistance level across simulated antibiotic consumption data and assumed antibiograms

Continued on next page

Appendix 1—table 4 continued

Symbol	Parameter	Unit	Distribution	Reference	Reference setting	Notes
ε	Colonization resistance	/	1–1 / Cauchy (2.21, 0.15)	estimated	/	From expert opinion
η	Resource competition	/	$(1/\gamma)$ / $(1/\gamma +$ Cauchy (73.09, 3.09))	estimated	/	From expert opinion
φ	Ecological release	/	Cauchy (2.97, 0.28)	estimated	/	From expert opinion

Appendix 1—table 5. Parameters and probability distributions for *E. coli*.

Symbol	Parameter	Unit	Distribution	Reference	Reference setting	Notes
β	Transmission rate	day^{-1}	Normal (0.0078, 0.00334)	*Gurieva et al., 2018*	13 European ICUs	/
α′	Endogenous acquisition rate	day^{-1}	Normal (0.0024, 0.000663)	*Gurieva et al., 2018*	13 European ICUs	/
γ	Natural clearance rate	day^{-1}	Normal (0.00269, 0.000216)	*Bar-Yoseph et al., 2016*	Mixed	Fit longitudinal colonization data using exponential decay model
c	Fitness cost of resistance	/	Normal (0.2, 0.02)	/	/	In absence of data for ESBL resistance, used same distribution as for MRSA
f_C	Admission fraction (colonized)	/	Normal (0.275, 0.0140)	*Ebrahimi et al., 2016*; *Gurieva et al., 2018*	Mixed	Estimated as the proportion of patients arriving to 13 European ICUs with ESBL-EC carriage, divided by the estimated proportion of *E. coli* that are ESBL-producing in a Hungarian hospital
f_R	Admission fraction (bearing resistant strain)	/	Normal (0.119, 0.0413)	*Ebrahimi et al., 2016*	Hungarian hospital	Proportion of fecal *E. coli* that were ESBL-producing from a non-outbreak setting
f_ω	Admission fraction (microbiota bearing ESBL gene)		Binomial (857, 0.0665)/857	*Pilmis et al., 2018*; *Vidal-Navarro et al., 2010*	2 French hospitals	Estimated by pooling 857 samples from two studies reporting fecal carriage of ESBL-producing species other than *E. coli*
r_S	Antibiotic resistance level (EC)	/	median 23.1% (range 9.6–36.5%)	Estimated	/	Cumulative resistance level across simulated antibiotic consumption data and assumed antibiograms
r_R	Antibiotic resistance level (ESBL-EC)	/	median 84.9% (range 77.4–92.2%)	Estimated	/	Cumulative resistance level across simulated antibiotic consumption data and assumed antibiograms
ε	Colonization resistance	/	1–1/Cauchy (6.06, 0.64)	Estimated	/	From expert opinion

Appendix 1—table 5 continued

Symbol	Parameter	Unit	Distribution	Reference	Reference setting	Notes
η	Resource competition	/	(1/γ)/(1/γ + Cauchy (76.38, 5.35))	Estimated	/	From expert opinion
φ	Ecological release	/	Cauchy (11.80, 0.80)	Estimated	/	From expert opinion
χ_e	HGT rate (equilibrium)	day^{-1}	χ_d/Log-Normal (1.36, 0.81)	Estimated	/	From expert opinion
χ_d	HGT rate (dysbiosis)	day^{-1}	-log(1-Weibull (0.94, 0.11)) / 10	Estimated	/	From expert opinion
ω	Proportion of patients whose microbiota acquire ESBL gene following antibiotic exposure	/	Binomial (132, 18/132)/132 × 0.382	*Agence nationale de sécurité du médicament et des produits de santé, 2017*; *Bar-Yoseph et al., 2016*	Mixed	The proportion of patients in a meta-analysis who, subsequent to treatment, express resistance to the antibiotic with which treated (18/132), multiplied by the proportion of ESBLs among antibiotics consumed in French hospitals (38.2%)

Appendix 1—table 6. Parameters and probability distributions for *K. pneumoniae*.

Symbol	Parameter	Unit	Distribution	Reference	Reference setting	Notes
β	Transmission rate	day^{-1}	Normal (0.029, 0.00842)	*Gurieva et al., 2018*	13 European ICUs	Estimate for non-*E. coli* Enterobacteriaceae
α′	Endogenous acquisition rate	day^{-1}	Normal (0.0048, 0.00133)	*Gurieva et al., 2018*	13 European ICUs	Estimate for non-*E. coli* Enterobacteriaceae
γ	Natural clearance rate	day^{-1}	Normal (0.00267, 0.000324)	*Bar-Yoseph et al., 2016*	Meta-analysis	Fit longitudinal colonization data using exponential decay model
c	Fitness cost of resistance	/	Normal (0.2, 0.02)	/	/	In absence of data for CP resistance, used same distribution as for MRSA
f_C	Admission fraction (colonized)	/	Binomial (11420, (928 / 11420)) / 11420	*Cravo Oliveira Hashiguchi et al., 2019*; *Gurieva et al., 2018*	Mixed	The proportion of patients arriving to 13 European ICUs with CP-KP carriage, divided by the estimated proportion of *K. pneumoniae* that produce carbapenemase in France
f_R	Admission fraction (bearing resistant strain)	/	Normal (0.01, 0.001)	*Cravo Oliveira Hashiguchi et al., 2019*	France	/

Continued on next page

Appendix 1—table 6 continued

Symbol	Parameter	Unit	Distribution	Reference	Reference setting	Notes
f_ω	Admission fraction (microbiota bearing CP gene)		Binomial (1135, 0.00441) / 1135	*Pantel et al., 2015*	7 French hospitals	Rectal carriage of carbapenemase-producing bacteria
r_S	Antibiotic resistance level (KP)	/	median 23.1% (range 9.6–36.5%)	estimated	/	Cumulative resistance level across simulated antibiotic consumption data and assumed antibiograms
r_R	Antibiotic resistance level (CP-KP)	/	median 91.7% (range 89.7–93.7%)	estimated	/	Cumulative resistance level across simulated antibiotic consumption data and assumed antibiograms
ε	Colonization resistance	/	1–1 / Cauchy (17.16, 0.97)	estimated	/	From expert opinion
η	Resource competition	/	$(1/\gamma)$ / $(1/\gamma$ + Cauchy (74.93, 4.03))	estimated	/	From expert opinion
ϕ	Ecological release	/	Cauchy (36.63, 0.82)	estimated	/	From expert opinion
χ_e	HGT rate (equilibrium)	day^{-1}	χ_d / Gamma (2.01,0.36)	estimated	/	From expert opinion
χ_d	HGT rate (dysbiosis)	day^{-1}	-log(1-Gamma (0.54, 3.67))/ 10	estimated	/	From expert opinion
ω	Proportion of patients whose microbiota acquire CP gene following antibiotic exposure		Binomial (132, 0.1363) / 132 × 0.0151	estimated from *Agence nationale de sécurité du médicament et des produits de santé, 2017*; *Bar-Yoseph et al., 2016*	Mixed	The proportion of patients in a meta-analysis who, subsequent to treatment, express resistance to the antibiotic with which treated (18/132), multiplied by the proportion of carbapenems among antibiotics consumed in French hospitals (1.5%)

Expert elicitation
Protocol

Expert elicitation is a scientific consensus methodology involving the estimation of unknown parameter values from subject-matter experts. We developed an expert elicitation protocol, using published recommendations for elicitation of clinical parameters,(*Johnson et al., 2010*) to characterize the role of microbiome dysbiosis in driving hospital colonization dynamics across the ARB included in this study (provided separately). First, the scientific context of the study was introduced, including the potential epidemiological relevance of microbiome-pathogen interactions, and potential roles for intraspecific strain competition and microbiome dysbiosis in explaining how antibiotics select for resistance. Second, the MATCH uncertainty elicitation tool and 'chips and bins' method were introduced, allowing experts to build distributions visually in the form of histograms to quantify parameter values and associated uncertainty. (*Morris et al., 2014*) Third, potential cognitive biases were reviewed and tips for reliable parameter estimation were provided. Finally, experts were asked to respond to questions and quantify their beliefs and uncertainty about how microbiome dysbiosis

among hospital patients affects pathogen colonization processes (acquisition, clearance, growth and horizontal gene transfer). It was stressed that the goal of the elicitation was not to characterize precise numerical estimates of particular mechanistic interactions, but rather to quantify the relative impact of microbiome dysbiosis on different colonization outcomes in the hospital setting. Experts were initially identified through a review of authors of relevant publications in the field. At the end of each interview, experts were further asked to refer us to additional experts in the form of snowball sampling. Elicitation results are reported anonymously, but all experts agreed to their acknowledgment in this article.

Results and interpretation

Of 23 invited experts, ten ultimately participated in elicitation interviews (response rate 43.5%). Their specialties include bacteriology, internal medicine, intensive care, infectious disease epidemiology and clinical microbiology. Model parameters, the clinical parameters that experts were asked to estimate, and assumed links between them are provided in *Appendix 1—table 7*. First, experts were asked about the relevance of intraspecific strain competition for the nosocomial epidemiology of each pathogen. Then, for key colonization parameters (β, α, γ, χ), experts were asked whether hospital patients experiencing antibiotic-induced dysbiosis are more or less likely to experience the corresponding colonization outcome than patients not experiencing dysbiosis (*Appendix 1—figure 8*). If yes, they were asked to quantify the relative impact of dysbiosis on that outcome i for each ARB j as a histogram (estimated using MATCH) given by a vector $x_{i,j,k}$ for each expert k. Experts made estimates for each ARB consecutively, such that parameters for each ARB were estimated relative to other included ARB.

Raw data for expert distributions are provided in *Appendix 1—figure 9*. Experts differed substantially in estimated ranges of different parameters, but Friedman's tests using medians of each parameter distribution suggested that the species rank order was conserved across experts, with *C. difficile* generally having the strongest estimated microbiome-pathogen interaction coefficients, and MRSA the weakest. To conserve species rank order when combining expert estimates $x_{i,j,k}$ to form pooled histograms, distributions were re-centred by the mean relative distance $z_{i,j}$ between each j and the reference ARB (taken as MRSA) over all experts k (*Appendix 1—figure 10*). For *C. difficile* and MRSA, HGT was excluded from simulations and pooled distributions were not re-centred. Each expert distribution was weighted equally, contributing to 10% of the final pooled distribution for each species and parameter. Pooled histograms were fit to six candidate distributions (normal, lognormal, Weibull, Cauchy, exponential and gamma), and the final distribution was selected as the fitted distribution giving the lowest Akaike Information Criterion (using the function fitdist from the R package fitdistrplus). Final fitted distributions for each parameter and ARB are given in *Appendix 1—table 3–6*, and for select parameters in *Figure 5*.

Among other observations, experts highlighted (i) uncertainty about an influence of strain competition on hospital colonization dynamics for all ARB, with the majority of experts believing strain competition was irrelevant for *C. difficile* but at least partially relevant for other ARB, (ii) unanimous certainty about a role for antibiotic-induced microbiome dysbiosis as a driver of colonization for *C. difficile*, ESBL-EC and CP-KP, with somewhat less certainty for MRSA, and (iii) certainty about a role for horizontal gene transfer (HGT) for ESBL-EC and CP-KP (*Appendix 1—figure 8*).

Appendix 1—table 7. Relationship between model parameters and the clinical parameters estimated by experts.

| Model parameter		Clinical parameter			Assumed relationship between model and clinical parameters
Name	Symbol	Description		Symbol	
Colonization resistance	ε	Relative risk of acquiring colonization among patients experiencing microbiome dysbiosis		RR_β	$\varepsilon = 1 - \frac{1}{RR_\beta}$
Resource competition	η	Excess duration of colonization among patients experiencing microbiome dysbiosis		d	$\eta = \frac{\frac{1}{\gamma}}{\frac{1}{\gamma}+d}$
Ecological release	ϕ	Relative risk of pathogen outgrowth among patients experiencing microbiome dysbiosis		RR_α	$\phi = RR_\alpha$

Continued on next page

Appendix 1—table 7 continued

Model parameter			Clinical parameter		Assumed relationship between model and clinical parameters
Name	Symbol	Description		Symbol	
HGT rate (dysbiosis)	χ_d	Proportion of antibiotic-exposed patients colonized with the specified species that acquire the specified resistance via HGT during their hospital stay		$p\chi_d$	$p_{\chi_d} = 1 - e^{-\chi_d \times \frac{1}{\mu}}$
HGT rate (equilibrium)	χ_e	Relative risk of acquiring the specified resistance via HGT among patients experiencing microbiome dysbiosis		$RR\chi$	$RR_{\chi} = \frac{\chi d}{\chi e}$
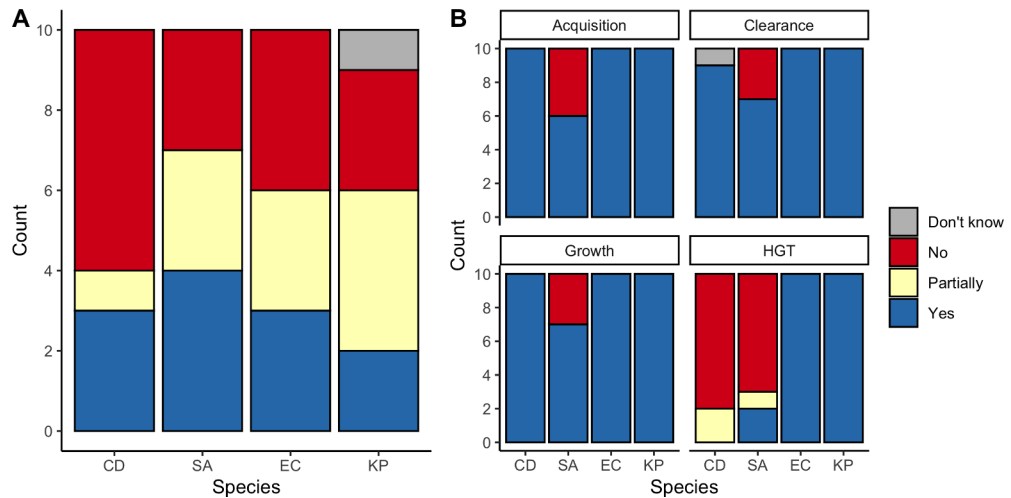
Appendix 1—figure 8. Expert belief about which mechanisms drive epidemiological dynamics of bacterial pathogens. (**A**) Expert belief in whether or not intraspecific strain competition influences nosocomial colonization dynamics for each pathogen. (**B**) Expert belief in whether or not each of the given colonization processes is affected by microbiome dysbiosis, and for HGT, whether or not this process is relevant in clinical settings. CD: *Clostridioides difficile*; SA: *Staphylococcus aureus*; EC: *Escherichia coli*; KP: *Klebsiella pneumoniae*; HGT: horizontal gene transfer.
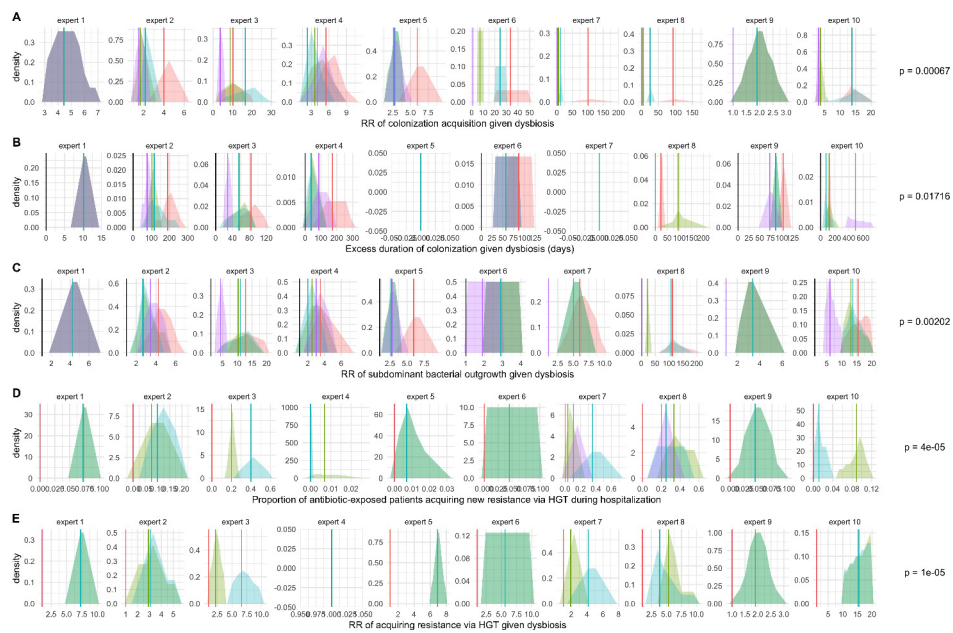
Appendix 1—figure 9. Expert elicitation results (raw data): expert belief and uncertainty about the impact of microbiome dysbiosis on nosocomial colonization dynamics of included bacterial pathogens (colors). Rows A through E represent, respectively, responses to questions two through six from the expert elicitation (protocol provided separately). Distributions were generated during expert interviews using the MATCH Uncertainty Elicitation Tool with the chips and bins method (*Morris et al., 2014*) Experts are anonymized and represented by different columns. Vertical bars represent medians of each distribution to visualize the rank order for each pathogen as estimated by each expert. p-values represent results of Friedman's tests for distribution medians, considering species as groups and experts as blocks for each question; when p<0.05, the species rank order across experts is interpreted as non-random.
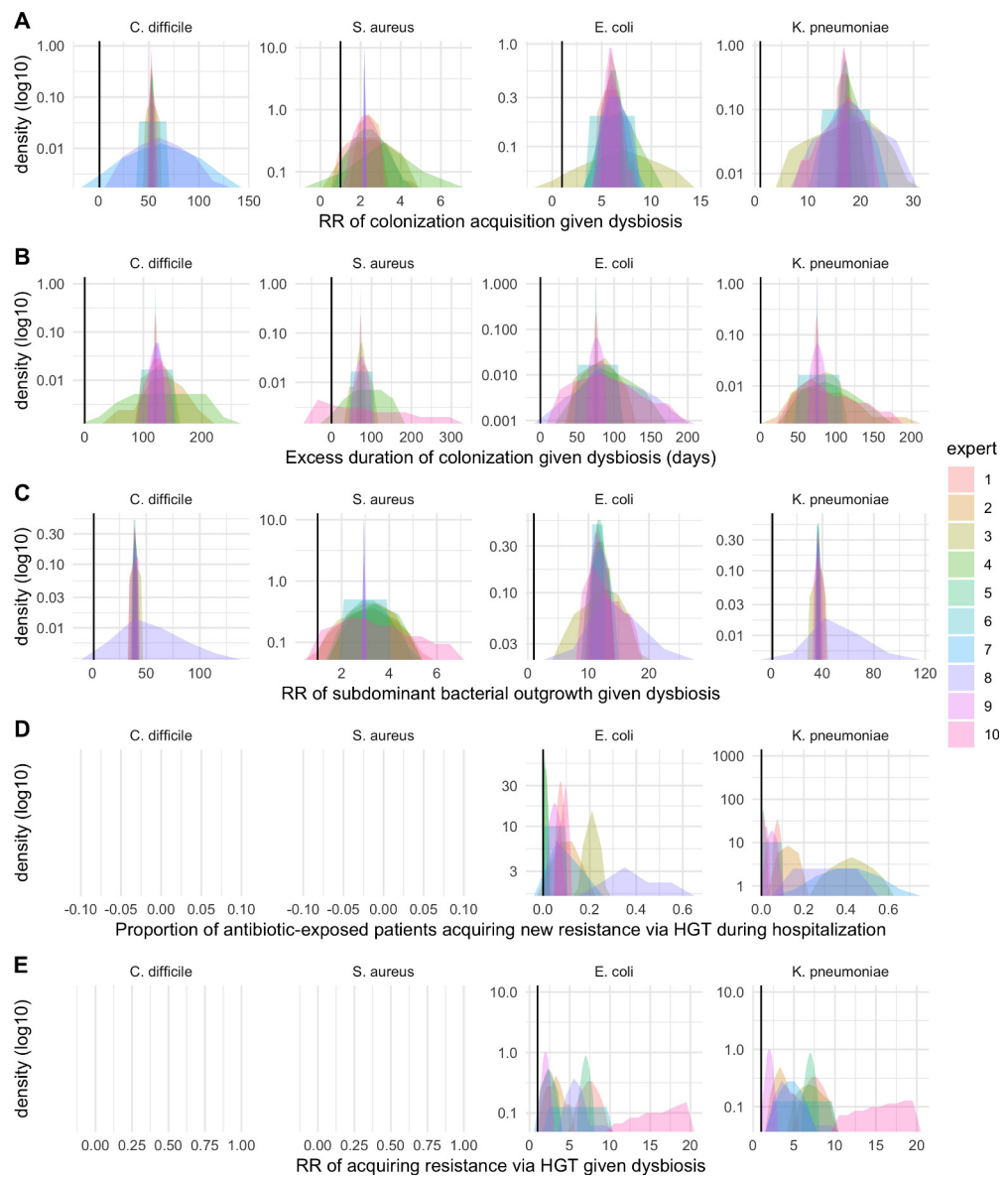
Appendix 1—figure 10. Expert elicitation results (re-centred data): expert belief and uncertainty about the impact of microbiome dysbiosis on nosocomial colonization dynamics of included bacterial pathogens (colors). Rows A through E represent, respectively, responses to questions two through six from the expert elicitation protocol (provided separately).

Antibiotic exposure data

Appendix 1—table 8. Antibiotic classes, their contribution to total hospital antibiotic consumption, their spectrum, and their relative rate of inducing microbiome dysbiosis.

Consumption data come from the French ANSM and are supplemented with data from Baggs et al. (*Agence nationale de sécurité du médicament et des produits de santé, 2017*; *Baggs et al., 2016*). The literature was used to classify antibiotic classes in terms of their spectrum, (*Abbara et al., 2020*; *Tan et al., 2017*) and relative rate of causing microbiome dysbiosis. (*Baggs et al., 2018*; *Brown et al., 2013*) The percentage column does not total to 100 due to rounding error.

| Antibiotic class	ACT code	% of consumption	Spectrum	Rate of inducing microbiome dysbiosis
Amoxicillin and beta-lactamase inhibitor	J01CR02	32.4	Broad	High
Penicillins with extended spectrum	J01CA	21.9	Narrow	Medium
Quinolones	J01M	11.0	Broad	High
C3G	J01DD	8.2	Broad	Very high
C1G	J01DB	3.7	Narrow	High
Macrolides	J01FA	3.4	Narrow	Medium
Imidazole	J01XD	2.9	Narrow	Medium
Piperacillin and beta-lactamase inhibitor	J01CR05	2.3	Broad	High
Aminoglycosides	J01G	2.3	Narrow	Low
Tetracyclines	J01A	2.0	Narrow	Low
Sulfonamides, trimethoprim	J01E	1.8	Narrow	Medium
Glycopeptides	J01XA	1.8	Narrow	Very high
Lincosamides	J01FF	1.6	Broad	Very high
Carbapenems	J01DH	1.5	Broad	High
Penicillins (other)	J01C_other	1.4	Narrow	Medium
C2G	J01DC	0.9	Narrow	High
C4G	J01DE	0.6	Broad	Very high
Other	Other	2.1	Narrow	Medium

Part 2: Supplementary results

### Baseline colonization dynamics
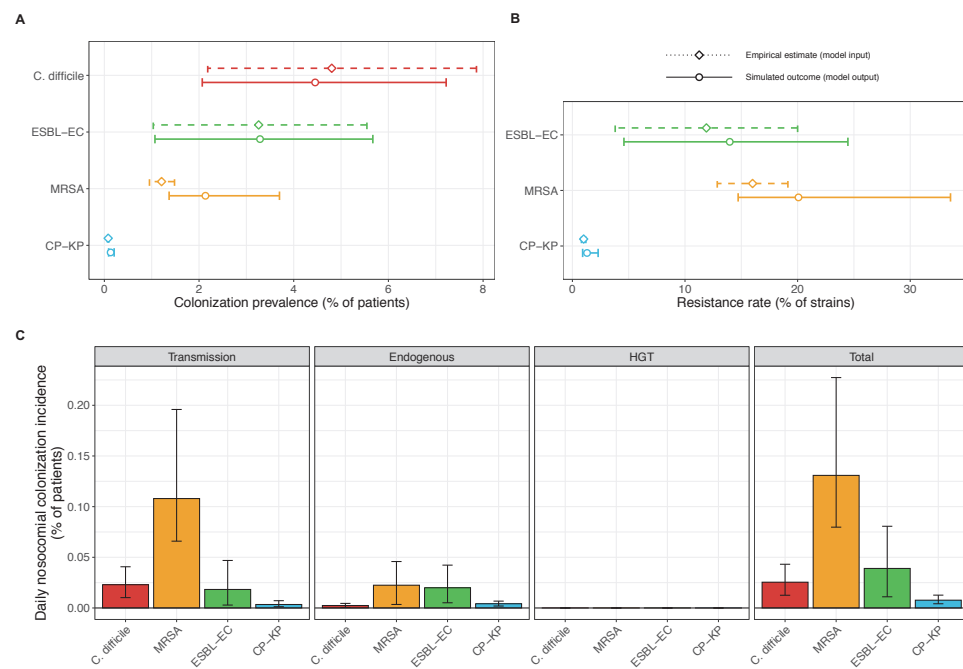
Appendix 1—figure 11. Baseline steady-state pathogen colonization outcomes for single-species

Appendix 1—figure 11 continued on next page

Appendix 1—figure 11 continued

simulations excluding the microbiome ($\varepsilon = 0$, $\eta = 0$, $\phi = 1$, $\chi = 0$). Compared to microbiome simulations (*Figure 6* in the main text), pathogens are less prevalent (**A**), and incidence is more than halved for all ARB except MRSA (**C**). However, resistance rates are largely unchanged (**B**). Points (**A and B**) and bars (**C**) represent medians, and error bars represent 95% uncertainty intervals across 10,000 Monte Carlo simulations.
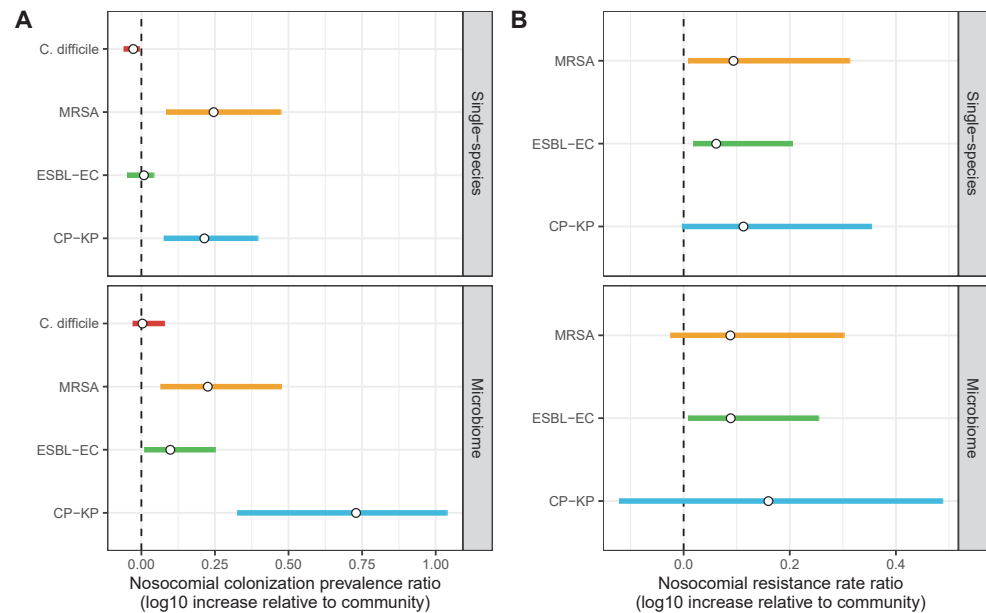
Appendix 1—figure 12. Change in ARB colonization outcomes in the hospital relative to the community ($\log_{10}$ scale), comparing single-species and microbiome simulations. (**A**) The ratio of colonization prevalence among hospital patients relative to baseline colonization prevalence in the community. (**B**) The ratio of resistance rates in the hospital relative to baseline resistance rates in the community. Points represent medians and error bars represent 95% uncertainty intervals across 10,000 Monte Carlo simulations.
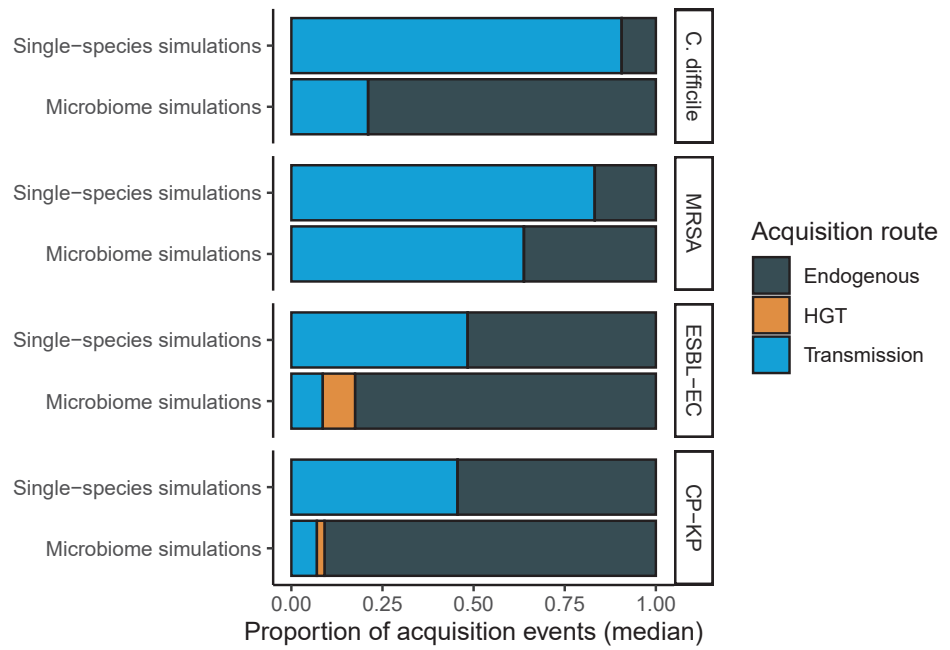
Appendix 1—figure 13. Different ARB spread in different ways, and the importance of different routes depends on potential microbiome interactions. Each shaded region represents the median estimated proportion of acquisition events explained by each acquisition route over 10,000 Monte Carlo simulations.
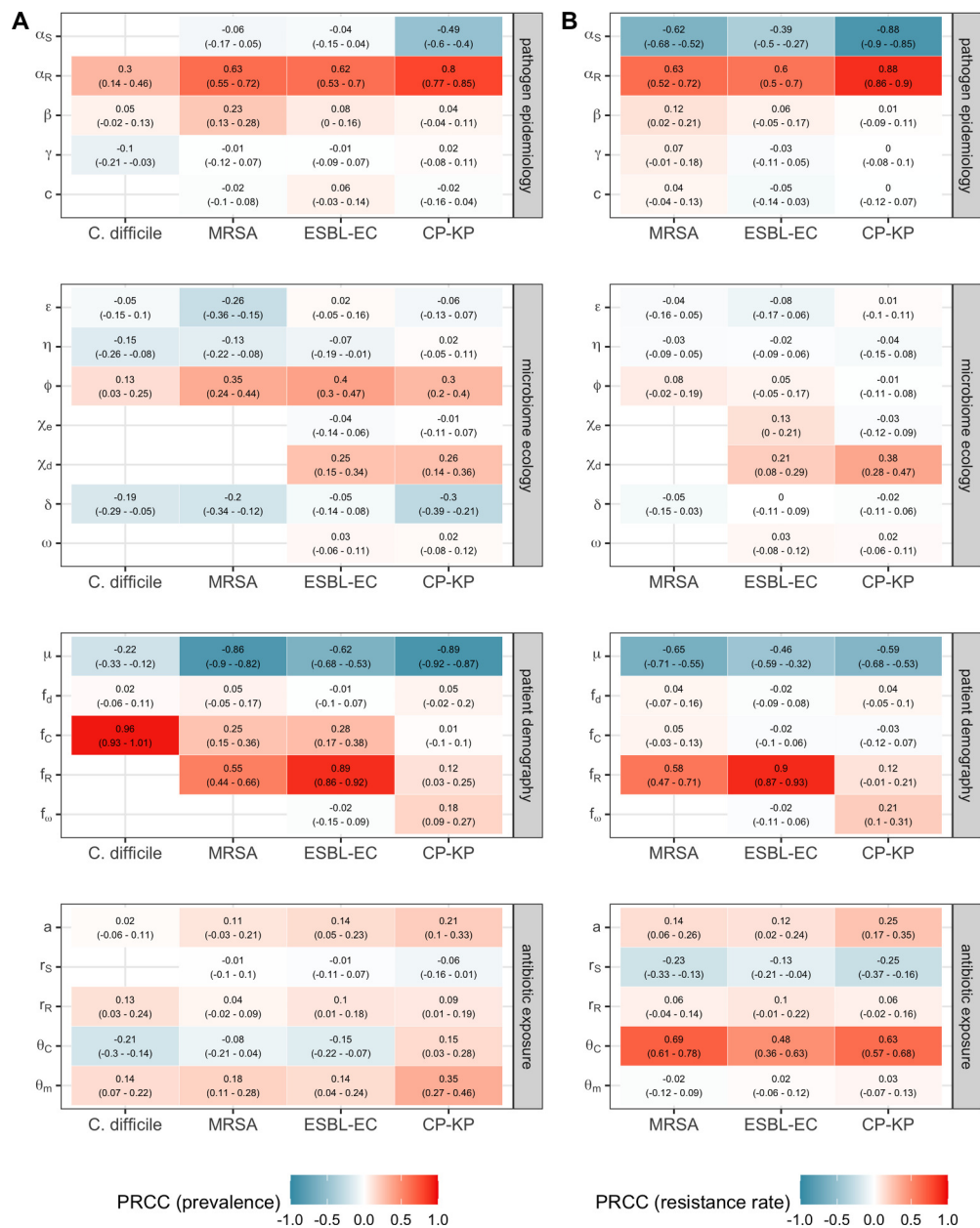
Appendix 1—figure 14. Multivariate sensitivity analysis describing partial rank correlation coefficients (PRCCs) between model parameters and two epidemiological outcomes evaluated at population dynamic equilibrium: in panel A, colonization prevalence of the focal strain P^R; in panel B, the pathogen resistance rate. For all pathogens, prevalence was positively associated with prior colonization upon hospital admission (f_C for *C. difficile*, f_R for MRSA, ESBL-EC and CP-KP) and ecological release (ϕ), and negatively associated with a higher rate of discharge and admission, i.e. shorter duration of hospitalisation (μ). Across ARB, higher rates of antibiotic-induced dysbiosis (θ_m) and microbiome recovery (δ) were generally positively and negatively associated with prevalence, respectively. Conversely, microbiome parameters were minimally associated with resistance rates, with the exception of the HGT rate among patients undergoing dysbiosis (χ_d).

Intervention evaluation
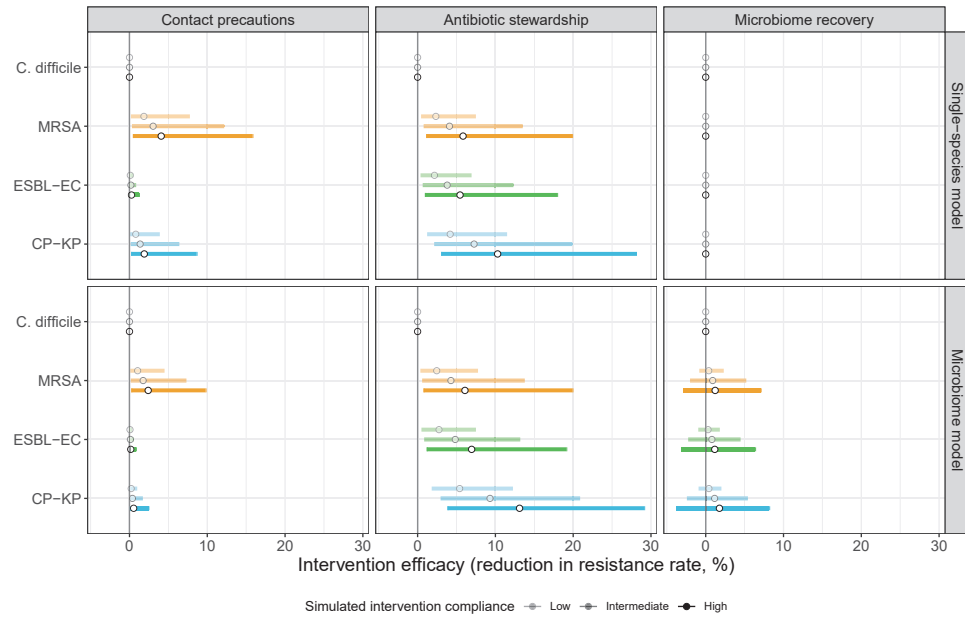
Appendix 1—figure 15. Compared to pathogen incidence (*Figure 7*), dynamic responses of pathogen resistance rates to public health interventions were similar across single-species and microbiome simulations (left panels, contact precautions; middle, antibiotic stewardship; right, microbiome recovery interventions). Top panels show results from simulations using 'single-species models' that only account for the focal pathogen species (including intraspecific strain competition for MRSA, ESBL-EC and CP-KP); bottom panels show simulation results when models also include microbiome-pathogen interactions and antibiotic-induced microbiome dysbiosis. For each intervention, three levels of intervention compliance (shading) are simulated. Points correspond to medians, and bars to 95% uncertainty intervals across 10,000 Monte Carlo simulations.
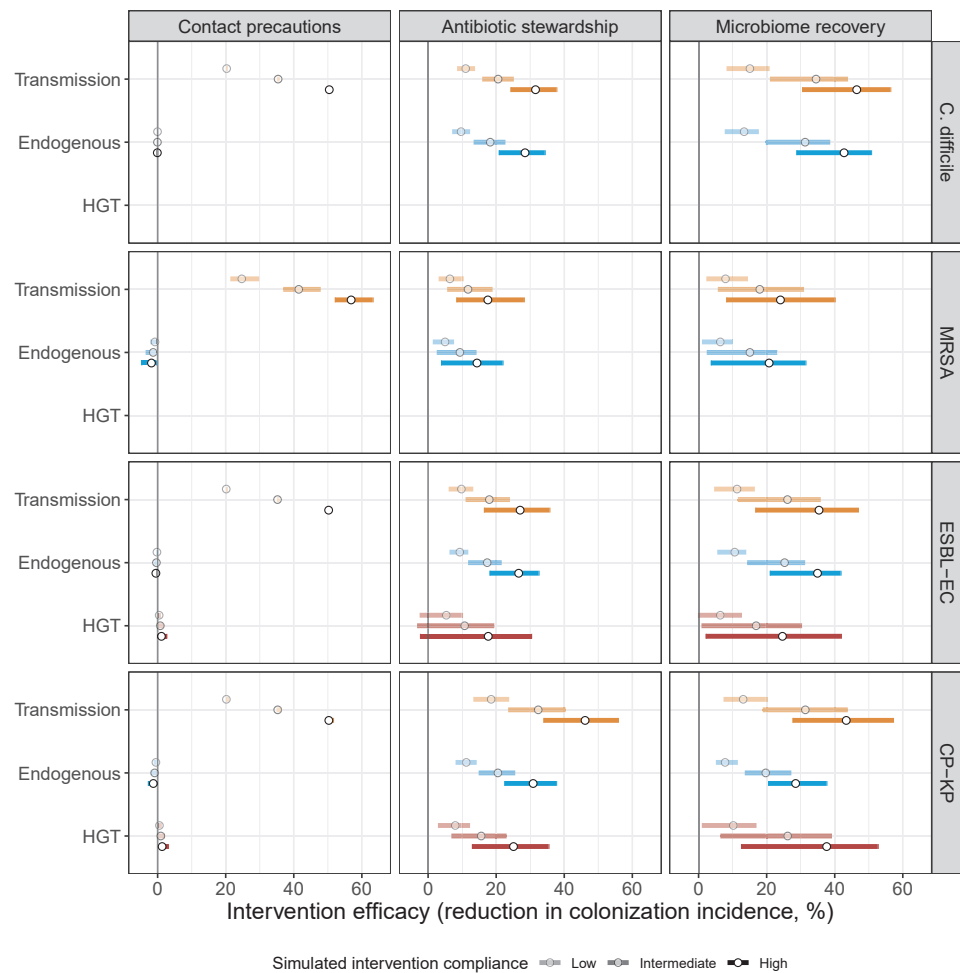
Appendix 1—figure 16. Interventions act on different routes of acquisition. Intervention efficacy (x-axis) for reducing colonization incidence via different routes of colonization acquisition (colors) for different interventions (columns) and ARB (rows). Unlike contact precautions, which only reduced incidence via transmission, antibiotic stewardship and microbiome recovery interventions reduced colonization incidence through all considered routes. Points correspond to medians, and bars to 95% uncertainty intervals across 10,000 Monte Carlo simulations.
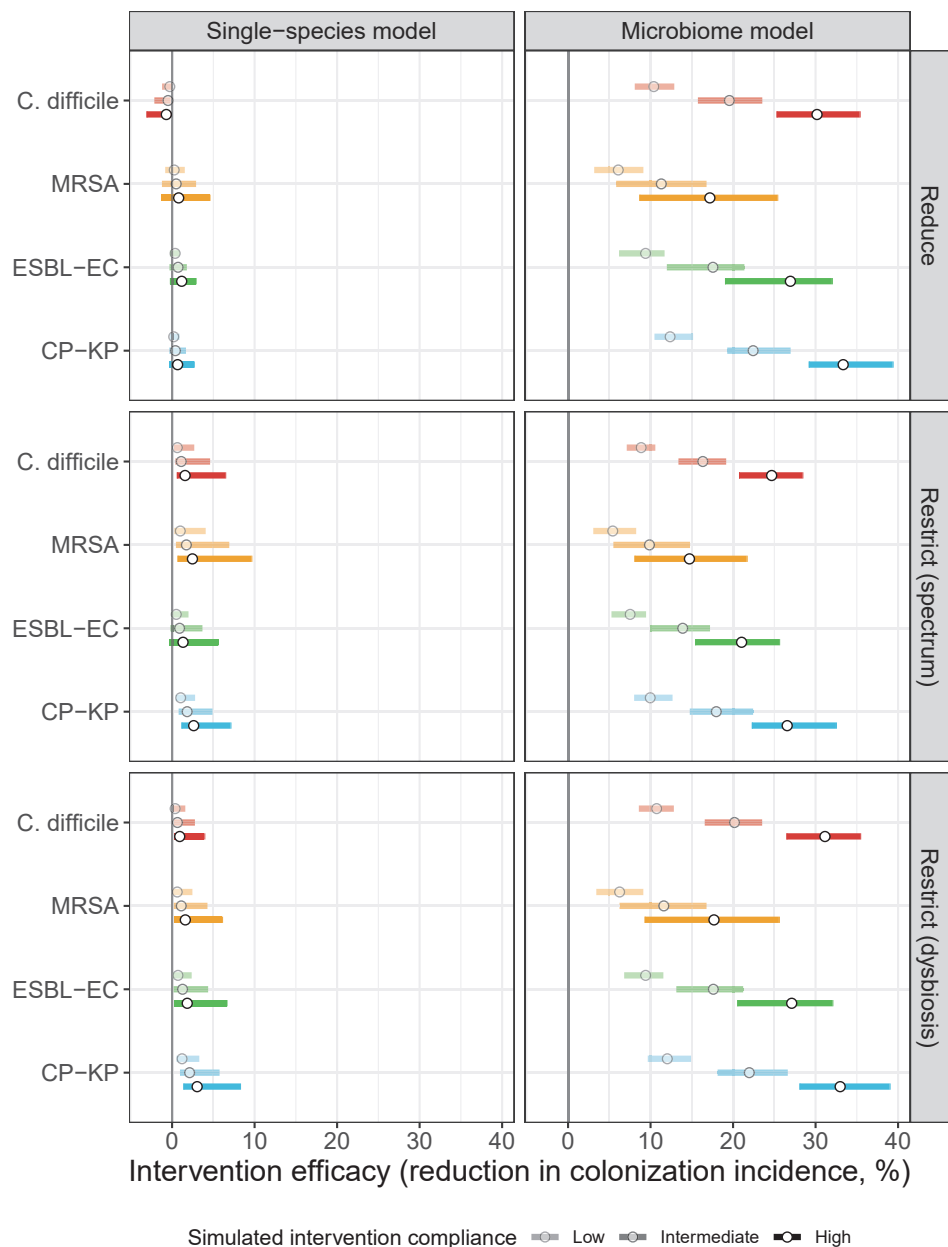
Appendix 1—figure 17. Intervention efficacy for three considered types of antibiotic stewardship: (**i**) reducing overall antibiotic prescribing, (ii) restricting broad-spectrum antibiotics in favour of narrow-spectrum antibiotics, and (iii) restricting antibiotics categorized as inducing microbiome dysbiosis at high or very high rates in favour of those that induce dysbiosis at medium or low rates. In microbiome simulations, restricting antibiotics that induce dysbiosis at a high rate was approximately as effective as reducing overall antibiotic prescribing. In single-species simulations, all stewardship interventions were of limited to negligible efficacy. Points correspond to medians, and bars to 95% uncertainty intervals across 10,000 Monte Carlo simulations.

Meta-analysis of hospital antibiotic stewardship interventions

To assess consistency of intervention outcomes with the literature, we compared antibiotic steward-ship results to a systematic review and meta-analysis of hospital antibiotic stewardship interventions

initially conducted by *Baur et al., 2017.* They included interventional studies published worldwide from Jan 1960 to May 2016 describing incidence of bacterial colonization or infection among hospital inpatients. Stewardship interventions were heterogeneous and included audits, antibiotic restriction, antibiotic cycling, antibiotic mixing, feedback, guideline implementation and education. The authors found no evidence of publication bias or small study effects.

Their analysis included 32 studies over 9 million patient-days, though stewardship interventions were co-implemented with other infection control measures (e.g. hand hygiene, patient isolation) in 31% of studies. When limited to stewardship, patients were still significantly less likely to experience colonization and infection (IRR=0.81, 0.67–0.97), but species-specific estimates were not made. When excluding studies that included non-stewardship interventions, ten studies remained for MRSA, (*Arda et al., 2007*; *Frank et al., 1997*; *Mach et al., 2007*; *Marra et al., 2009*; *Meyer et al., 2010*; *Miyawaki et al., 2010*; *Peto et al., 2008*; *Smith et al., 2008*; *Yeo et al., 2012*; *Zou et al., 2015*) seven for *C. difficile*, (*Borde et al., 2015*; *Dubrovskaya et al., 2012*; *Frank et al., 1997*; *Leung et al., 2011*; *Lübbert et al., 2014*; *Malani et al., 2013*; *Schön et al., 2011*) two for ESBL-*E. coli*, (*Arda et al., 2007*; *Chong et al., 2013*) and one for CP-*K. pneumoniae* (*Arda et al., 2007*) For ESBL-*E.* coli, we further included studies of ESBL-producing Enterobacteriaceae and Gram-negative bacteria (*Grohs et al., 2014*; *Takesue et al., 2010*) Using their published data and methodology, we calculated incidence risk ratios (IRR) using the standard inverse-variance method, and pooled IRRs across species using mixed-effects meta-analysis models (R package *metafor*). Results for each study and pooled results for each pathogen are presented in *Appendix 1—figure 18*.
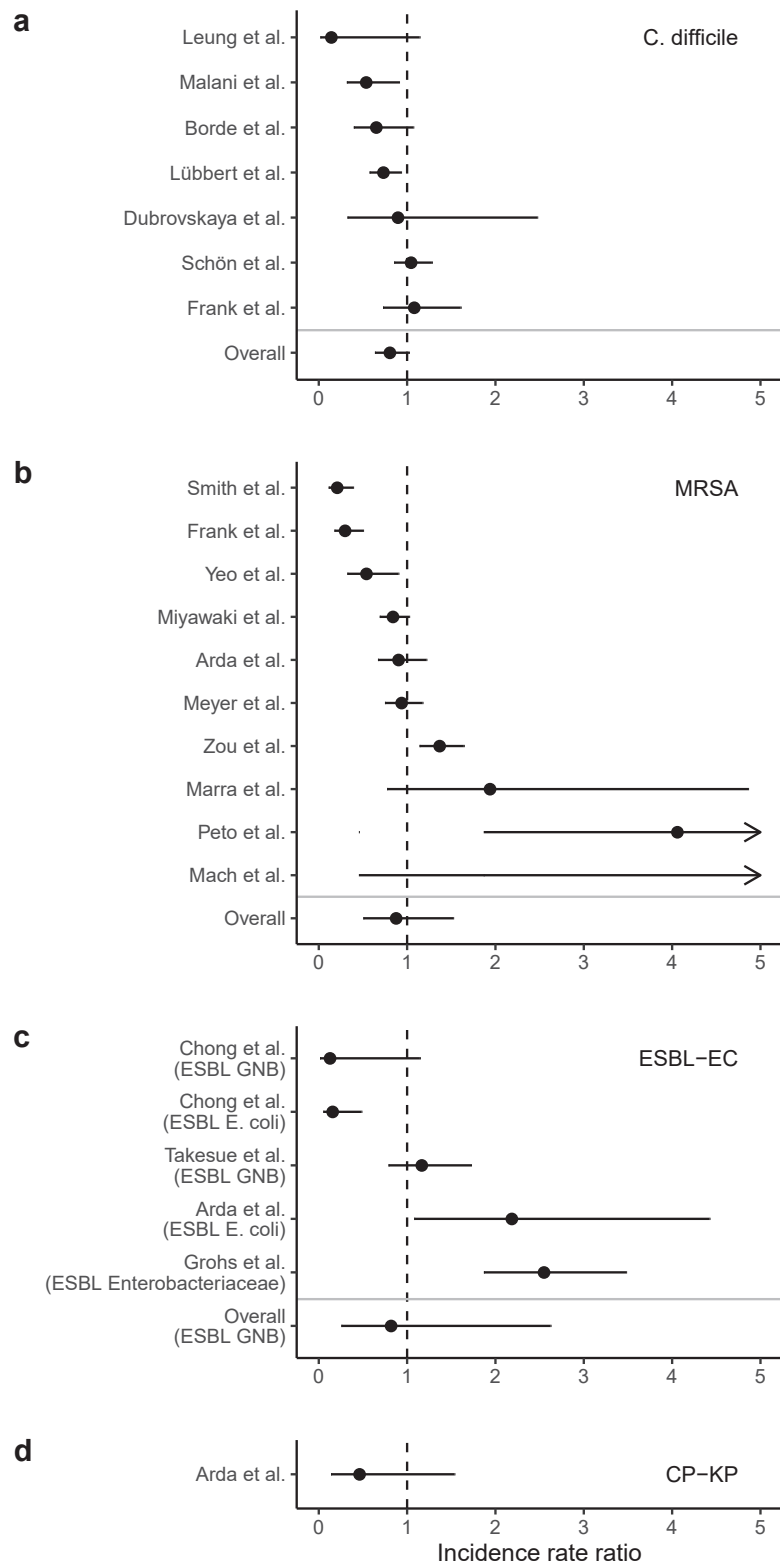
Appendix 1—figure 18. Incidence rate ratios (IRRs) for ARB colonization and infection among hospital inpatients exposed to antibiotic stewardship interventions. IRRs were calculated using data presented in *Baur et al., 2017* Results are stratified by four pathogens: (**a**) *C. difficile*, (**b**) methicillin-resistant *S. aureus*, (**c**) ESBL-producing *E. coli* (and here also including ESBL-producing

Appendix 1—figure 18 continued on next page

Appendix 1—figure 18 continued

Enterobacteriaceae or Gram-negative bacteria), and (**d**) carbapenemase-producing *K. pneumoniae*. Points represent means and bars represent 95% confidence intervals.